8th International Particle Accelerator Conference

COPENHAGEN, DENMARK, 2017 MAY 14—19

Towards Diffraction Limited Storage Ring Based Light Sources

Liu Lin
Brazilian Synchrotron Light Laboratory - LNLS

IPAC17

8th International Particle Accelerator Conference

COPENHAGEN, DENMARK, 2017 MAY 14—19

Towards Diffraction Limited Storage Ring Based Light Sources

Highlights from Sirius, the Brazilian Light Source Project

Liu Lin
Brazilian Synchrotron Light Laboratory - LNLS

Outline

- The new generation of Storage Ring Light Sources
- High brightness and coherence
  - Low emittance
  - Phase-space matching
- Sirius, the Brazilian Light Source Project
  - Lattice design highlights: low beta sections
  - Light source & beamline integration: improved solution for CARNAÚBA beamline
- Conclusion

The new generation of storage rings

emittance scaling

$$\epsilon_0 \propto \frac{\gamma^2}{N_B^3}$$

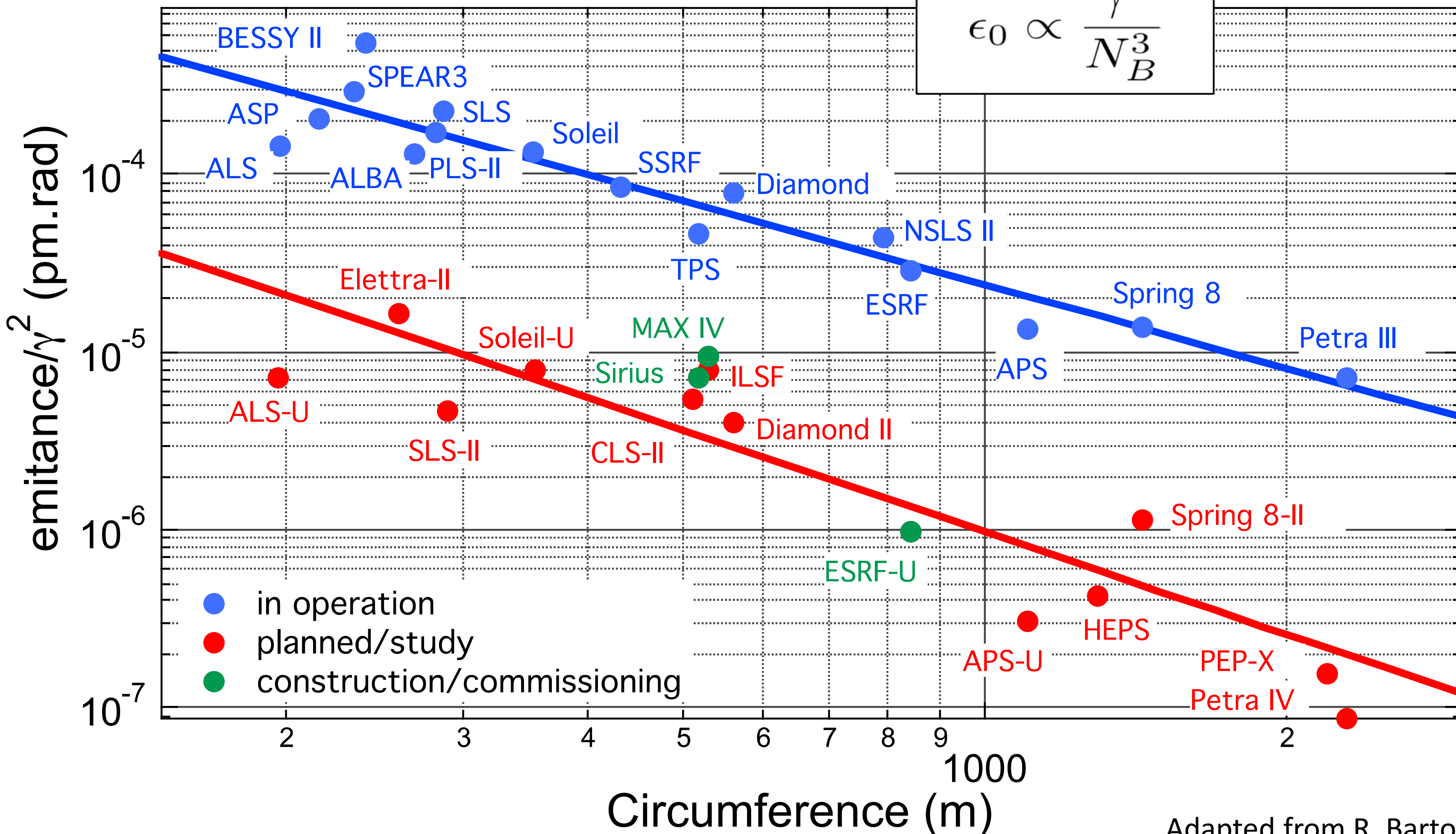

Adapted from R. Bartollini

The new generation of storage rings

emittance scaling

$$\epsilon_0 \propto \frac{\gamma^2}{N_B^3}$$

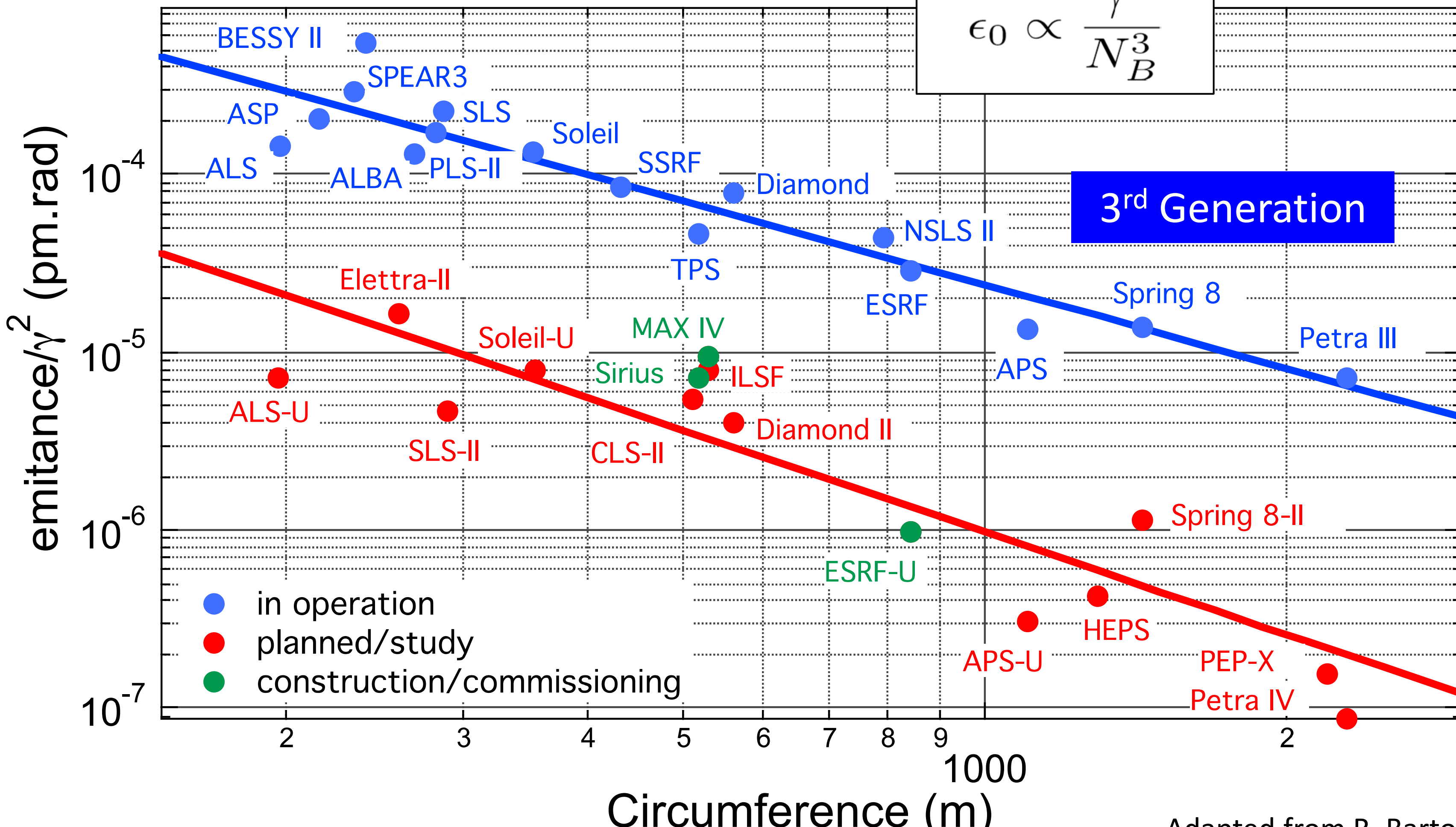

Adapted from R. Bartollini

The new generation of storage rings

emittance scaling

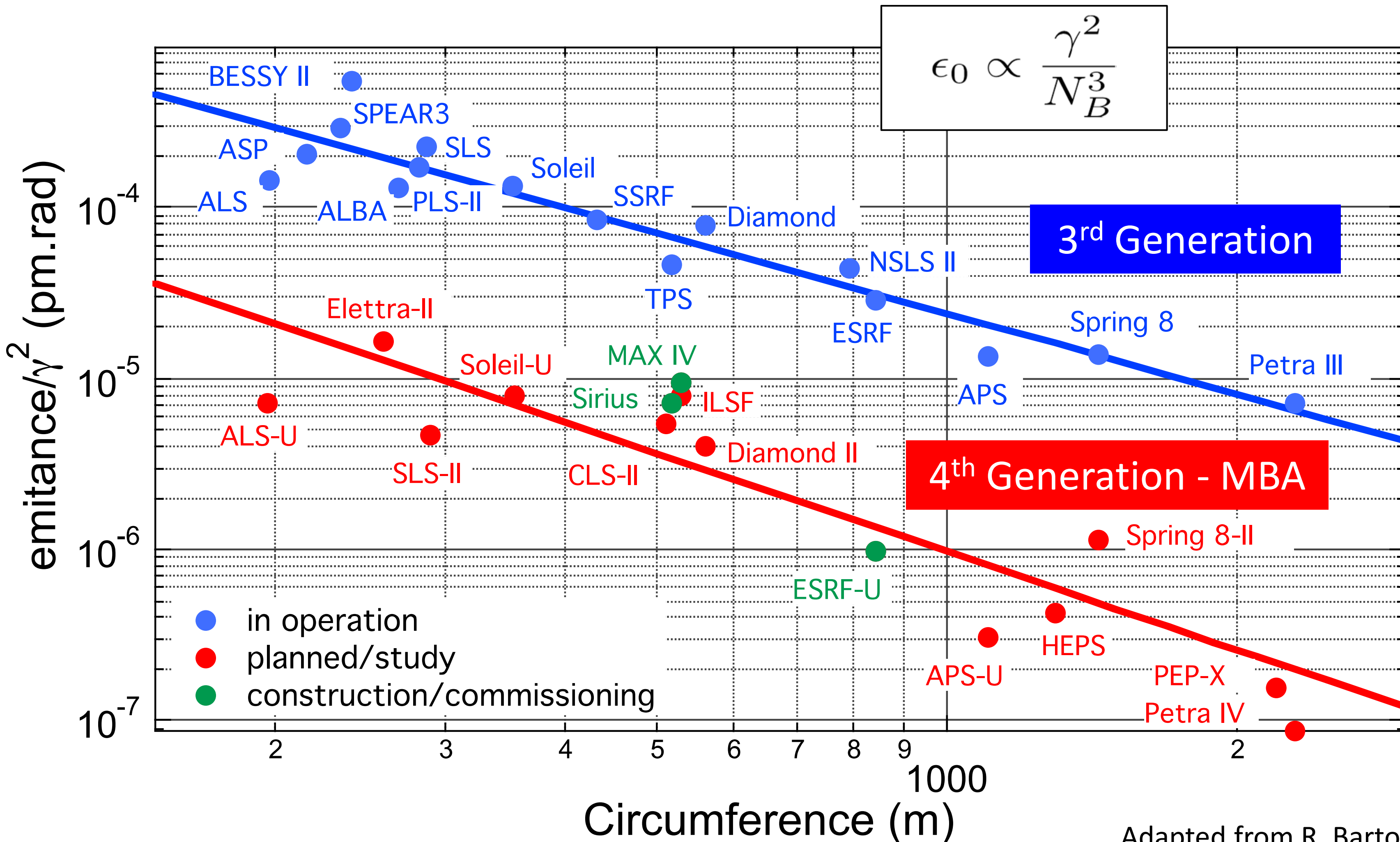

Adapted from R. Bartollini

Some new storage rings and upgrade plans

Machine	Energy [GeV]	Circum. [m]	N_B	Emit. [pm]	status
MAX-IV	3	528	140	330	operation, new
Sirius	3	518	100	250	construction, new
ESRF-U	6	844	224	135	construction, upgrade
ALS-U	2	196	108	109	planned, upgrade
APS-U	6	1104	280	42	planned, upgrade
CLS-II	3	510	147	186	planned, new
Diamond-II	3	561	144	140	planned, upgrade
Elettra-II	2	259	72	250	planned, upgrade
HEPS	6	1296	336	59	planned, new
ILSF	3	528	100	275	planned, new
PEP-X	4.5	2199		12	planned, upgrade
PETRA-IV	6	2304	504	12	planned, upgrade
SLS-II	2.4	290	84	103	planned, upgrade
Soleil-II	2.75	354	104	230	planned, upgrade
Spring8-II	6	1436	200	157	planned, upgrade

Planned machines are at different planning stages.

Storage ring spectral brilliance (brightness)

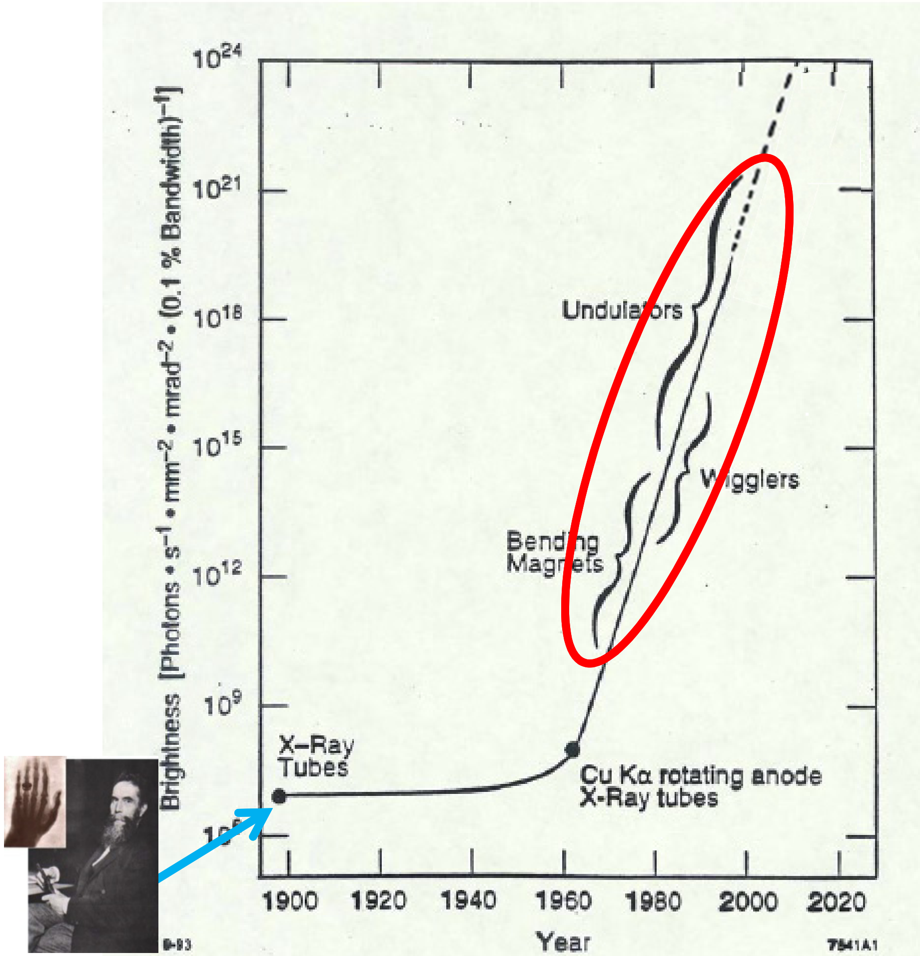

Herman Winick March 26, 2007

4th Generation

emittance reduction with MBA lattices, high performance IDs, high coherent flux

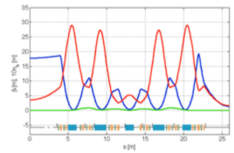

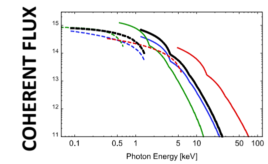

3rd Generation

DBA, TBA lattices with straight sections for wigglers and undulators, high brilliance

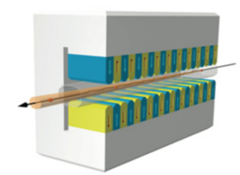

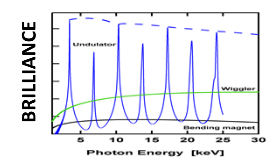

2nd Generation

dedicated sources from bending magnets, high flux

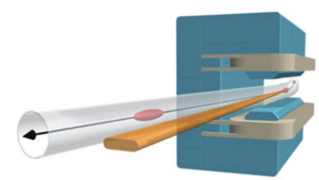

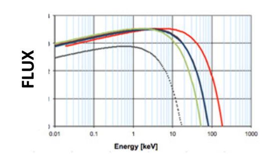

1st Generation

parasitic operation in colliders, bending magnets

Spectral brilliance and coherent fraction

- Spectral brilliance: Flux density in phase space

$$B(\lambda) \propto \frac{F(\lambda)}{\left(\epsilon_{x,e^-} \otimes \epsilon_r(\lambda)\right) \left(\epsilon_{y,e^-} \otimes \epsilon_r(\lambda)\right)}$$

Spectral brilliance and coherent fraction

- Spectral brilliance: Flux density in phase space

$$B(\lambda) \propto \frac{F(\lambda)}{\left(\epsilon_{x,e^-} \otimes \epsilon_r(\lambda)\right) \ \left(\epsilon_{y,e^-} \otimes \epsilon_r(\lambda)\right)}$$

Photon flux [photons/s/0.1% bw]

Spectral brilliance and coherent fraction

- Spectral brilliance: Flux density in phase space

$$B(\lambda) \propto \frac{F(\lambda)}{\left(\epsilon_{x,e^-} \otimes \epsilon_r(\lambda)\right) \left(\epsilon_{y,e^-} \otimes \epsilon_r(\lambda)\right)}$$

Photon flux [photons/s/0.1% bw]

electron beam emittance

Spectral brilliance and coherent fraction

- Spectral brilliance: Flux density in phase space

$$B(\lambda) \propto \frac{F(\lambda)}{\left(\epsilon_{x,e^-} \otimes \epsilon_r(\lambda)\right)\ \left(\epsilon_{y,e^-} \otimes \epsilon_r(\lambda)\right)}$$

Photon flux [photons/s/0.1% bw]

electron beam emittance

photon limiting emittance

- Spectral brilliance: Flux density in phase space

$$B(\lambda) \propto \frac{F(\lambda)}{\left(\epsilon_{x,e^-} \otimes \epsilon_r(\lambda)\right) \left(\epsilon_{y,e^-} \otimes \epsilon_r(\lambda)\right)}$$

Photon flux [photons/s/0.1% bw]

electron beam emittance

photon limiting emittance

$$\epsilon_r = \sigma_r \sigma_{r'} = \frac{\lambda}{4\pi}$$ for Gaussian beam

$$\epsilon_r = \sigma_r \sigma_{r'} \approx \frac{\lambda}{2\pi}$$ for undulator beam

Spectral brilliance and coherent fraction

- Spectral brilliance: Flux density in phase space

$$B(\lambda) \propto \frac{F(\lambda)}{\left(\epsilon_{x,e^-} \otimes \epsilon_r(\lambda)\right)\ \left(\epsilon_{y,e^-} \otimes \epsilon_r(\lambda)\right)}$$

Photon flux [photons/s/0.1% bw]

electron beam emittance

photon limiting emittance

$\epsilon_r = \sigma_r \sigma_{r'} = \dfrac{\lambda}{4\pi}$ for Gaussian beam

$\epsilon_r = \sigma_r \sigma_{r'} \approx \dfrac{\lambda}{2\pi}$ for undulator beam

- Coherent fraction for undulator radiation

$$f_{coh} = \frac{(\lambda/2\pi)^2}{\left(\epsilon_{x,e^-} \otimes \epsilon_r(\lambda)\right)\ \left(\epsilon_{y,e^-} \otimes \epsilon_r(\lambda)\right)}$$

Spectral brilliance and coherent fraction

- Spectral brilliance: Flux density in phase space

$$B(\lambda) \propto \frac{F(\lambda)}{\left(\epsilon_{x,e^-} \otimes \epsilon_r(\lambda)\right)\ \left(\epsilon_{y,e^-} \otimes \epsilon_r(\lambda)\right)}$$

Photon flux [photons/s/0.1% bw]

electron beam emittance

photon limiting emittance

$$\epsilon_r = \sigma_r \sigma_{r'} = \frac{\lambda}{4\pi}$$ for Gaussian beam

$$\epsilon_r = \sigma_r \sigma_{r'} \approx \frac{\lambda}{2\pi}$$ for undulator beam

- Coherent fraction for undulator radiation

$$f_{coh} = \frac{(\lambda/2\pi)^2}{\left(\epsilon_{x,e^-} \otimes \epsilon_r(\lambda)\right)\ \left(\epsilon_{y,e^-} \otimes \epsilon_r(\lambda)\right)}$$

- Diffraction limited storage ring

$$\epsilon_{x,y} \approx \epsilon_r(\lambda) = \frac{\lambda}{2\pi}$$

Spectral brilliance and coherent fraction

- Spectral brilliance: Flux density in phase space

$$B(\lambda) \propto \frac{F(\lambda)}{\left(\epsilon_{x,e^-} \otimes \epsilon_r(\lambda)\right) \left(\epsilon_{y,e^-} \otimes \epsilon_r(\lambda)\right)}$$

Photon flux [photons/s/0.1% bw]

electron beam emittance

photon limiting emittance

$\epsilon_r = \sigma_r \sigma_{r'} = \frac{\lambda}{4\pi}$ for Gaussian beam

$\epsilon_r = \sigma_r \sigma_{r'} \approx \frac{\lambda}{2\pi}$ for undulator beam

- Coherent fraction for undulator radiation

$$f_{coh} = \frac{(\lambda/2\pi)^2}{\left(\epsilon_{x,e^-} \otimes \epsilon_r(\lambda)\right) \left(\epsilon_{y,e^-} \otimes \epsilon_r(\lambda)\right)}$$

- Diffraction limited storage ring

$$\epsilon_{x,y} \approx \epsilon_r(\lambda) = \frac{\lambda}{2\pi}$$

$\varepsilon_{x,y} \approx$ 100 pm.rad
diffraction limit for 2 keV

$\varepsilon_{x,y} \approx$ 20 pm.rad
diffraction limit for 10 keV

Achieving low emittance with MBA

$$\epsilon_x = C_q \ \frac{\gamma^2}{J_x} \ \frac{\oint \mathcal{H}(s) \ h(s)^3 ds}{\oint h(s)^2 ds}$$

Achieving low emittance with MBA

$$\epsilon_x = C_q \frac{\gamma^2}{J_x} \frac{\oint \mathcal{H}(s)\ h(s)^3 ds}{\oint h(s)^2 ds}$$

damping partition

Achieving low emittance with MBA

$$\epsilon_x = C_q \frac{\gamma^2}{J_x} \frac{\oint \mathcal{H}(s)\ h(s)^3 ds}{\oint h(s)^2 ds}$$

damping partition

curvature function
$h(s) = 1/\rho(s)$

Achieving low emittance with MBA

$$\epsilon_x = C_q \frac{\gamma^2}{J_x} \frac{\oint \mathcal{H}(s)\ h(s)^3 ds}{\oint h(s)^2 ds}$$

damping partition

dispersion's betatron amplitude

$$\mathcal{H} = \frac{\eta^2 + (\alpha\eta + \beta\eta')^2}{\beta}$$

curvature function

$$h(s) = 1/\rho(s)$$

η: dispersion function

β, α: Twiss functions

Achieving low emittance with MBA

$$\epsilon_x = C_q \frac{\gamma^2}{J_x} \frac{\oint \mathcal{H}(s)\ h(s)^3 ds}{\oint h(s)^2 ds}$$

dispersion's betatron amplitude

$$\mathcal{H} = \frac{\eta^2 + (\alpha\eta + \beta\eta')^2}{\beta}$$

η: dispersion function
β, α: Twiss functions

damping partition

curvature function

$$h(s) = 1/\rho(s)$$

Emittance depends on optics at places where radiation is emitted (dipoles).

Achieving low emittance with MBA

$$\epsilon_x = C_q \frac{\gamma^2}{J_x} \frac{\oint \mathcal{H}(s)\ h(s)^3 ds}{\oint h(s)^2 ds}$$

damping partition

dispersion's betatron amplitude

$$\mathcal{H} = \frac{\eta^2 + (\alpha\eta + \beta\eta')^2}{\beta}$$

curvature function

$$h(s) = 1/\rho(s)$$

η: dispersion function

β, α: Twiss functions

Emittance depends on optics at places where radiation is emitted (dipoles).

Double bend achromat - DBA

Multiple bend achromat – MBA

many small dipoles to keep horizontal focus in each dipole

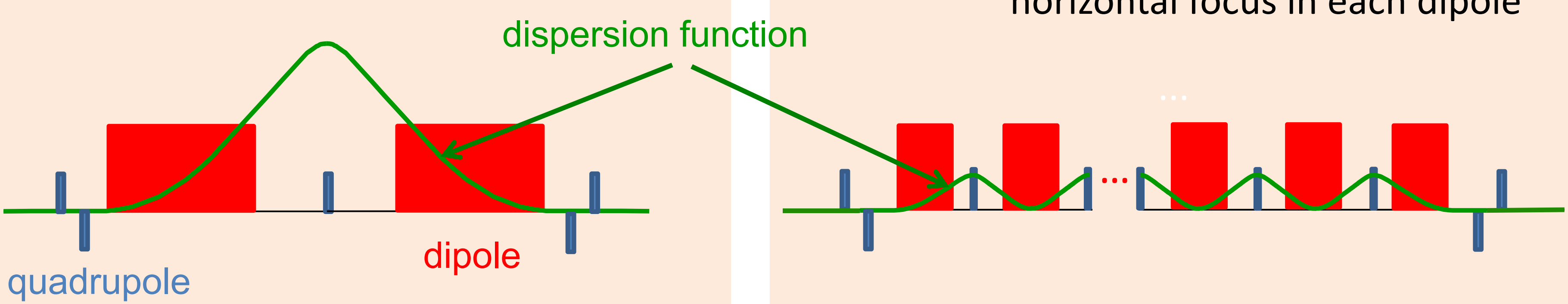

The Multi Bend Achromat Challenges

Courtesy: Ricardo Rodrigues

MBA

The Multi Bend Achromat Challenges

Courtesy: Ricardo Rodrigues

MBA → Many short cells

The Multi Bend Achromat Challenges

Courtesy: Ricardo Rodrigues

MBA → Many short cells → Small beam emittance

The Multi Bend Achromat Challenges

Courtesy: Ricardo Rodrigues

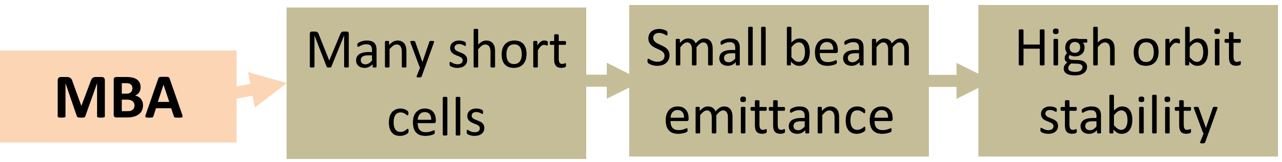

The Multi Bend Achromat Challenges

Courtesy: Ricardo Rodrigues

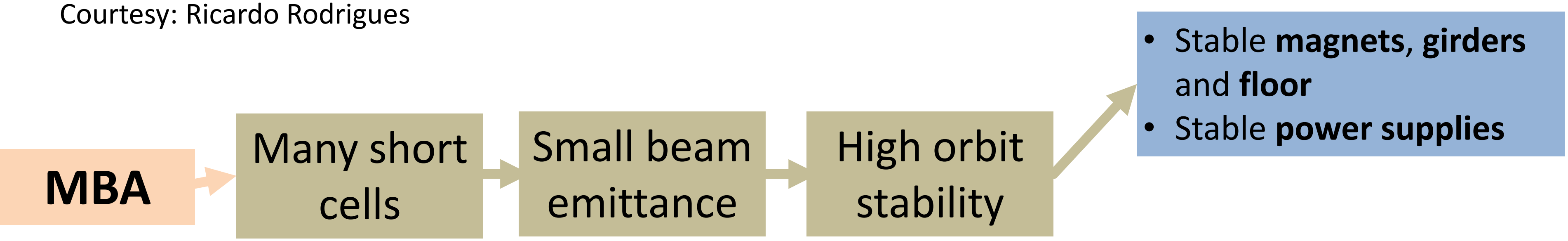

The Multi Bend Achromat Challenges

Courtesy: Ricardo Rodrigues

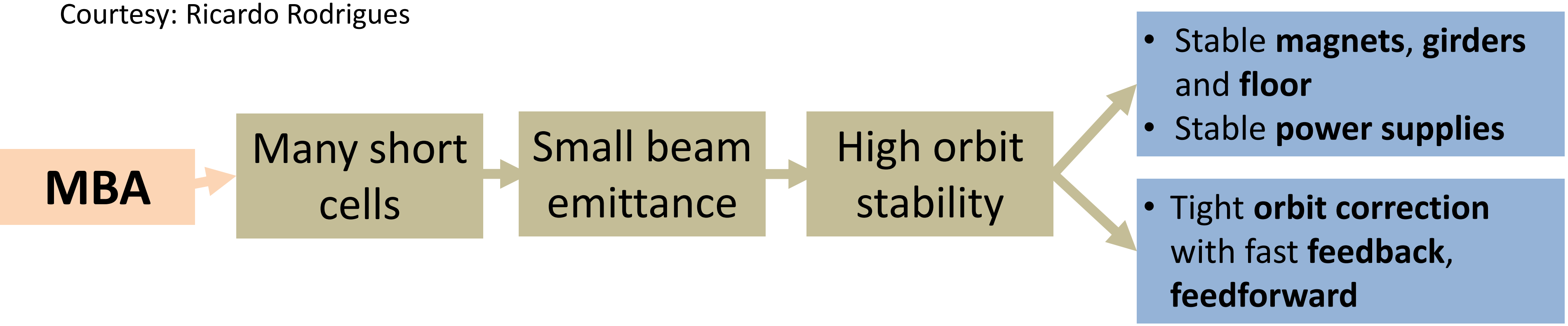

The Multi Bend Achromat Challenges

Courtesy: Ricardo Rodrigues

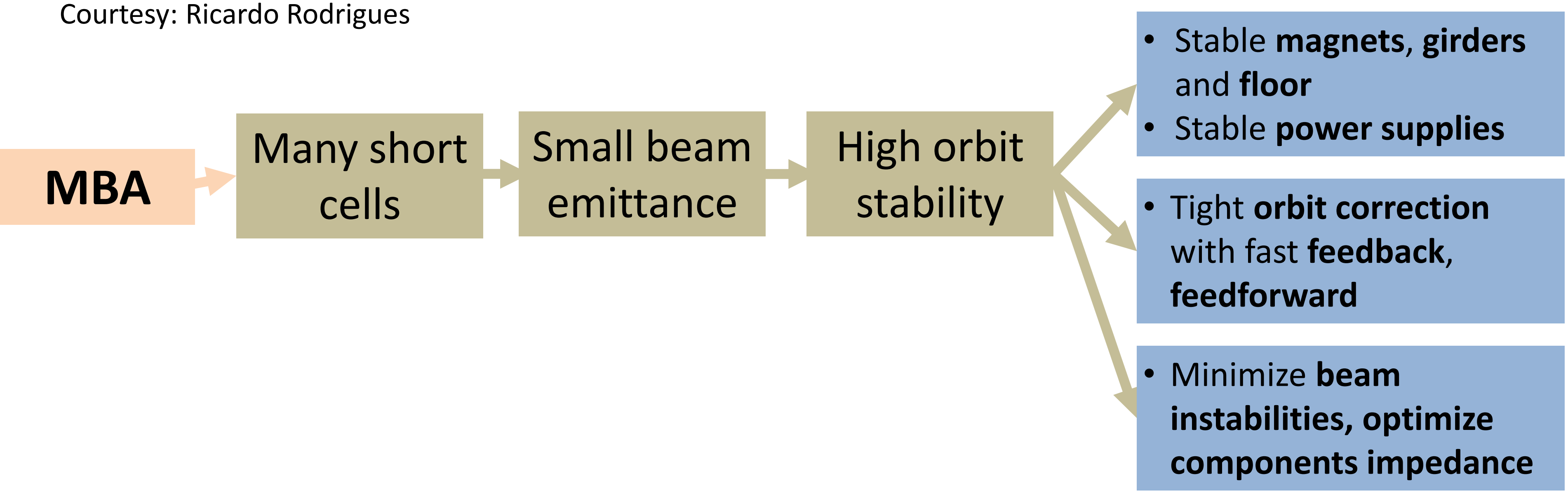

The Multi Bend Achromat Challenges

Courtesy: Ricardo Rodrigues

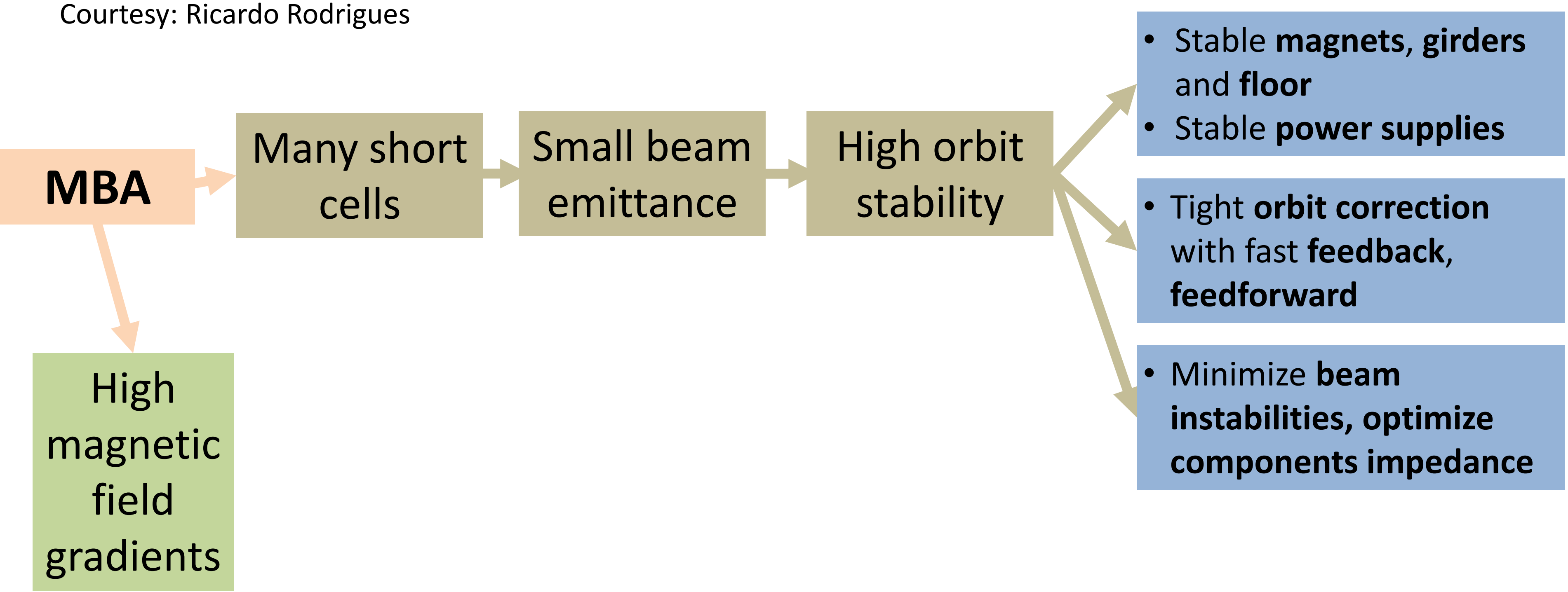

The Multi Bend Achromat Challenges

Courtesy: Ricardo Rodrigues

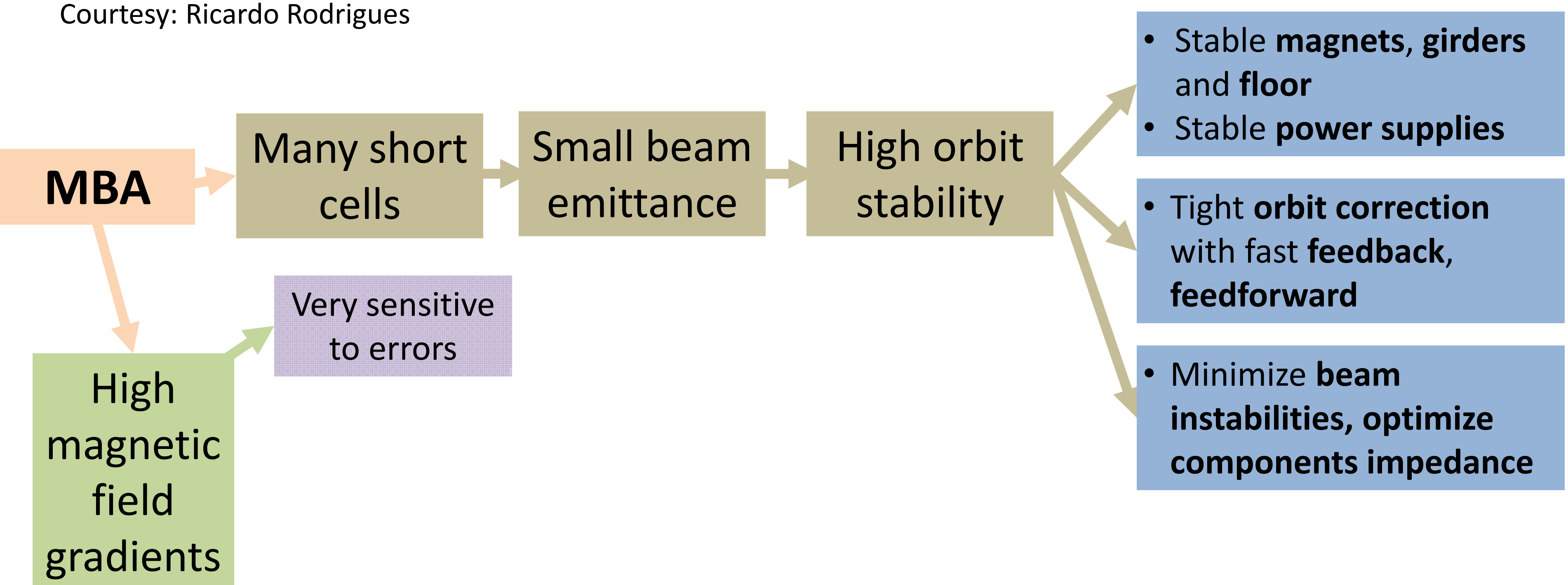

The Multi Bend Achromat Challenges

Courtesy: Ricardo Rodrigues

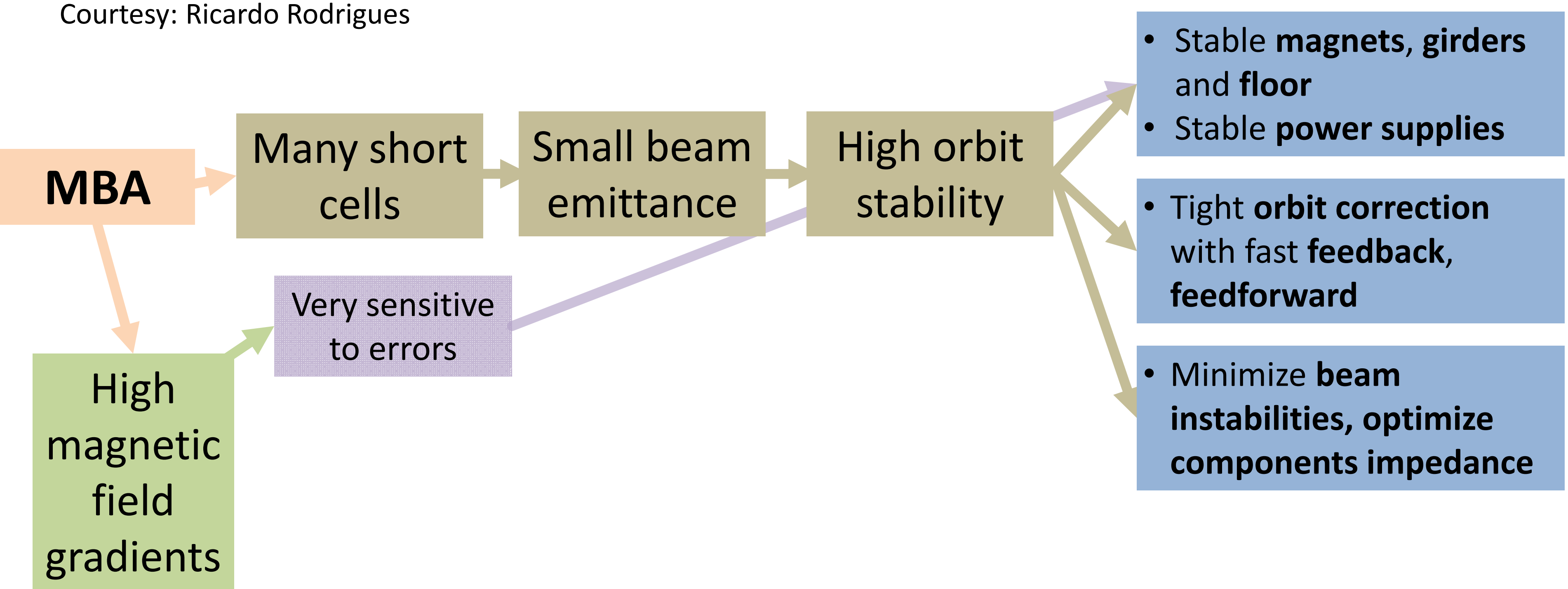

The Multi Bend Achromat Challenges

Courtesy: Ricardo Rodrigues

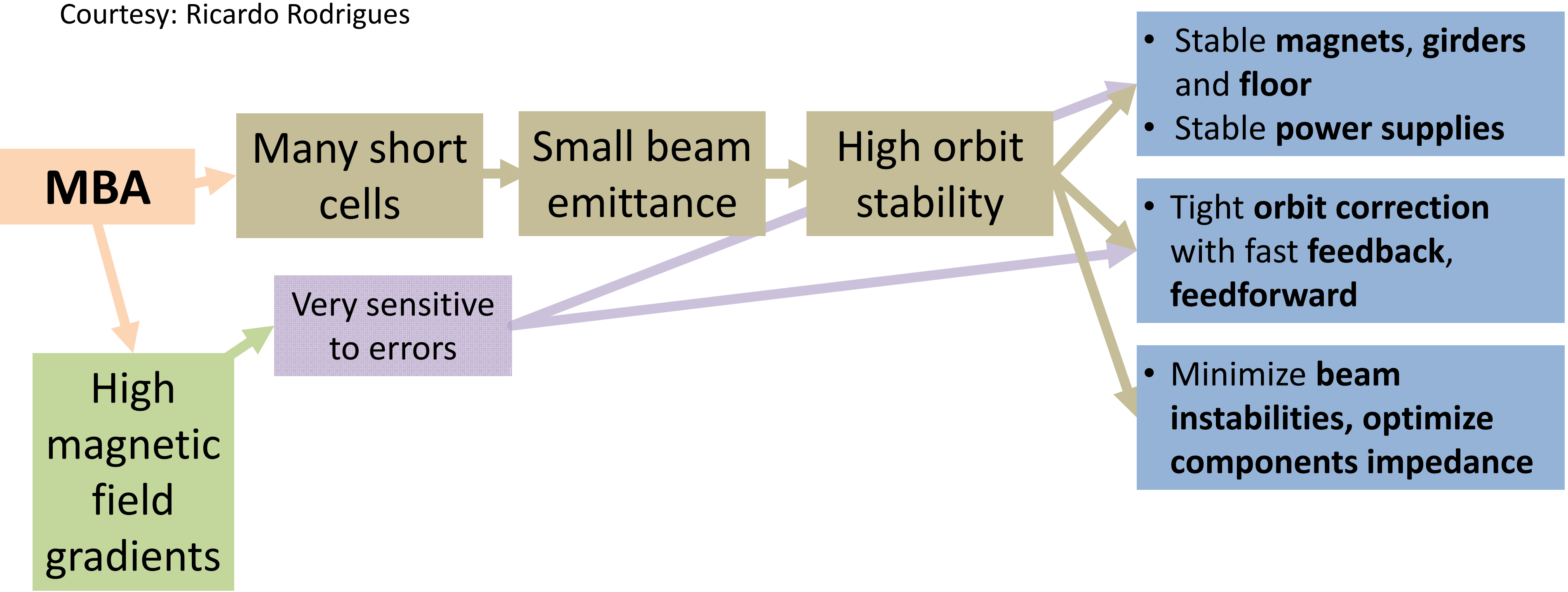

The Multi Bend Achromat Challenges

Courtesy: Ricardo Rodrigues

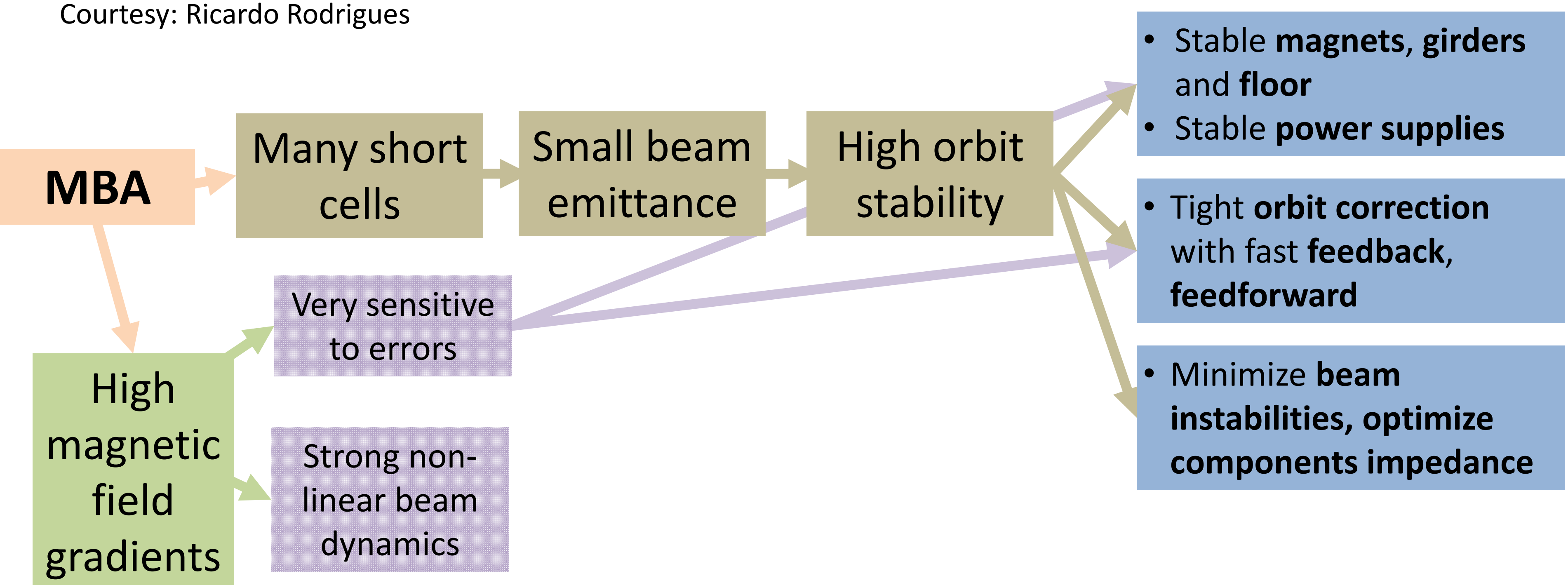

The Multi Bend Achromat Challenges

Courtesy: Ricardo Rodrigues

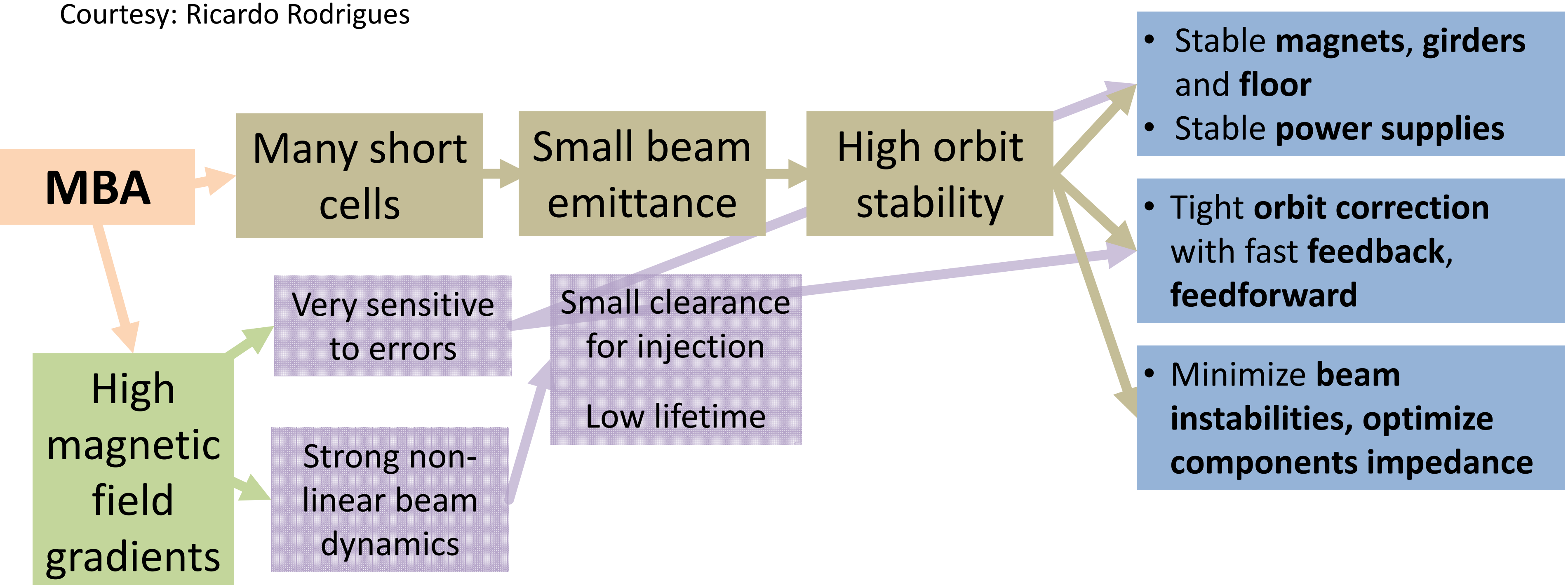

The Multi Bend Achromat Challenges

Courtesy: Ricardo Rodrigues

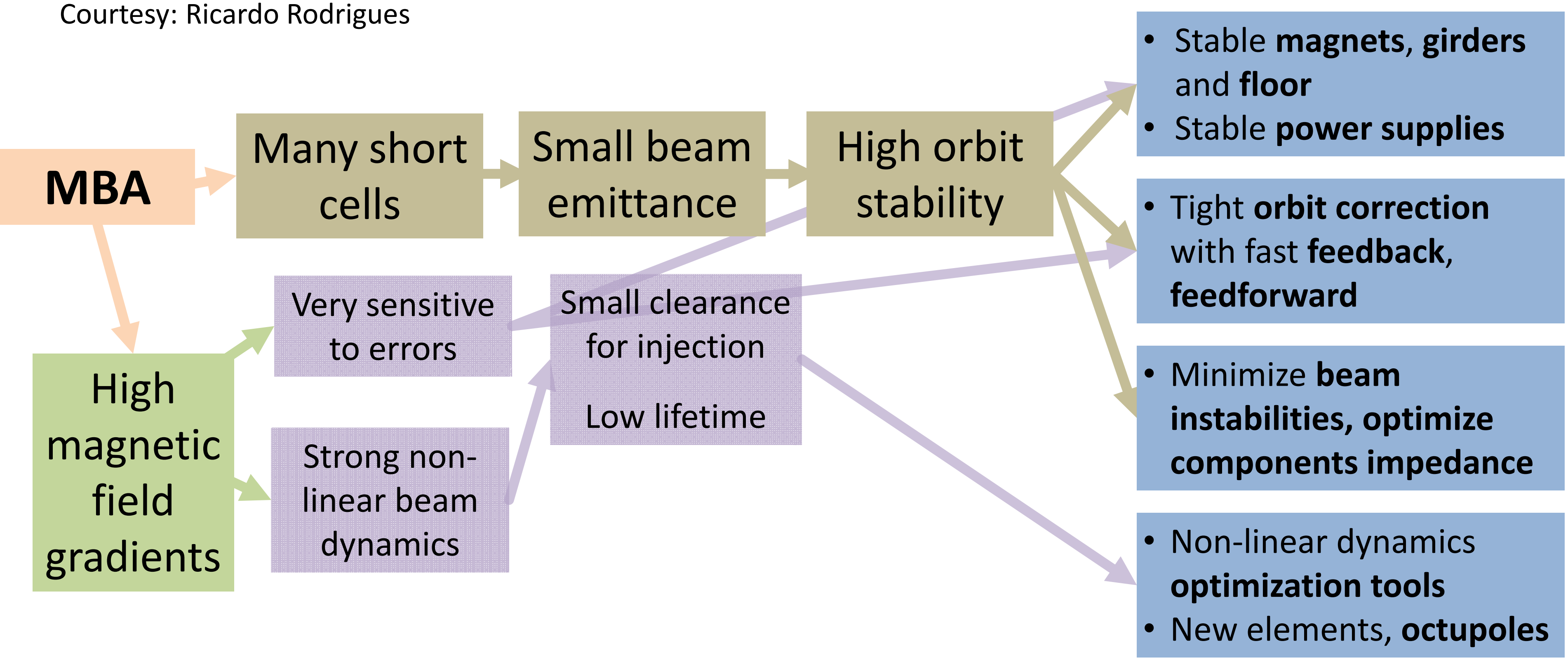

The Multi Bend Achromat Challenges

Courtesy: Ricardo Rodrigues

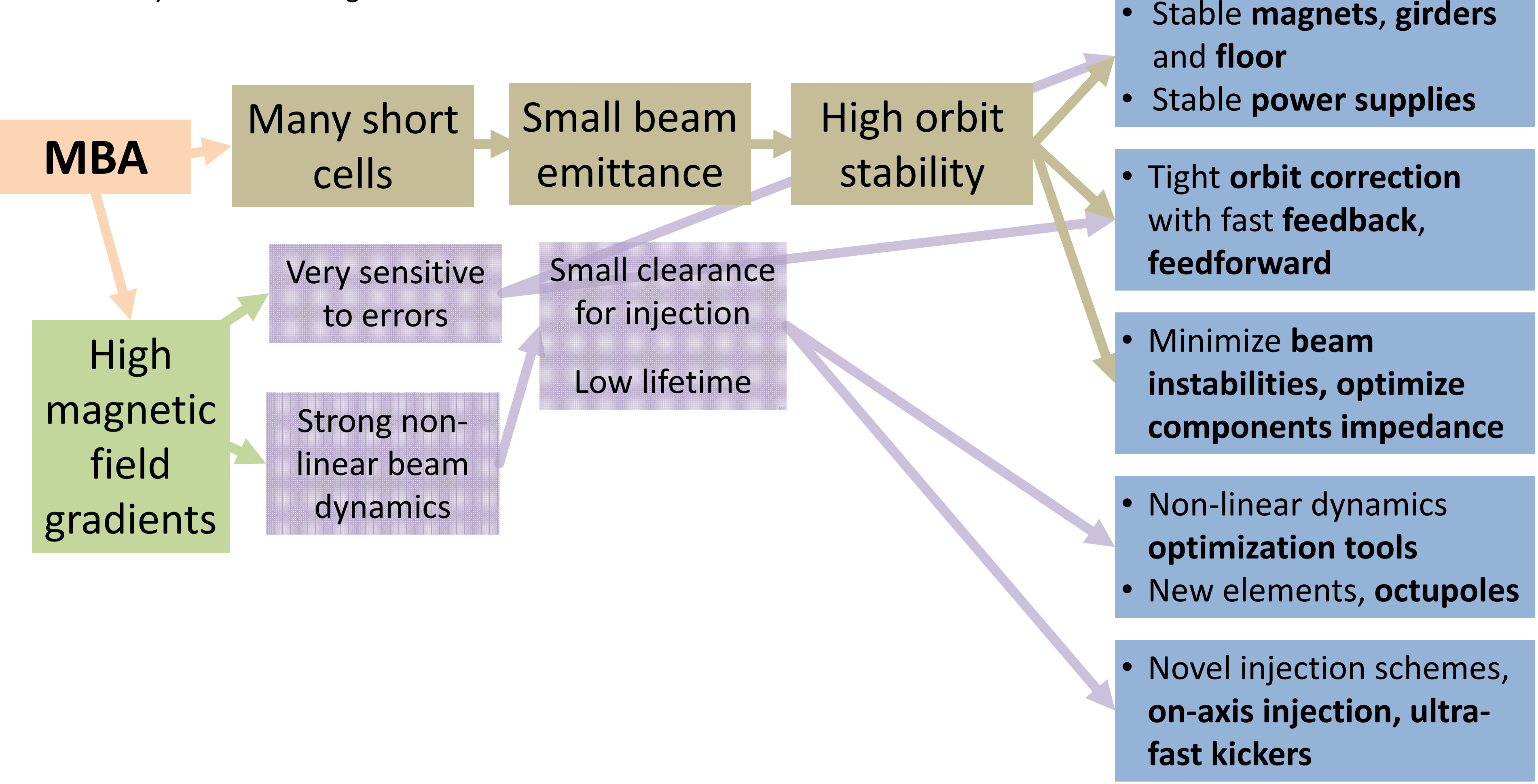

The Multi Bend Achromat Challenges

Courtesy: Ricardo Rodrigues

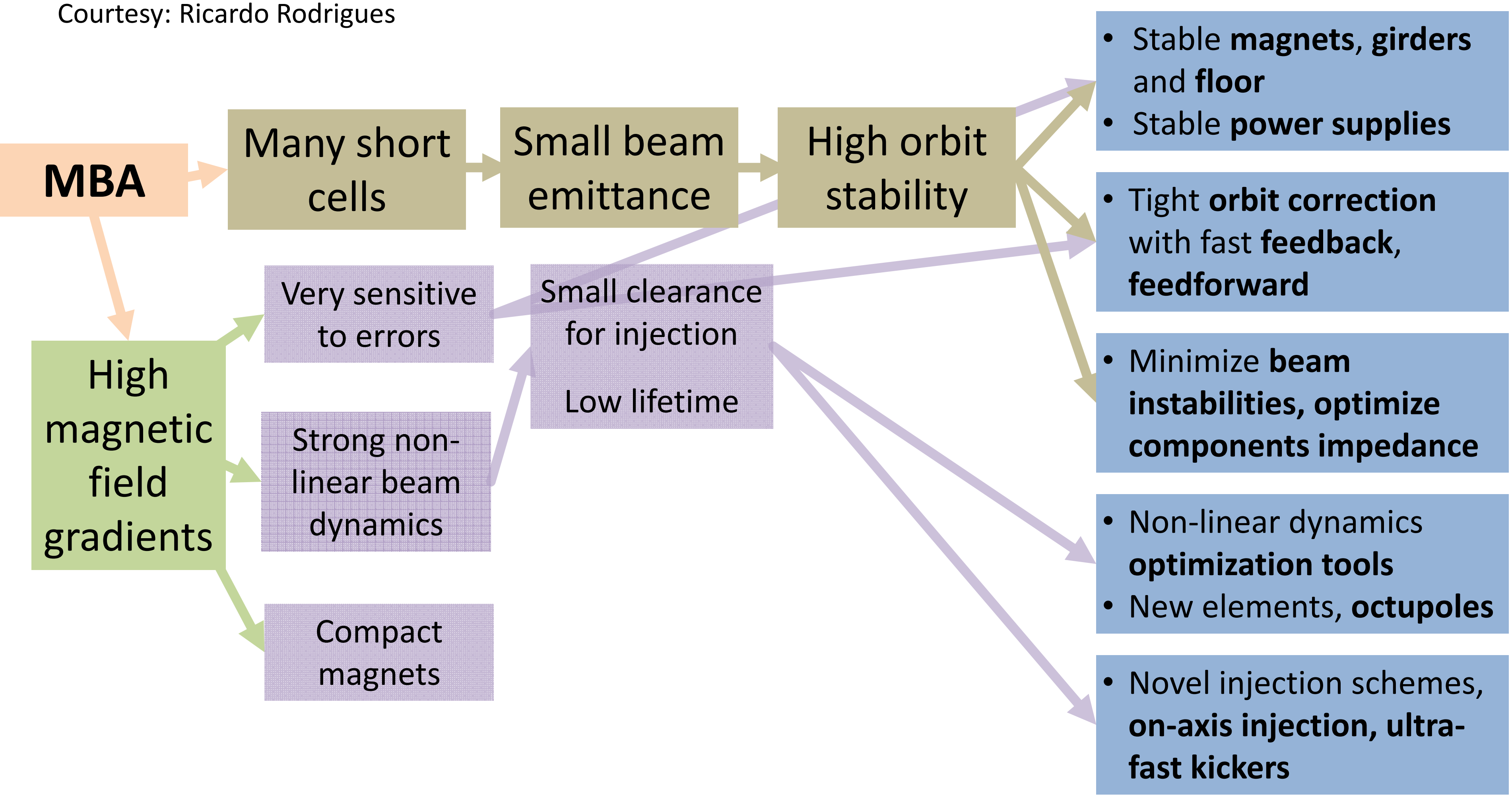

The Multi Bend Achromat Challenges

Courtesy: Ricardo Rodrigues

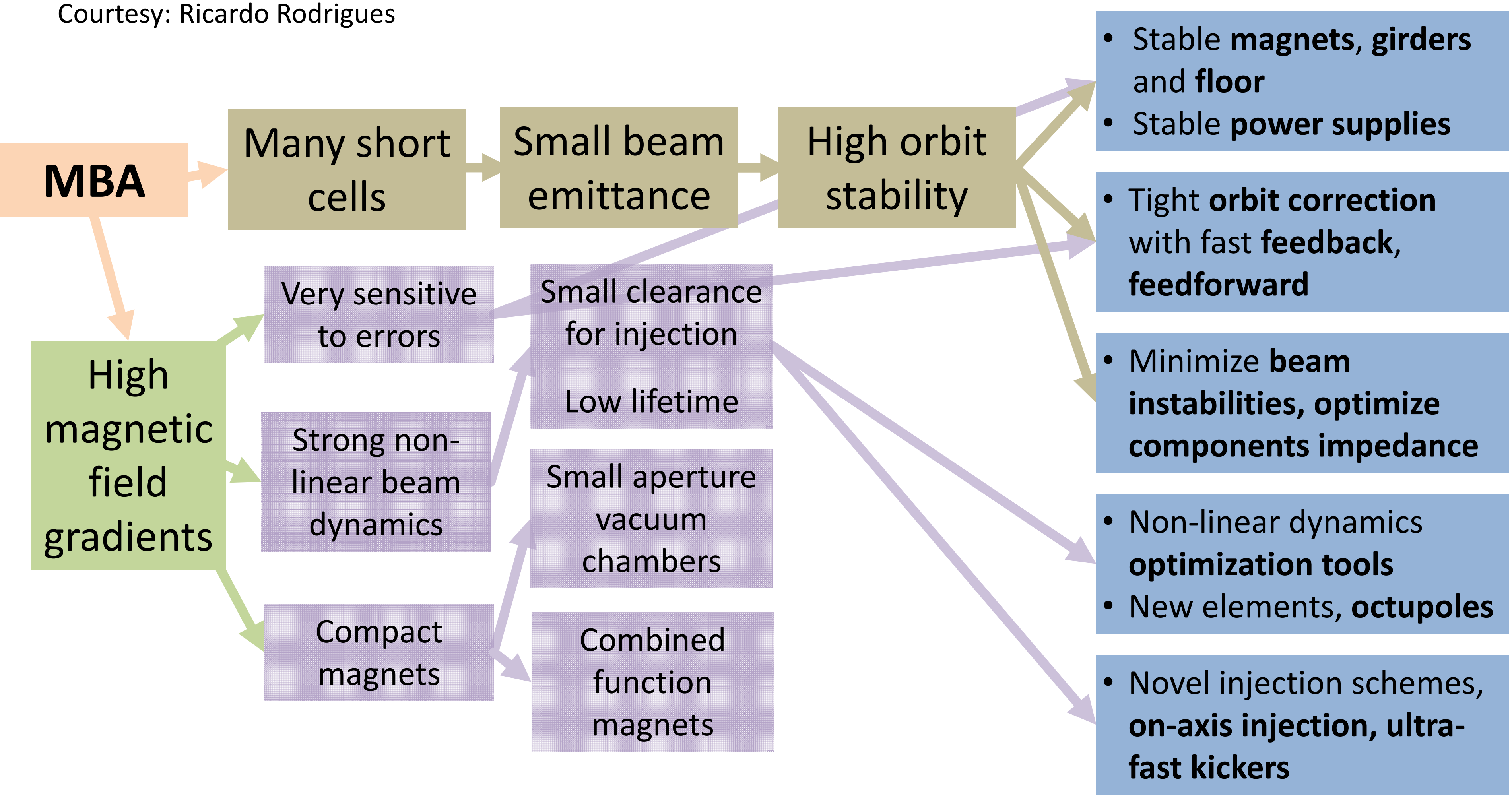

The Multi Bend Achromat Challenges

Courtesy: Ricardo Rodrigues

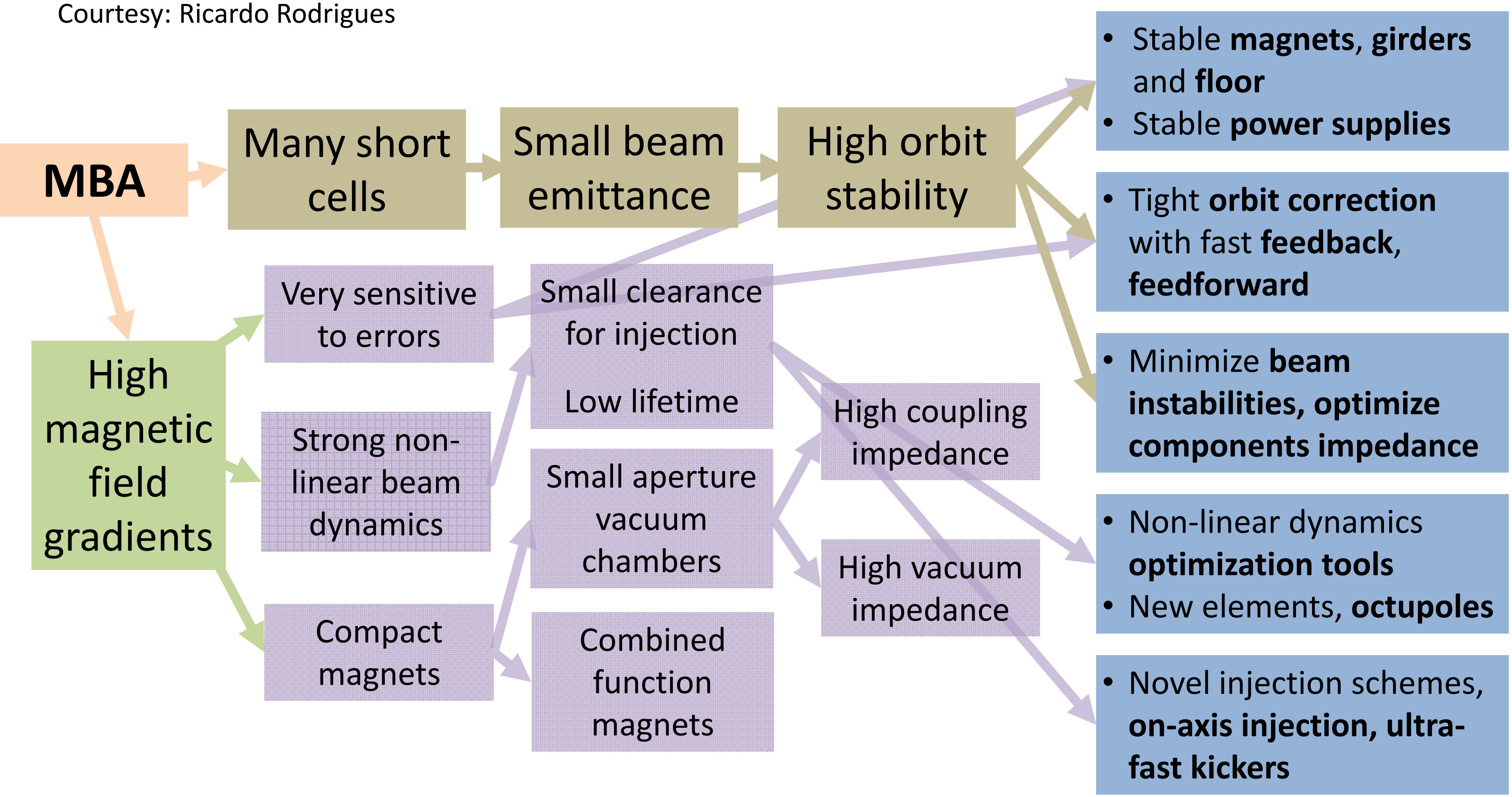

The Multi Bend Achromat Challenges

Courtesy: Ricardo Rodrigues

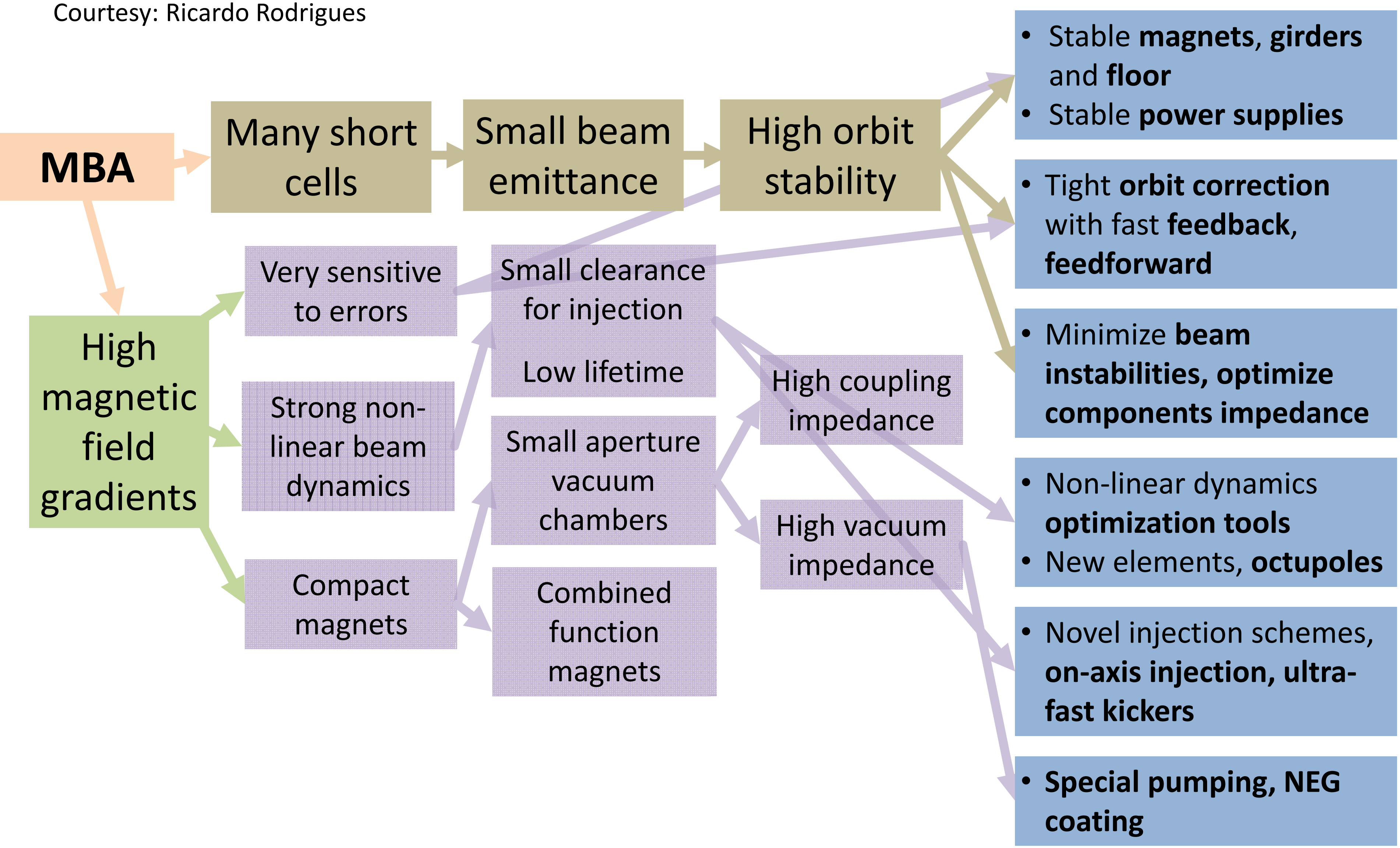

The Multi Bend Achromat Challenges

Courtesy: Ricardo Rodrigues

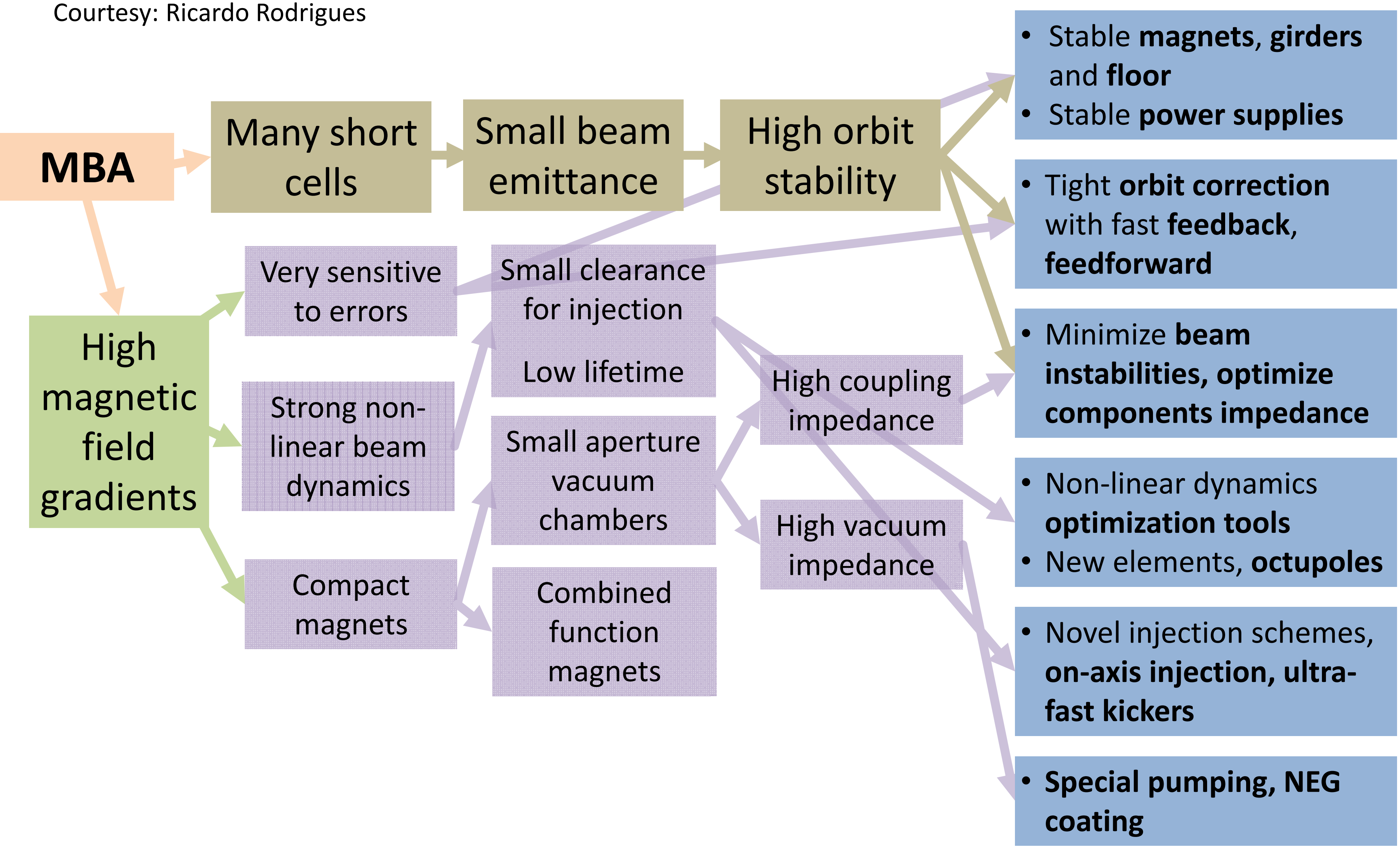

The Multi Bend Achromat Challenges

Courtesy: Ricardo Rodrigues

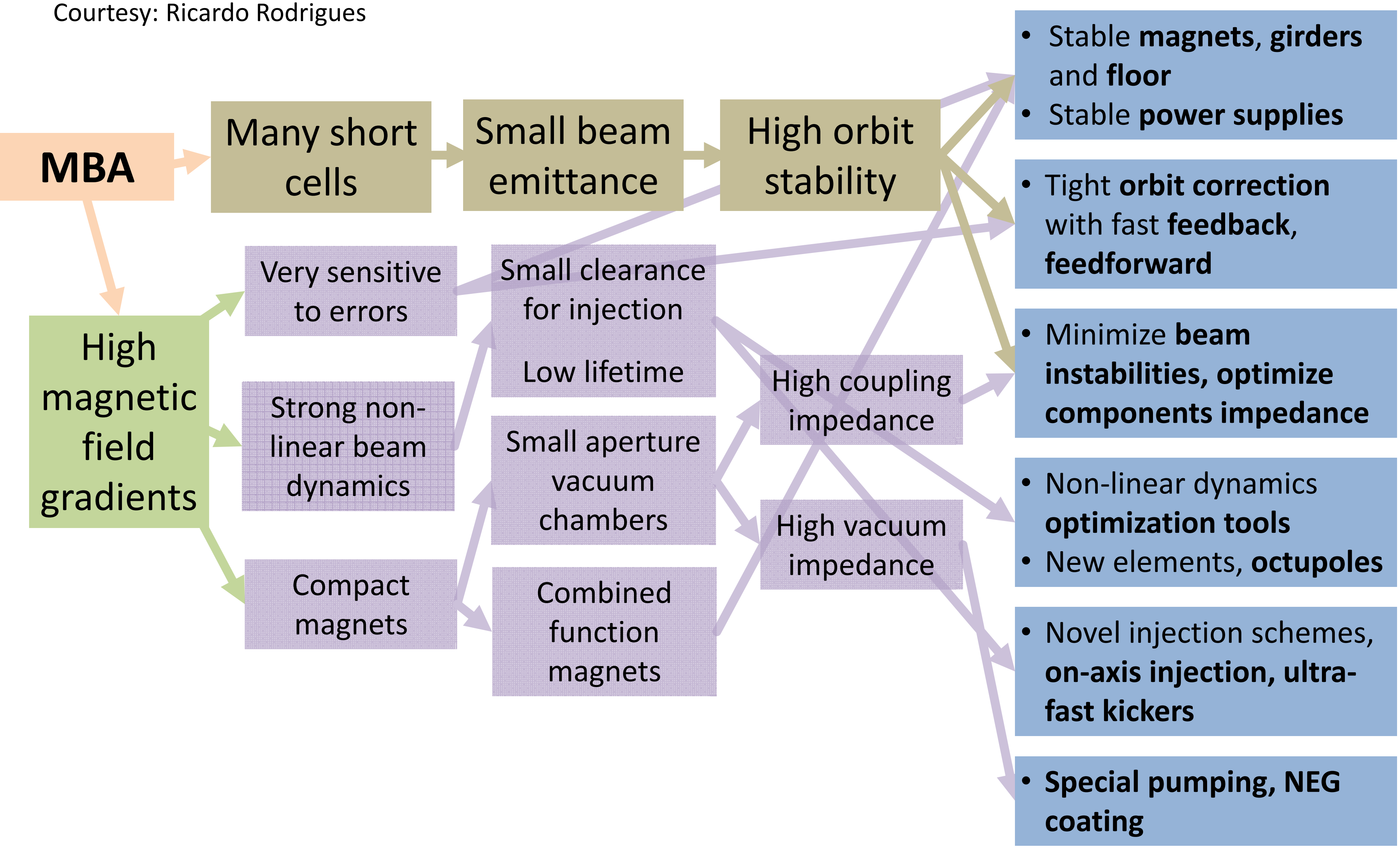

The Multi Bend Achromat Challenges

Courtesy: Ricardo Rodrigues

MBA

Many short cells

Small beam emittance

High orbit stability

High magnetic field gradients

Very sensitive to errors

Strong non-linear beam dynamics

Compact magnets

Small clearance for injection

Low lifetime

Small aperture vacuum chambers

Combined function magnets

High coupling impedance

High vacuum impedance

- Stable **magnets, girders** and **floor**
- Stable **power supplies**

- Tight **orbit correction** with fast **feedback, feedforward**

- Minimize **beam instabilities, optimize components impedance**

- Non-linear dynamics **optimization tools**
- New elements, **octupoles**

- Novel injection schemes, **on-axis injection, ultra-fast kickers**

- **Special pumping, NEG coating**

Recent advances in accelerator technology, simulation tools, new design ideas, etc, are helping to overcome the challenges but many issues are still open and require R&D.

Other ingredients to reduce emittance

- Increase damping partition number J_x by adding transverse field gradient in dipoles.

$$J_x = 1 - \frac{\oint (1 - 2n)\eta |h(s)^3| ds}{\oint h(s)^2 ds}$$

Other ingredients to reduce emittance

- Increase damping partition number J_x by adding transverse field gradient in dipoles.

$$J_x = 1 - \frac{\oint (1-2n)\eta |h(s)^3| ds}{\oint h(s)^2 ds}$$

- Longitudinal dipole gradient

$$\epsilon_x \propto \oint \mathcal{H}(s)\, h(s)^3 ds$$

  - Curvature function $h(s) = 1/\rho(s)$
  - To keep product small: compensate variation in $\mathcal{H}(s)$ with variation in $h(s)$
  - Radiate more (high curvature) where $\mathcal{H}(s)$ is small.

Other ingredients to reduce emittance

- Increase damping partition number J_x by adding transverse field gradient in dipoles.

$$J_x = 1 - \frac{\oint (1 - 2n)\eta |h(s)^3| ds}{\oint h(s)^2 ds}$$

- Longitudinal dipole gradient

$$\epsilon_x \propto \oint \mathcal{H}(s)\, h(s)^3 ds$$

  - Curvature function $h(s) = 1/\rho(s)$
  - To keep product small: compensate variation in $\mathcal{H}(s)$ with variation in $h(s)$
  - Radiate more (high curvature) where $\mathcal{H}(s)$ is small.
- Achromatic cells and low field dipoles to enhance emittance reduction with Insertion Devices.

Other ingredients to reduce emittance

- Increase damping partition number J_x by adding transverse field gradient in dipoles.

$$J_x = 1 - \frac{\oint (1 - 2n)\eta |h(s)^3| ds}{\oint h(s)^2 ds}$$

- Longitudinal dipole gradient

$$\epsilon_x \propto \oint \mathcal{H}(s)\, h(s)^3 ds$$

  - Curvature function $h(s) = 1/\rho(s)$
  - To keep product small: compensate variation in $\mathcal{H}(s)$ with variation in $h(s)$
  - Radiate more (high curvature) where $\mathcal{H}(s)$ is small.
- Achromatic cells and low field dipoles to enhance emittance reduction with Insertion Devices.
- Different dipole lengths, shorter dipoles at cell ends, where $\eta = \eta' = 0$.

Other ingredients to reduce emittance

- Increase damping partition number J_x by adding transverse field gradient in dipoles.

$$J_x = 1 - \frac{\oint (1-2n)\eta |h(s)^3| ds}{\oint h(s)^2 ds}$$

- Longitudinal dipole gradient

$$\epsilon_x \propto \oint \mathcal{H}(s)\, h(s)^3 ds$$

  - Curvature function $h(s) = 1/\rho(s)$
  - To keep product small: compensate variation in $\mathcal{H}(s)$ with variation in $h(s)$
  - Radiate more (high curvature) where $\mathcal{H}(s)$ is small.
- Achromatic cells and low field dipoles to enhance emittance reduction with Insertion Devices.
- Different dipole lengths, shorter dipoles at cell ends, where $\eta = \eta' = 0$.
- Increase damping with Damping Wigglers → energy spread increases.

Other ingredients to reduce emittance

- Increase damping partition number J_x by adding transverse field gradient in dipoles.

$$J_x = 1 - \frac{\oint (1 - 2n)\eta |h(s)^3| ds}{\oint h(s)^2 ds}$$

- Longitudinal dipole gradient

$$\epsilon_x \propto \oint \mathcal{H}(s)\, h(s)^3 ds$$

  - Curvature function $h(s) = 1/\rho(s)$
  - To keep product small: compensate variation in $\mathcal{H}(s)$ with variation in $h(s)$
  - Radiate more (high curvature) where $\mathcal{H}(s)$ is small.
- Achromatic cells and low field dipoles to enhance emittance reduction with Insertion Devices.
- Different dipole lengths, shorter dipoles at cell ends, where $\eta = \eta' = 0$.
- Increase damping with Damping Wigglers → energy spread increases.
- Anti-bends (SLS). Disentangle dispersion η and beta function β_x.

Diffraction Limit: low emittance is not all! Phase space matching

Electron beam and radiation phase-space

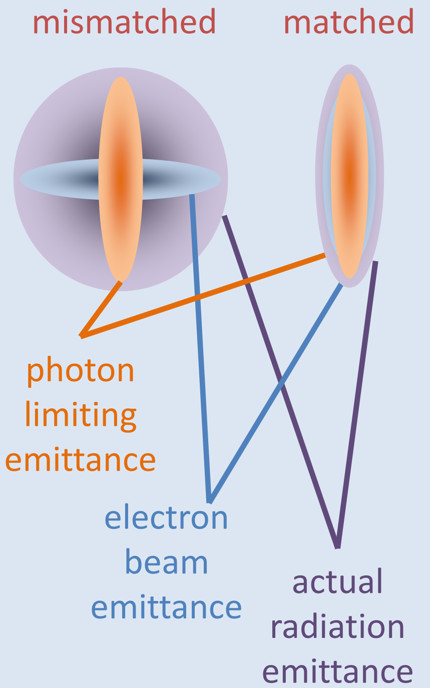

Matching condition

$$\beta_e = \frac{\sigma_e}{\sigma'_e} = \frac{\sigma_r}{\sigma'_r}$$

Diffraction Limit: low emittance is not all! Phase space matching

IPAC17

LNLS sirius

Electron beam and radiation phase-space

mismatched matched

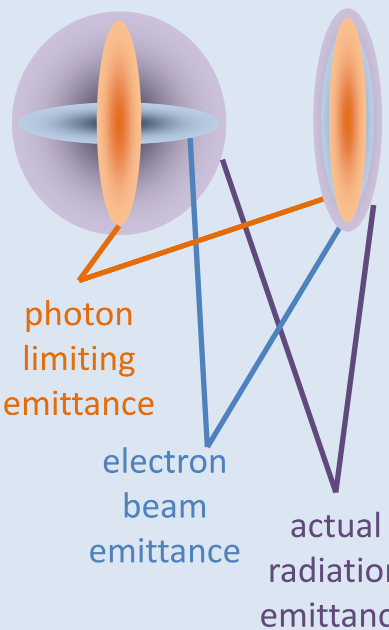

Matching condition

$$\beta_e = \frac{\sigma_e}{\sigma'_e} = \frac{\sigma_r}{\sigma'_r}$$

Highest brilliance from undulator of length L is achieved when

$$\beta_{x,y}^{opt} \approx \frac{L}{\pi}$$

$$\beta_{x,y}^{opt} \sim 1 - 2m$$

Ryan R. Lindberg and Kwang-Je Kim (2015)

COMPACT REPRESENTATIONS OF PARTIALLY … Phys. Rev. ST Accel. Beams **18**, 090702 (2015)

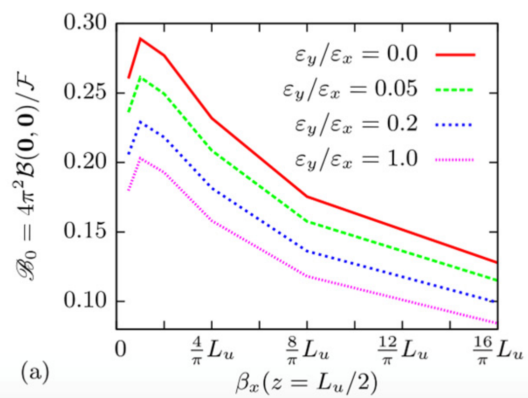

(a)

IV. CONCLUSIONS

In this paper we have described three different coherent mode representations of partially coherent undulator radiation. We began with the well-known Gaussian-Schell decomposition in terms of Gauss-Hermite modes, which is valid provided the electron beam emittance is much larger than the natural radiation emittance $\lambda/4\pi$. In this largely incoherent case the specifics of the single-electron undulator field are unimportant. We then refined our analysis to include the situation when the electron beam emittance ε_y in one direction is arbitrary, and found that the modes along y are determined by solving a matrix

Diffraction Limit: low emittance is not all! Phase space matching

Electron beam and radiation phase-space

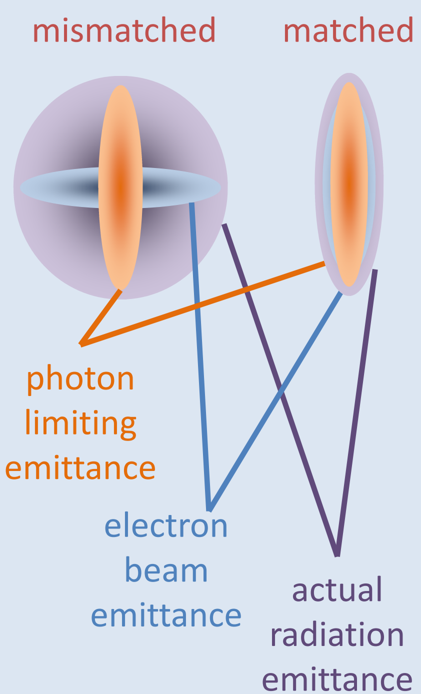

Matching condition

$$\beta_e = \frac{\sigma_e}{\sigma'_e} = \frac{\sigma_r}{\sigma'_r}$$

Highest brilliance from undulator of length L is achieved when

$$\beta_{x,y}^{opt} \approx \frac{L}{\pi} \qquad \beta_{x,y}^{opt} \sim 1 - 2m$$

Ryan R. Lindberg and Kwang-Je Kim (2015)

COMPACT REPRESENTATIONS OF PARTIALLY … Phys. Rev. ST Accel. Beams **18**, 090702 (2015)

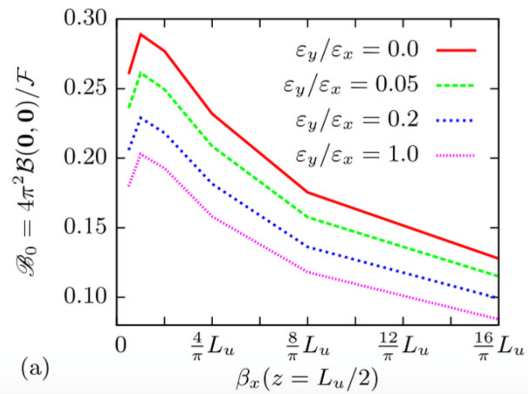

(a)

IV. CONCLUSIONS

In this paper we have described three different coherent mode representations of partially coherent undulator radiation. We began with the well-known Gaussian-Schell decomposition in terms of Gauss-Hermite modes, which is valid provided the electron beam emittance is much larger than the natural radiation emittance $\lambda/4\pi$. In this largely incoherent case the specifics of the single-electron undulator field are unimportant. We then refined our analysis to include the situation when the electron beam emittance ε_y in one direction is arbitrary, and found that the modes along y are determined by solving a matrix

Figure 8(a) shows that the coherence is maximized when $\beta_x \approx L_u/\pi$ (or $\hat{\beta}_x \approx 1$), which indicates that the "natural" Rayleigh range of undulator radiation $Z_R \approx \beta_x \approx L_u/\pi$. Unfortunately, it is nearly impossible for lattice designers to make the beta functions in both x and y be simultaneously that small, and typically $\beta_x > 3L_u/\pi$.

very similar: the profiles when β_x is increased by a factor of 16 can be approximately obtained by multiplying those in Fig. 8(b) by 1.3. Figure 8(c) plots the profiles along x as we vary β_x. Each plot is approximately Gaussian, and we see that the angular spread decreases as β_x increases. More careful inspection shows that the width of the angular

090702-14

Phase space matching (from SPECTRA)

SINGLE PHOTON'S "PHASE SPACE" (900 eV)
(Wigner Distribution Function)
from single electron

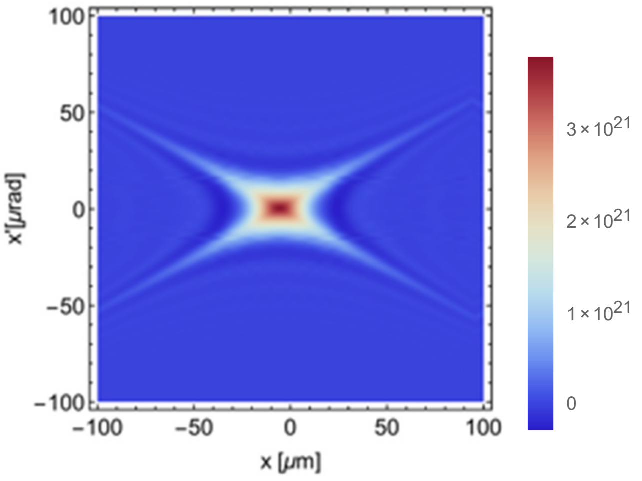

Courtesy: Harry Westfahl Jr.

Phase space matching (from SPECTRA)

SINGLE PHOTON'S "PHASE SPACE" (900 eV)
(Wigner Distribution Function)
from single electron

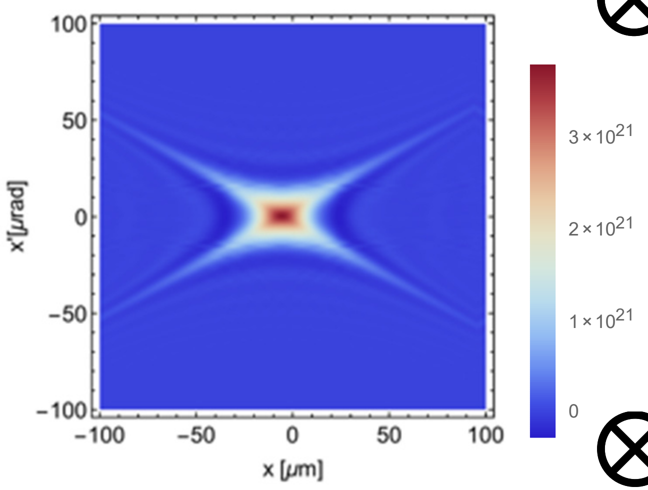

⊗

ELECTRONS PHASE SPACE
(HORIZONTAL)

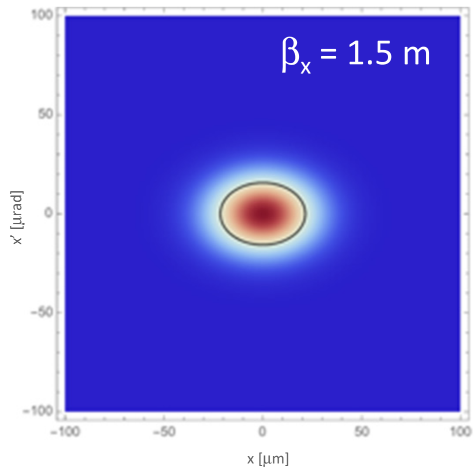

=

AVERAGE PHOTON'S "PHASE SPACE"
(Wigner Distribution Function=Brilliance)

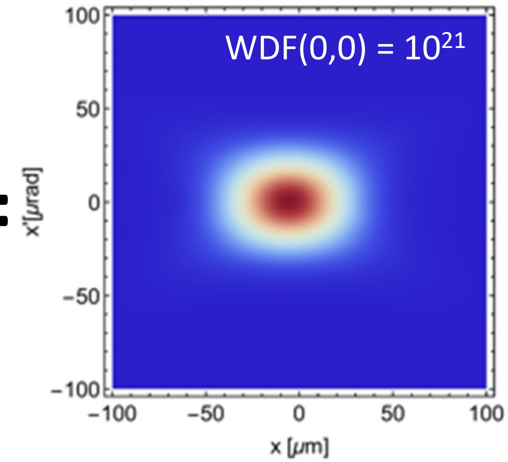

⊗

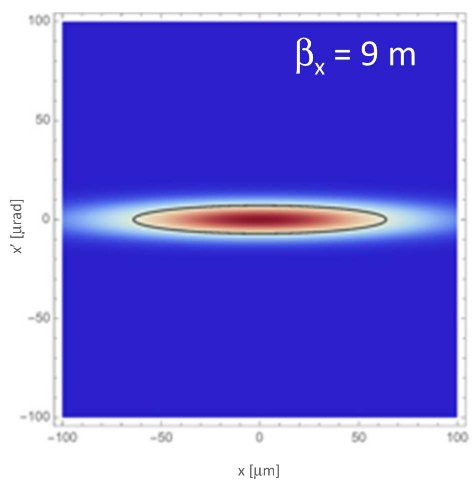

=

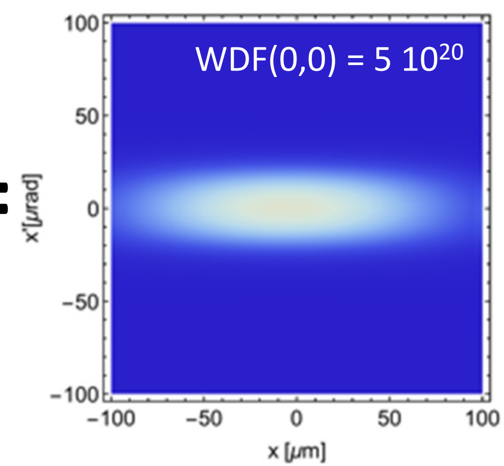

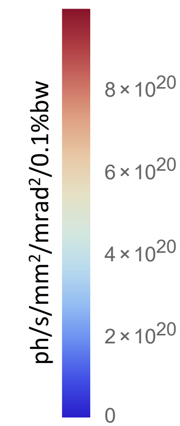

Courtesy: Harry Westfahl Jr.

Sirius, the Brazilian Light Source Project

First beam 2018 – Open in 2019

Budget

• Accelerators	100 M US$
• 13 beamlines	140 M US$
• Building	213 M US$
• Human Res	57 M US$
• Total	510 M US$

Schedule

• Jan.2015	start of building construction
• Oct.2017	start of machine installation
• Jul.2018	start of SR commissioning
• Sep.2018	phase 1 operation (20mA, NCC)
• Feb.2019	phase 2 operaton (100mA, SCC)

CNPEM Campus

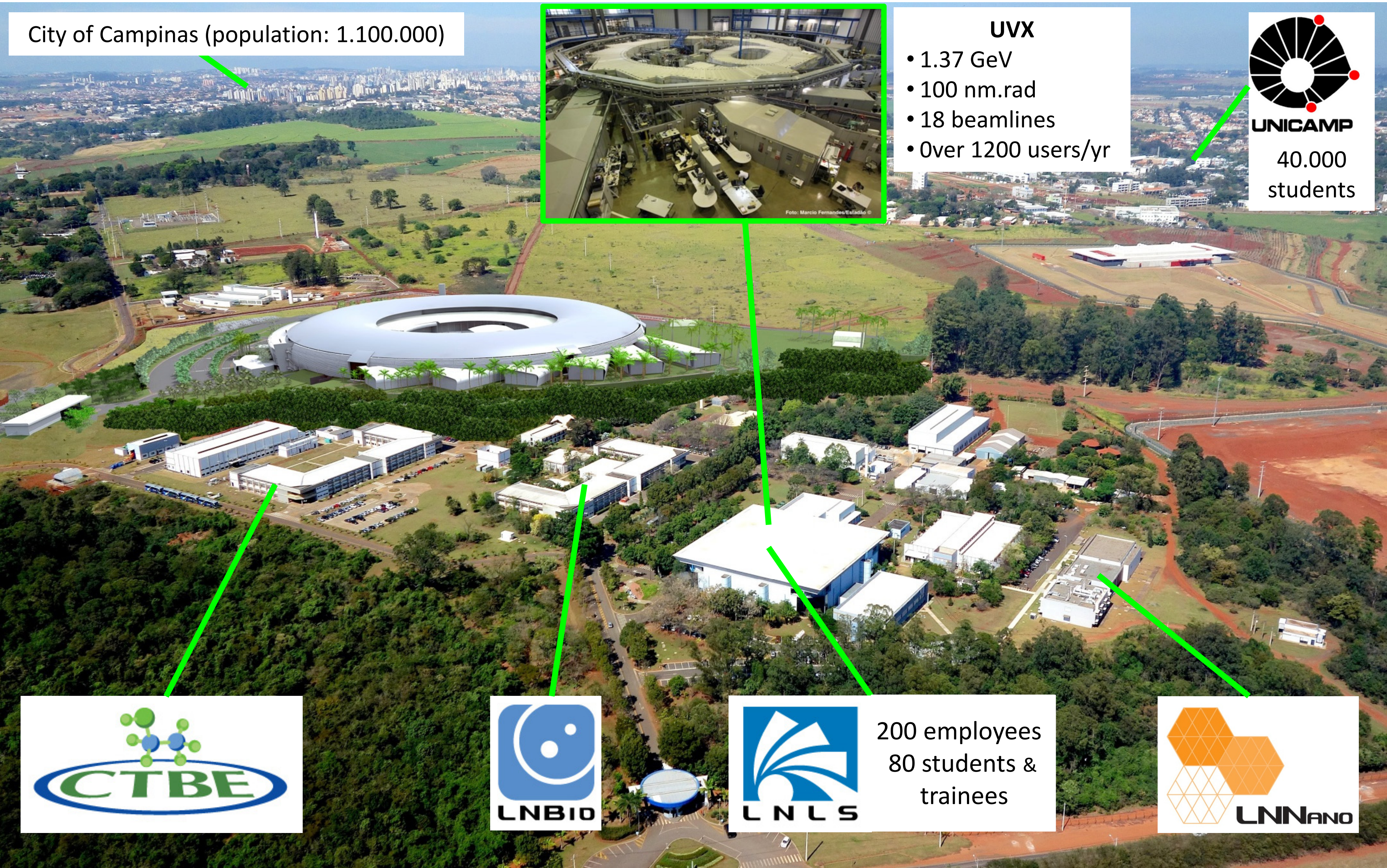

Sirius main parameters

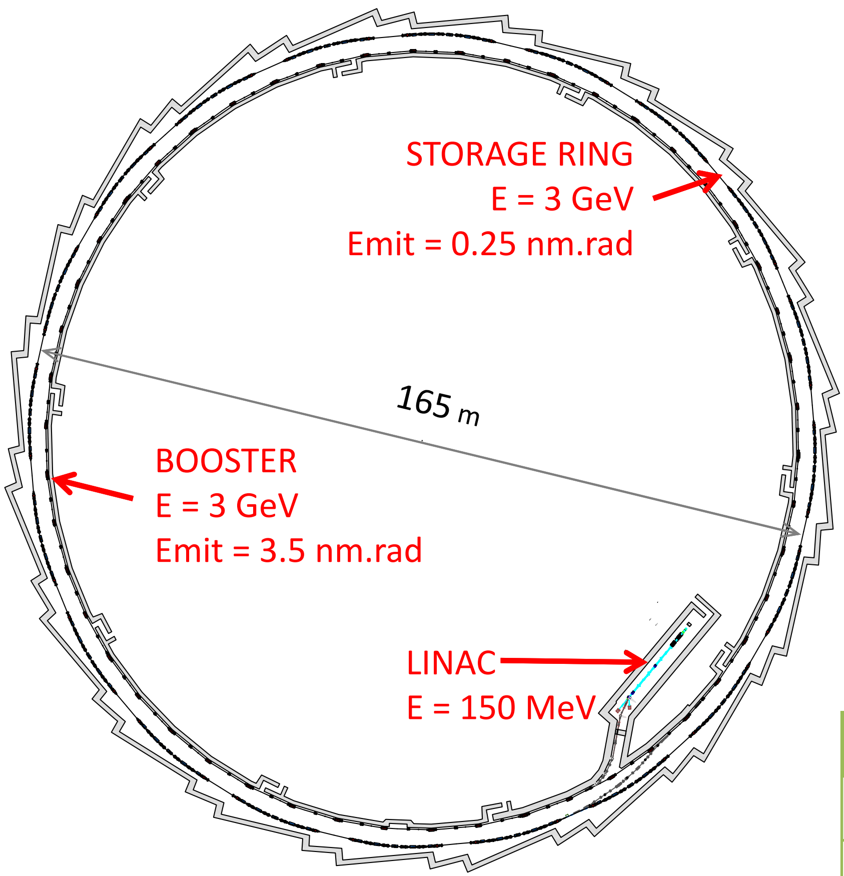

Storage Ring	
Beam energy	3.0 GeV
Circumference	518.4 m
Lattice	20 x 5BA
Hor. emittance (bare lat.)	0.25 nm.rad
Hor. emittance (with IDs)	→ 0.15 nm.rad
Betatron tunes (H/V)	49.11 / 14.17
Natural chrom. (H/V)	-119.0 / -81.2
rms energy spread	0.85×10^{-3}
Energy loss/turn (dipoles)	473 keV
Dam. times (H/V/L) [ms]	16.9 / 22.0 / 12.9
Nominal current, top up	350 mA

Booster	
Circumference	496.8 m
Emittance @ 3 GeV	3.5 nm.rad
Lattice	50 Bend
Cycling frequency	2 Hz

The Sirius 5BA magnet lattice

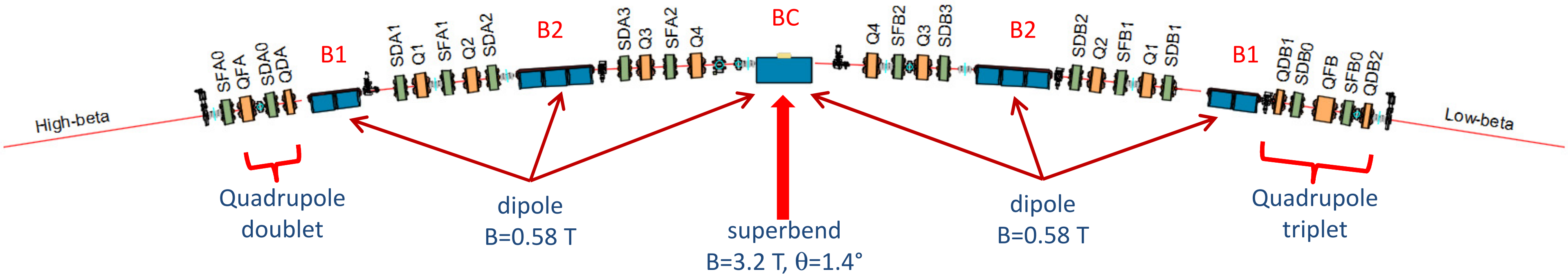

The Sirius 5BA magnet lattice

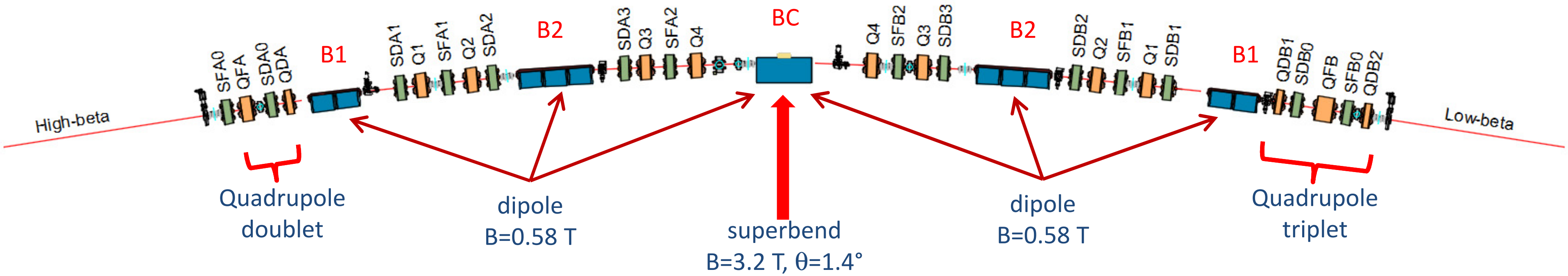

- 20 - 5BA arcs and 2 types of straight sections for insertion devices:
  - 5 **high β_x** straight sections of **7.0 m** – matching with quad **doublets**.
  - 15 **low β_x** straight sections of **6.0 m** – matching with quad **triplets**.

The Sirius 5BA magnet lattice

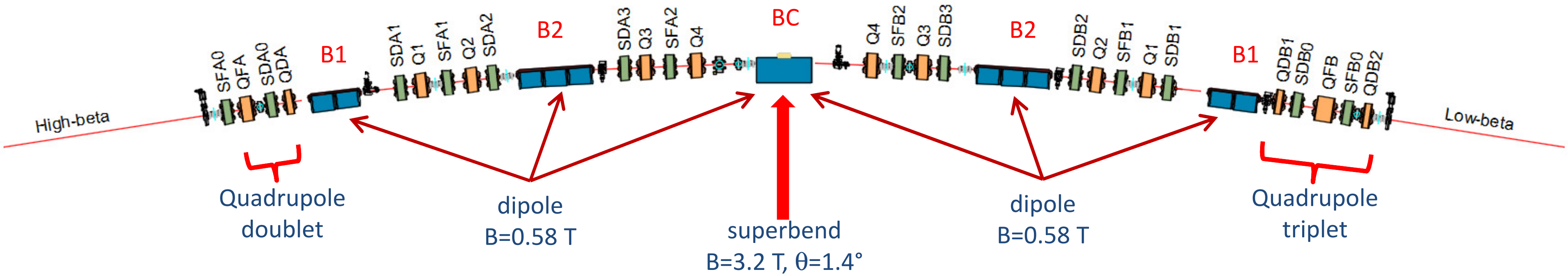

- 20 - 5BA arcs and 2 types of straight sections for insertion devices:
  - 5 **high β_x** straight sections of **7.0 m** – matching with quad **doublets**.
  - 15 **low β_x** straight sections of **6.0 m** – matching with quad **triplets**.
- 20 PM longitudinal gradient superbends
  - sharp peak field of B_p= 3.2 T in the center → critical photon energy of e_c = 19.2 keV

The Sirius 5BA magnet lattice

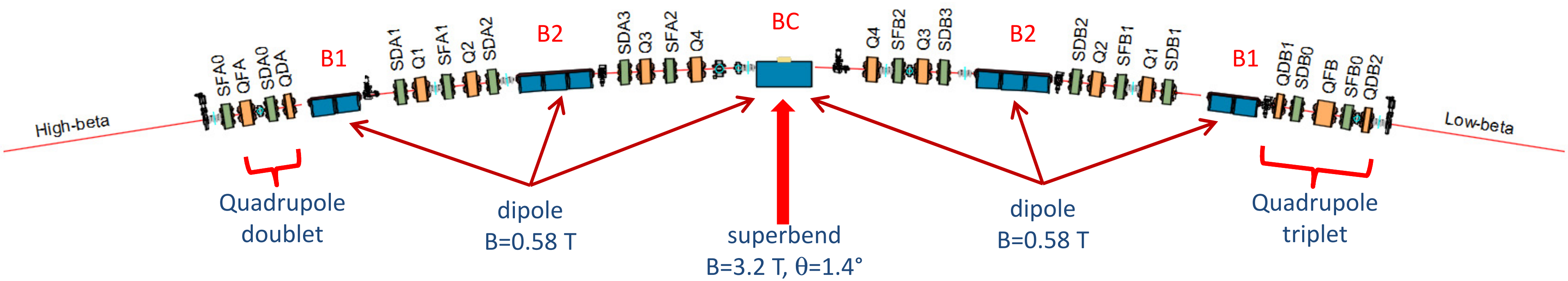

- 20 - 5BA arcs and 2 types of straight sections for insertion devices:
  - 5 **high β_x** straight sections of **7.0 m** – matching with quad **doublets**.
  - 15 **low β_x** straight sections of **6.0 m** – matching with quad **triplets**.
- 20 PM longitudinal gradient superbends
  - sharp peak field of B_p= 3.2 T in the center → critical photon energy of e_c = 19.2 keV
- Low field (0.58 T) EM and PM dipoles with transverse field gradient (7.8 T/m)

The Sirius 5BA magnet lattice

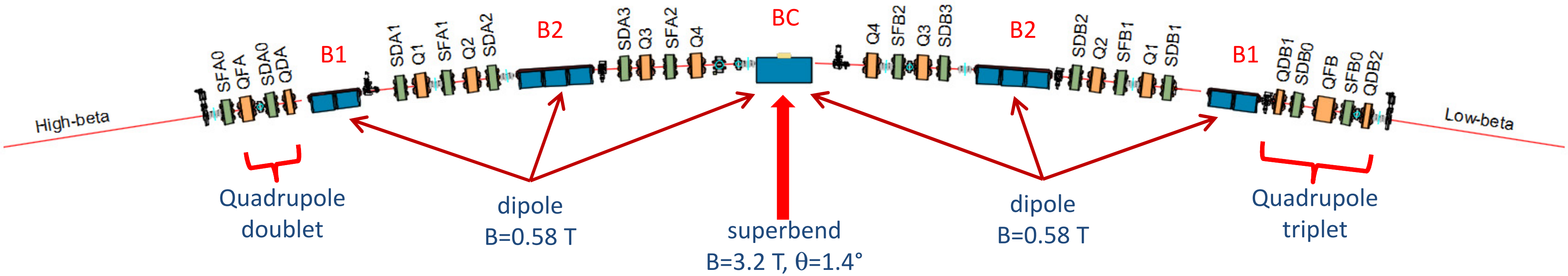

- 20 - 5BA arcs and 2 types of straight sections for insertion devices:
  - 5 **high β_x** straight sections of **7.0 m** – matching with quad **doublets**.
  - 15 **low β_x** straight sections of **6.0 m** – matching with quad **triplets**.
- 20 PM longitudinal gradient superbends
  - sharp peak field of B_p= 3.2 T in the center → critical photon energy of e_c = 19.2 keV
- Low field (0.58 T) EM and PM dipoles with transverse field gradient (7.8 T/m)
- 13 quadrupoles/cell, 14 sextupoles/cell, no octupoles

The Sirius 5BA magnet lattice

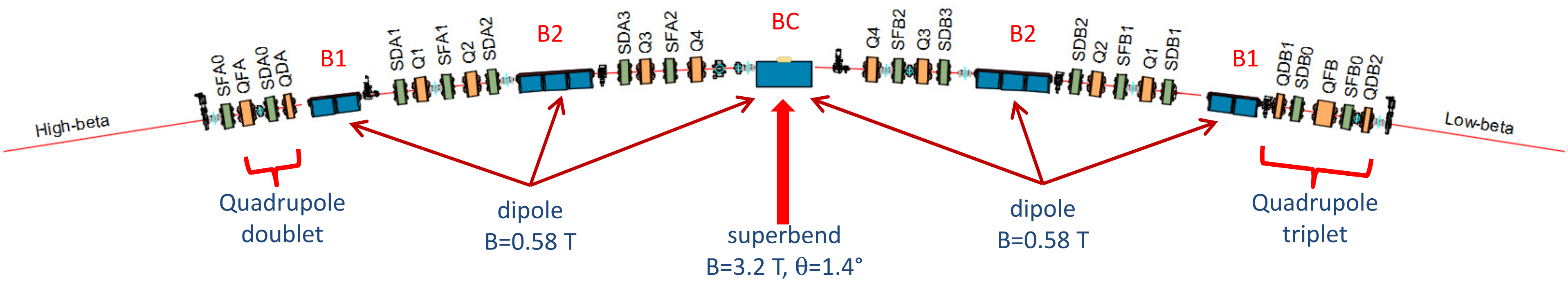

- 20 - 5BA arcs and 2 types of straight sections for insertion devices:
  - 5 **high β_x** straight sections of **7.0 m** – matching with quad **doublets**.
  - 15 low β_x straight sections of **6.0 m** – matching with quad **triplets**.
- 20 PM longitudinal gradient superbends
  - sharp peak field of B_p= 3.2 T in the center → critical photon energy of e_c = 19.2 keV
- Low field (0.58 T) EM and PM dipoles with transverse field gradient (7.8 T/m)
- 13 quadrupoles/cell, 14 sextupoles/cell, no octupoles
- Different lengths for B1 and B2 (but same unit block)

The Sirius 5BA magnet lattice

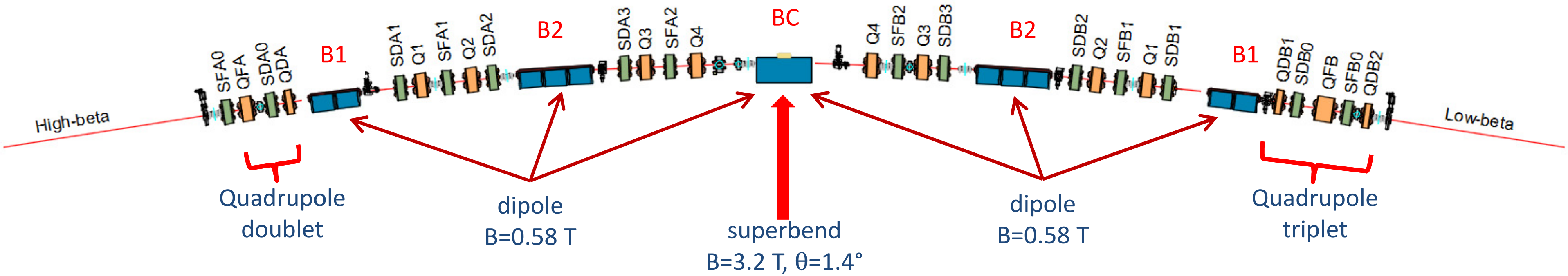

- 20 - 5BA arcs and 2 types of straight sections for insertion devices:
  - 5 **high β_x** straight sections of **7.0 m** – matching with quad **doublets**.
  - 15 low β_x straight sections of **6.0 m** – matching with quad **triplets**.
- 20 PM longitudinal gradient superbends
  - sharp peak field of B_p= 3.2 T in the center → critical photon energy of e_c = 19.2 keV
- Low field (0.58 T) EM and PM dipoles with transverse field gradient (7.8 T/m)
- 13 quadrupoles/cell, 14 sextupoles/cell, no octupoles
- Different lengths for B1 and B2 (but same unit block)
- NEG coated copper beam pipe ∅ = 24 mm (internal)

Superbends (no wigglers allowed)

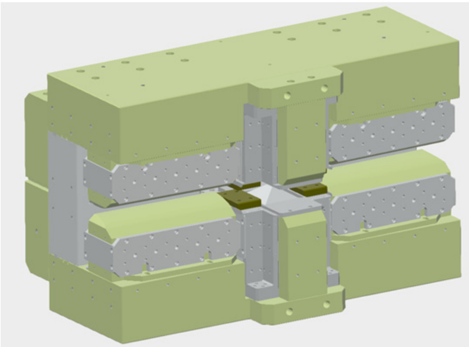

Permanent magnet (NdFeB)

High field insert (3.2 T) superbend

- 19 keV critical energy at peak
- Hard X-rays produced only at beamline exit
- Total energy loss/turn from dipoles = 473 keV

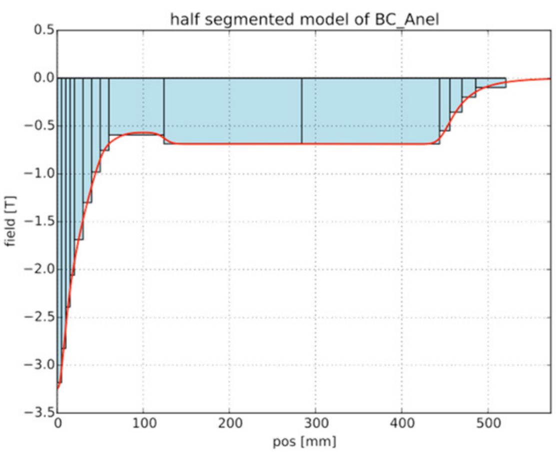

Superbends (no wigglers allowed)

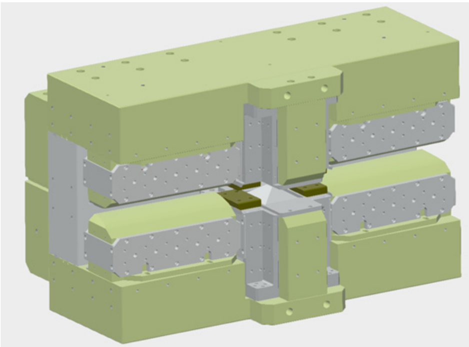

Permanent magnet (NdFeB)

High field insert (3.2 T) superbend

- 19 keV critical energy at peak
- Hard X-rays produced only at beamline exit
- Total energy loss/turn from dipoles = 473 keV

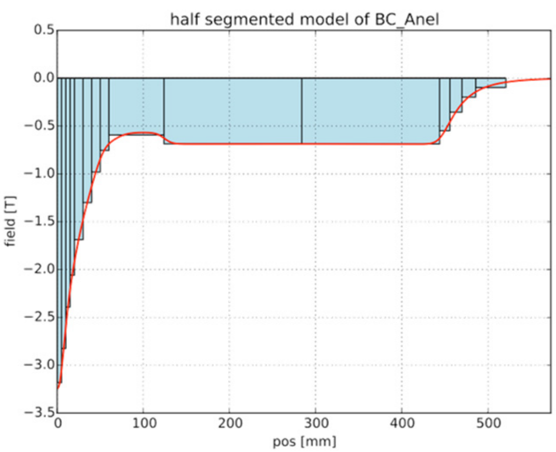

From SRW:

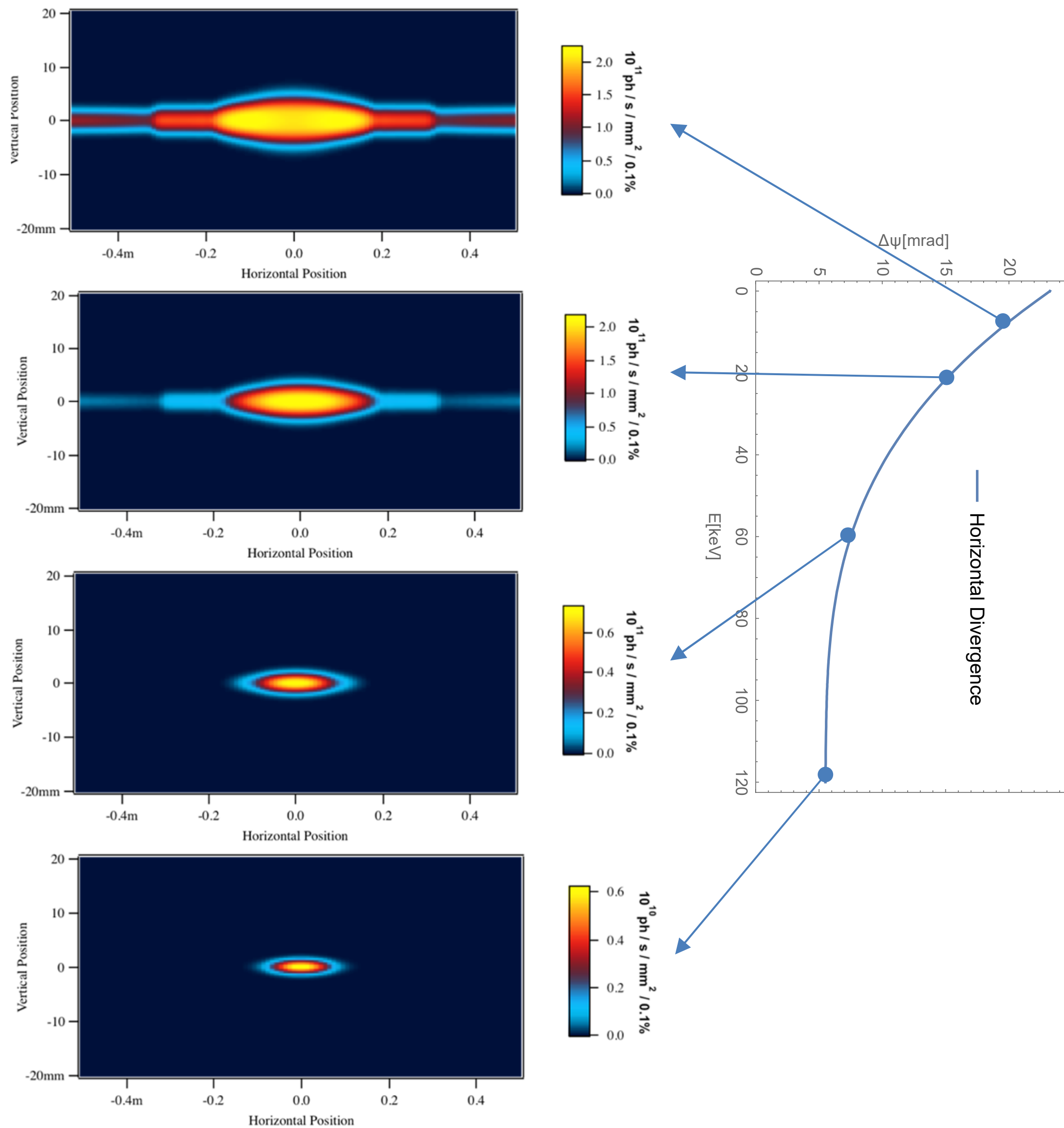

Sirius optics

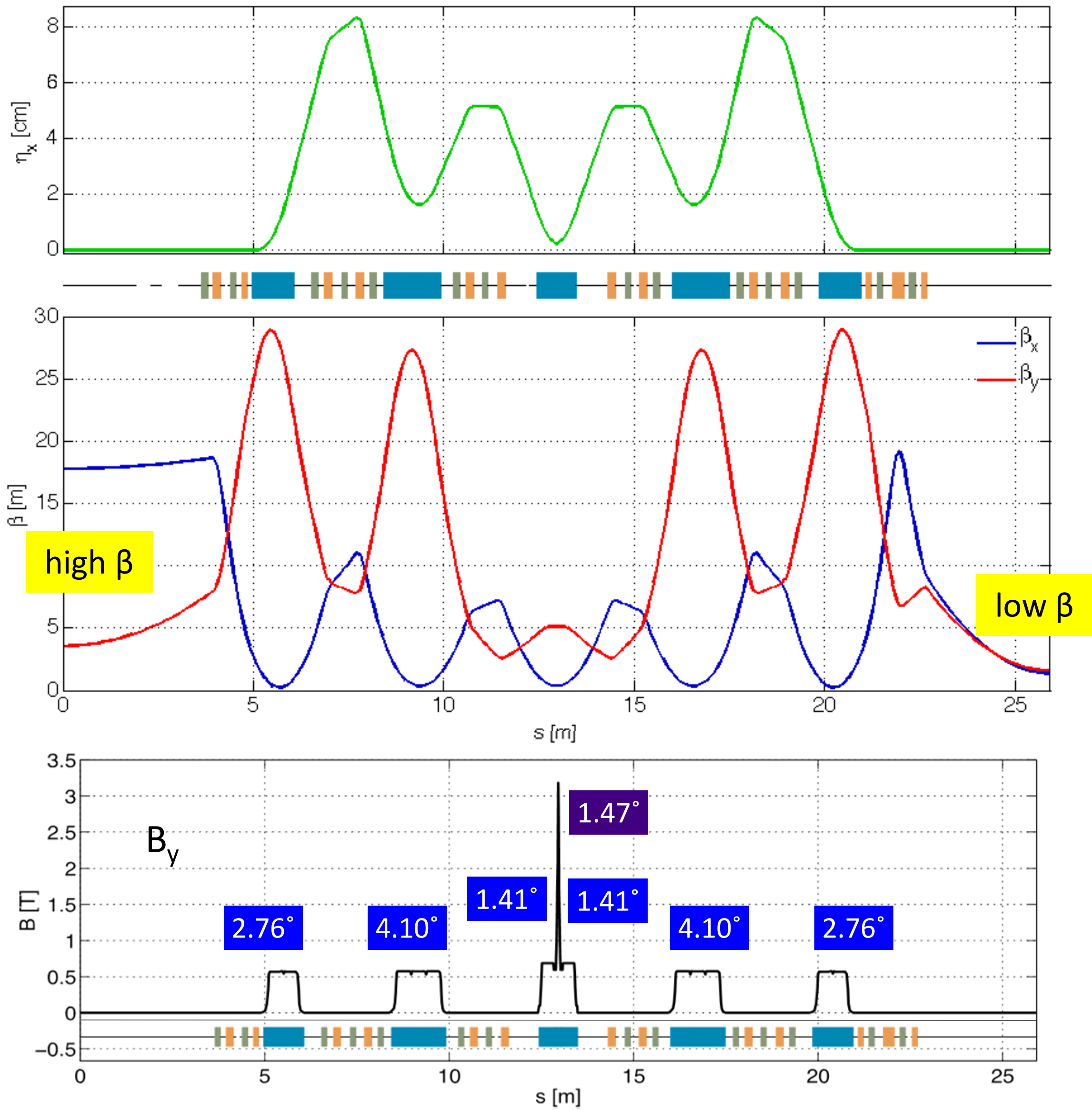

- 5-fold symmetric optics with 5 high and 15 low β sections.
- Achromatic cells.
- At low β sections
  - $\beta_x \approx \beta_y \approx 1.5$ m
  - Optimized electron and photon beam phase-space matching for undulators.
- At superbend
  - Strong focusing of dispersion and β_x functions
  - Beam size: 9.6 x 3.6 μm^2

Sirius optics

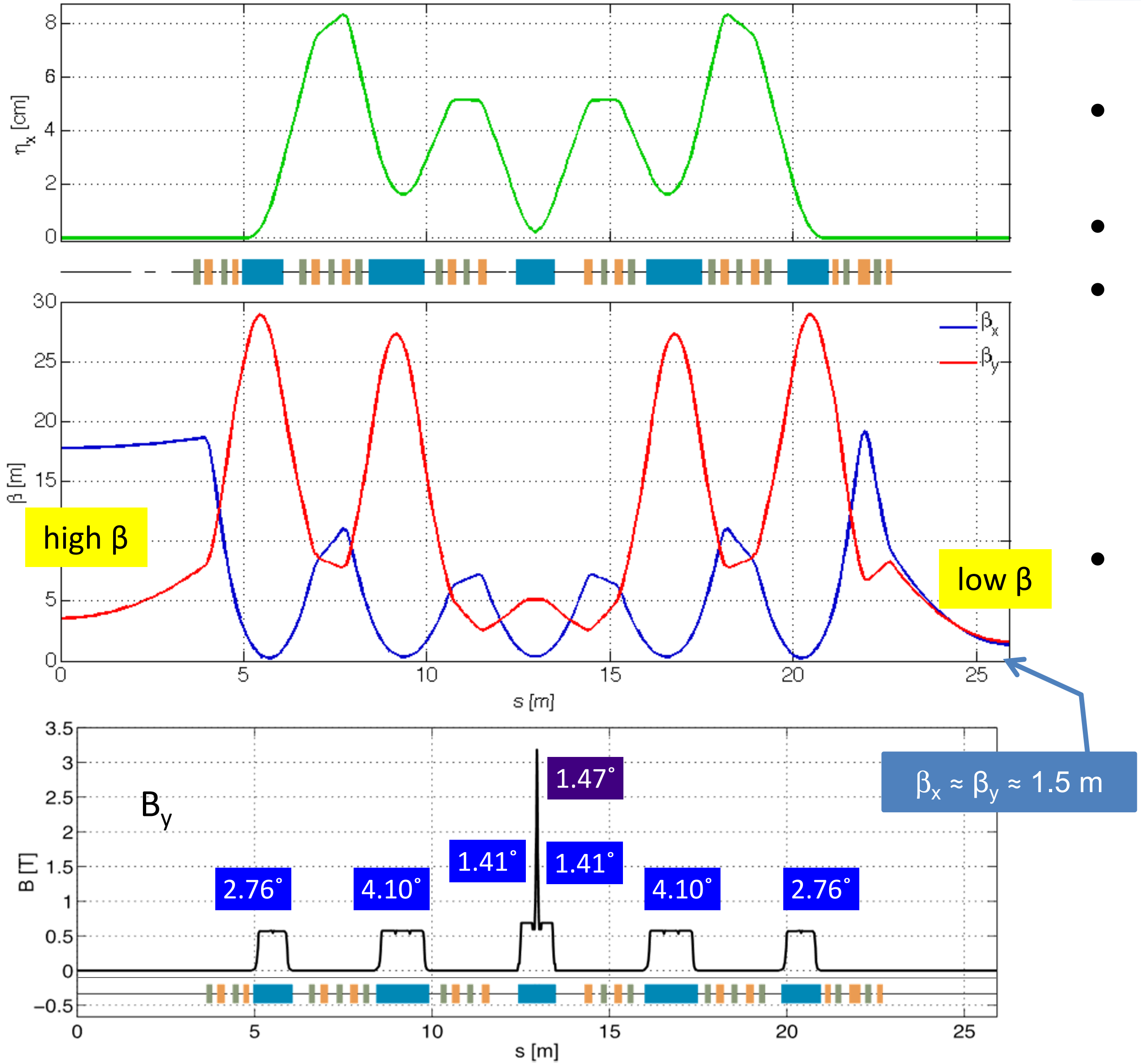

- 5-fold symmetric optics with 5 high and 15 low β sections.
- Achromatic cells.
- At low β sections
  - $\beta_x \approx \beta_y \approx 1.5$ m
  - Optimized electron and photon beam phase-space matching for undulators.
- At superbend
  - Strong focusing of dispersion and β_x functions
  - Beam size: 9.6 x 3.6 μm^2

Sirius optics

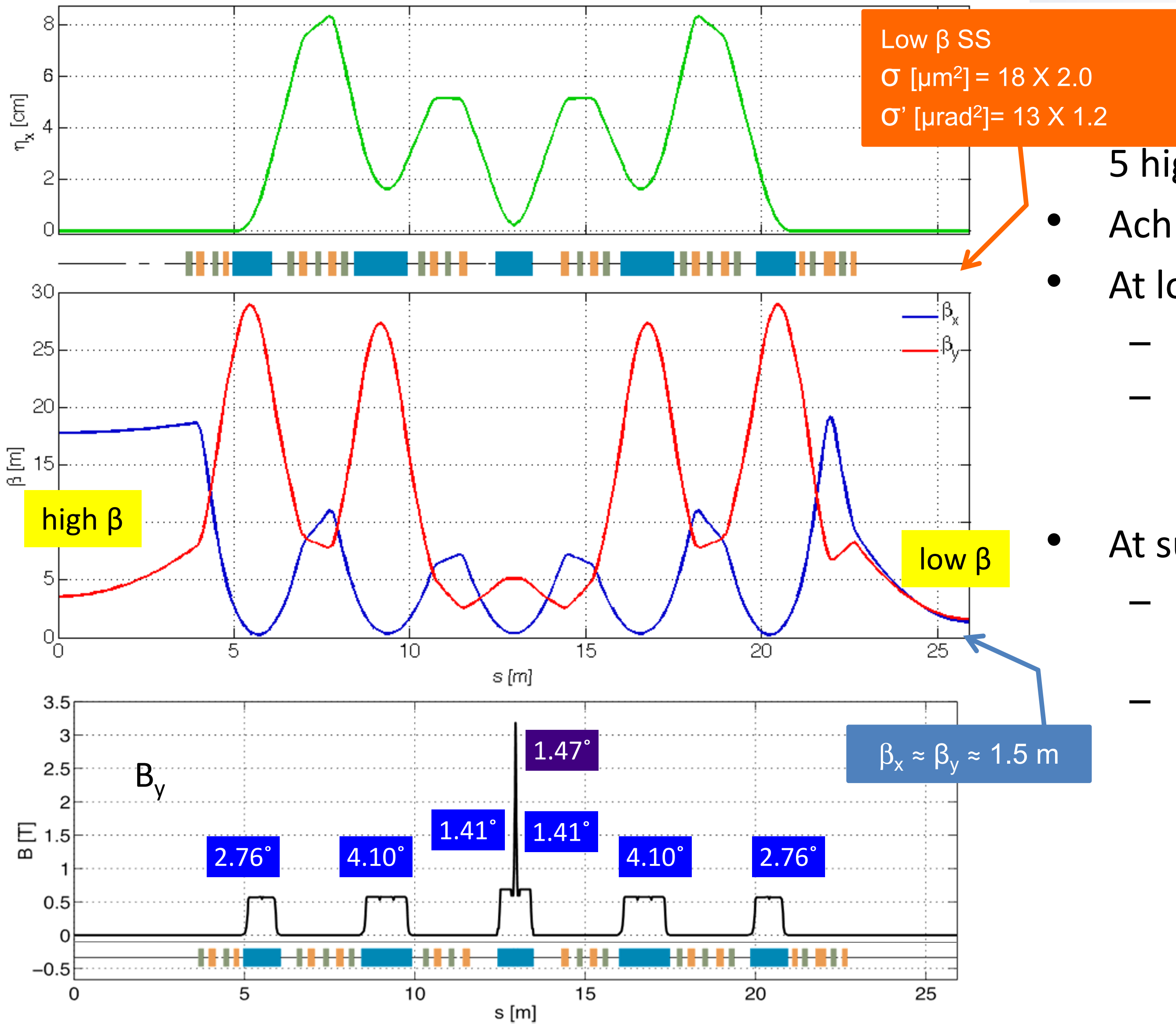

- …d symmetric optics with 5 high and 15 low β sections.
- Achromatic cells.
- At low β sections
  - $\beta_x \approx \beta_y \approx 1.5$ m
  - Optimized electron and photon beam phase-space matching for undulators.
- At superbend
  - Strong focusing of dispersion and β_x functions
  - Beam size: 9.6 x 3.6 μm^2

Sirius optics

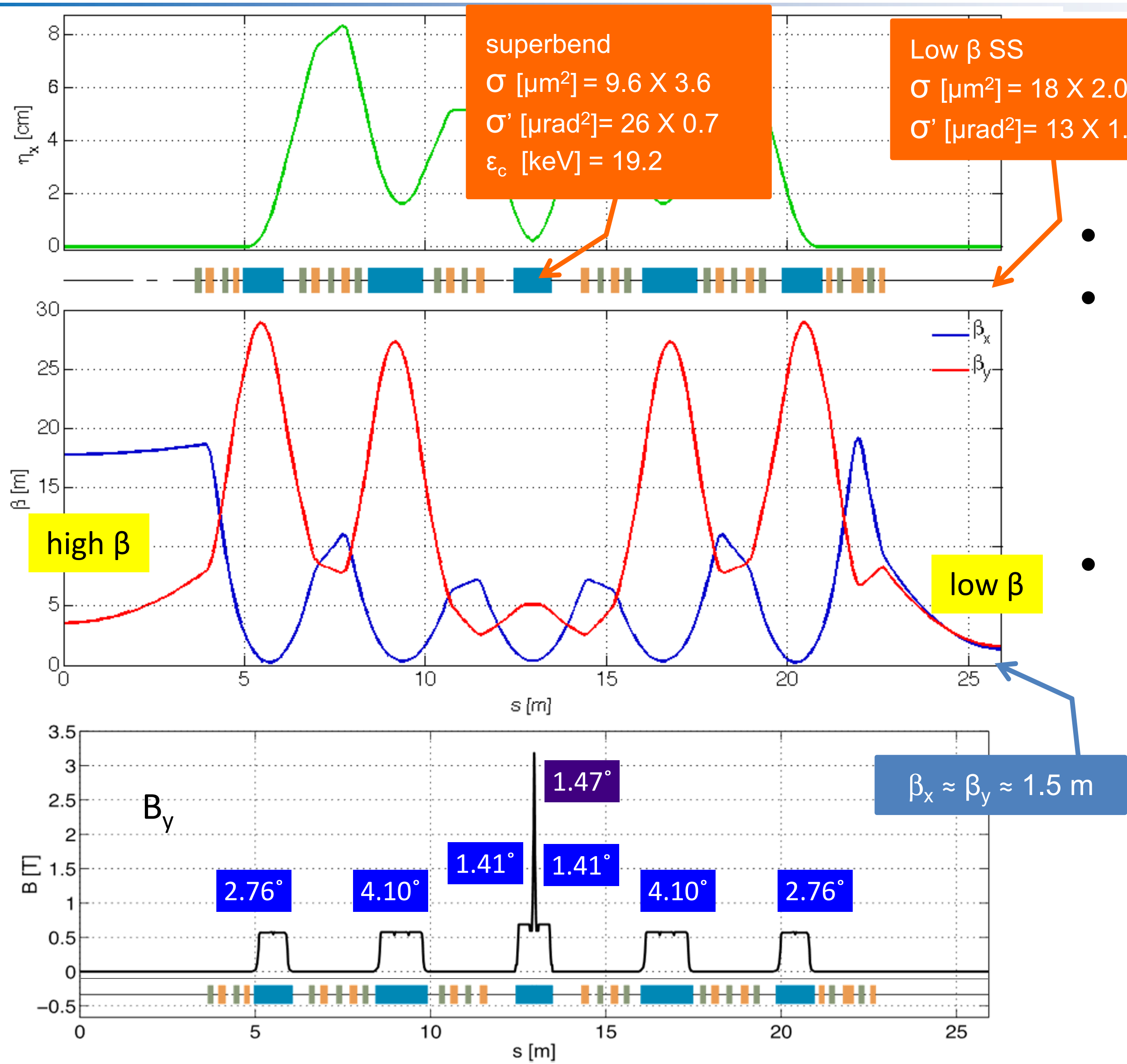

...d symmetric optics with 5 high and 15 low β sections.

- Achromatic cells.
- At low β sections
  - $\beta_x \approx \beta_y \approx 1.5$ m
  - Optimized electron and photon beam phase-space matching for undulators.
- At superbend
  - Strong focusing of dispersion and β_x functions
  - Beam size: 9.6 x 3.6 μm^2

Sirius optics

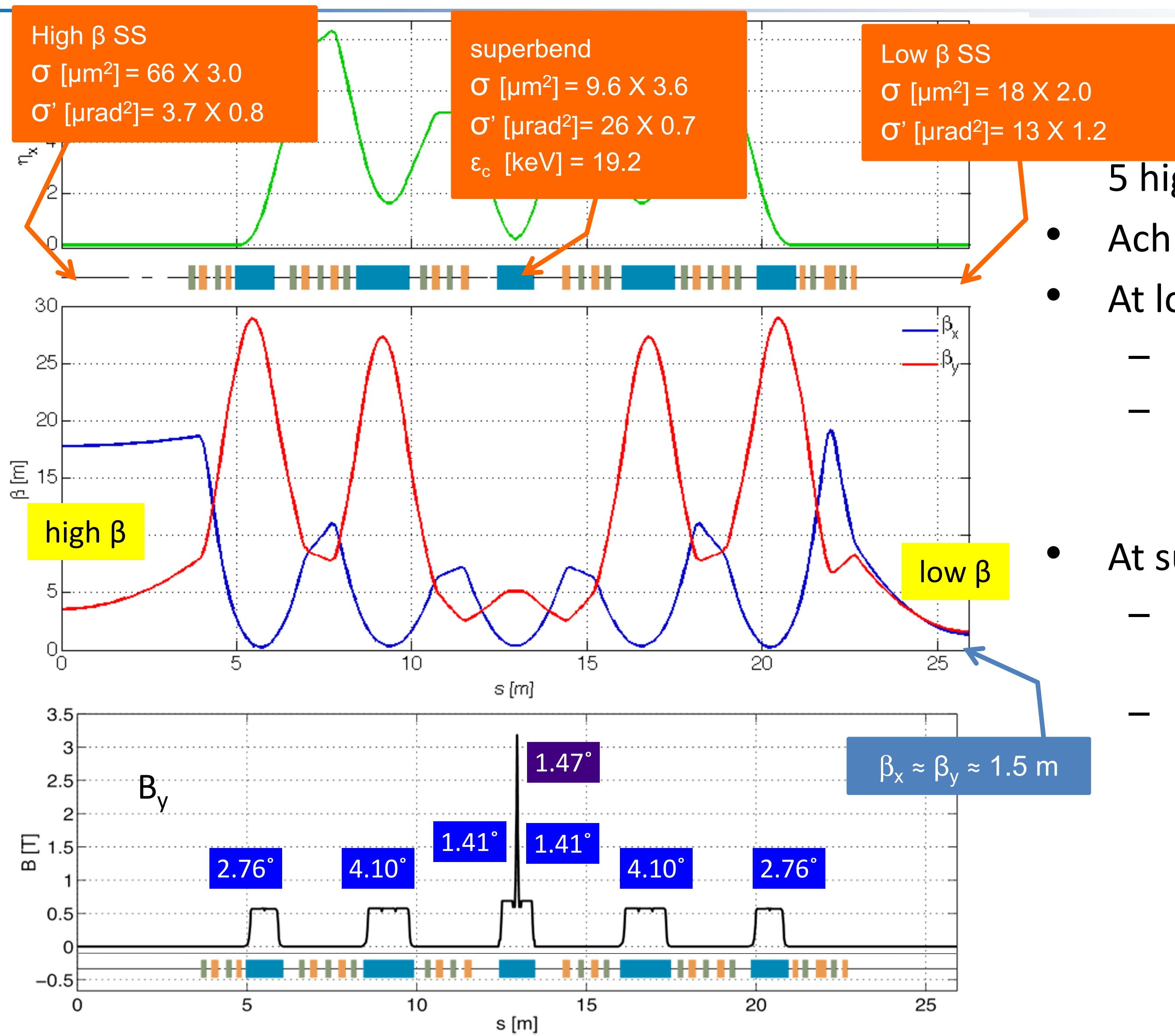

- …d symmetric optics with 5 high and 15 low β sections.
- Achromatic cells.
- At low β sections
  - $\beta_x \approx \beta_y \approx 1.5$ m
  - Optimized electron and photon beam phase-space matching for undulators.
- At superbend
  - Strong focusing of dispersion and β_x functions
  - Beam size: 9.6 x 3.6 μm^2

New low β_x operation mode

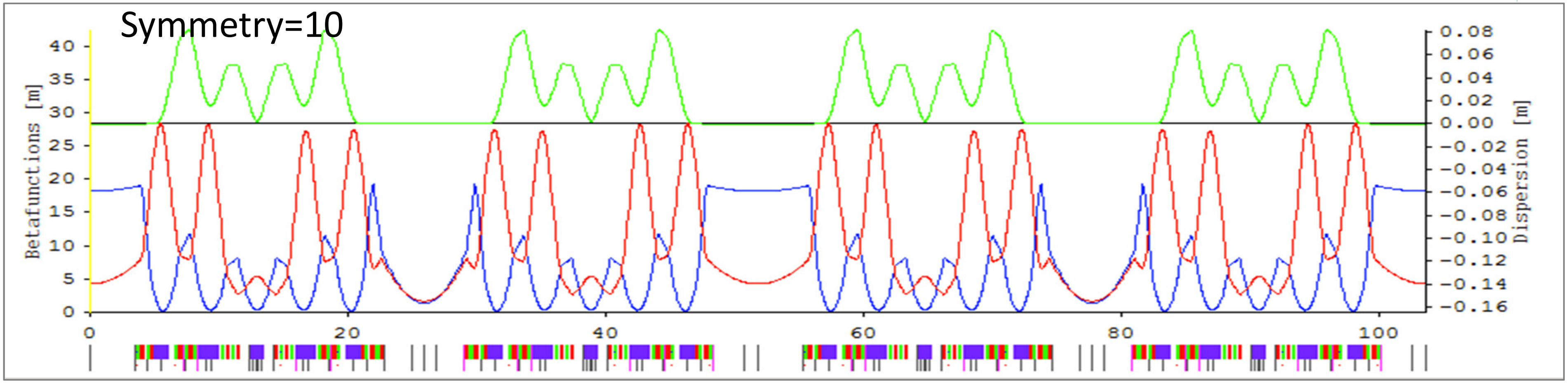

New low β_x operation mode

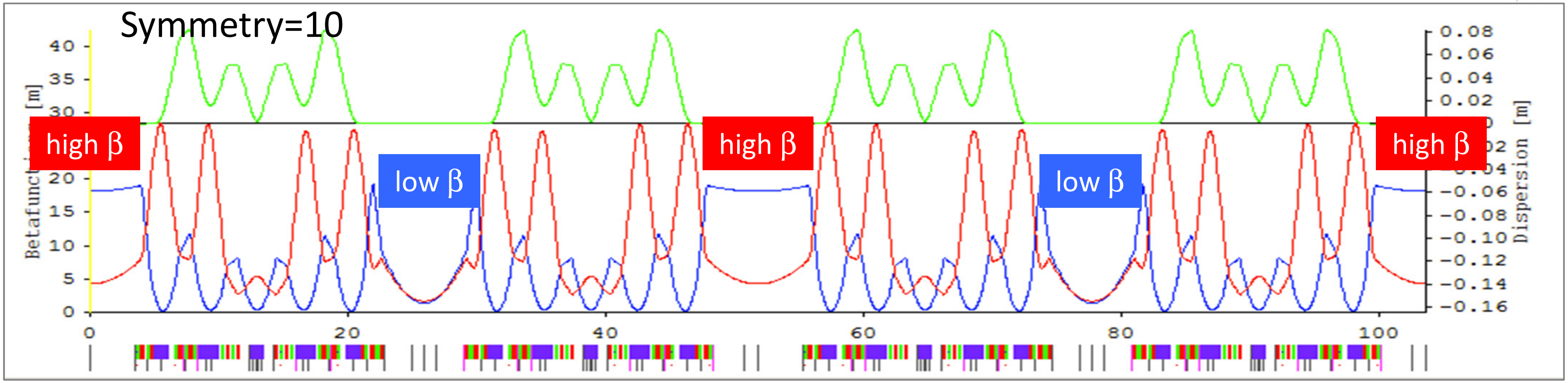

New low β_x operation mode

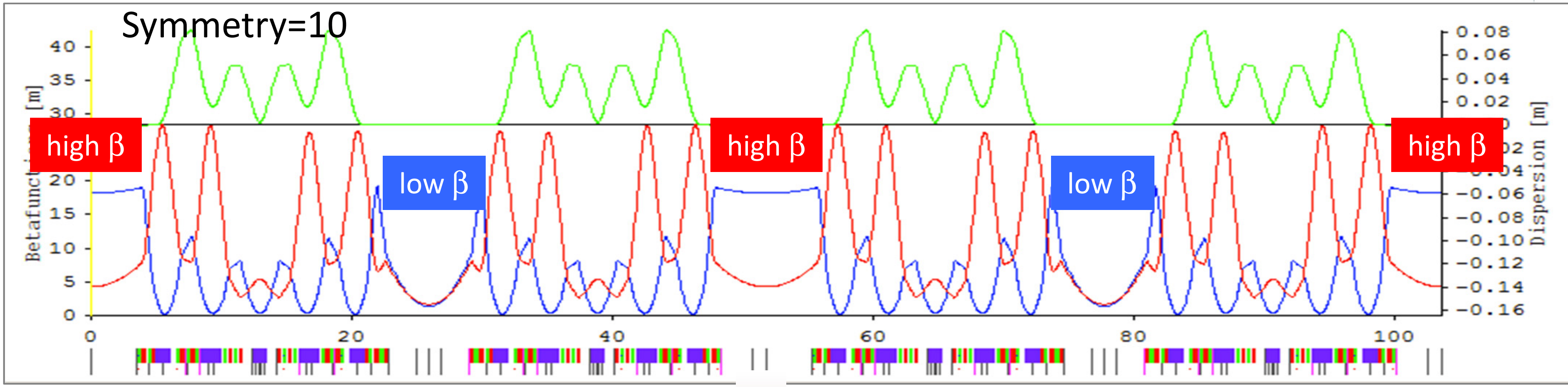

New low β_x operation mode

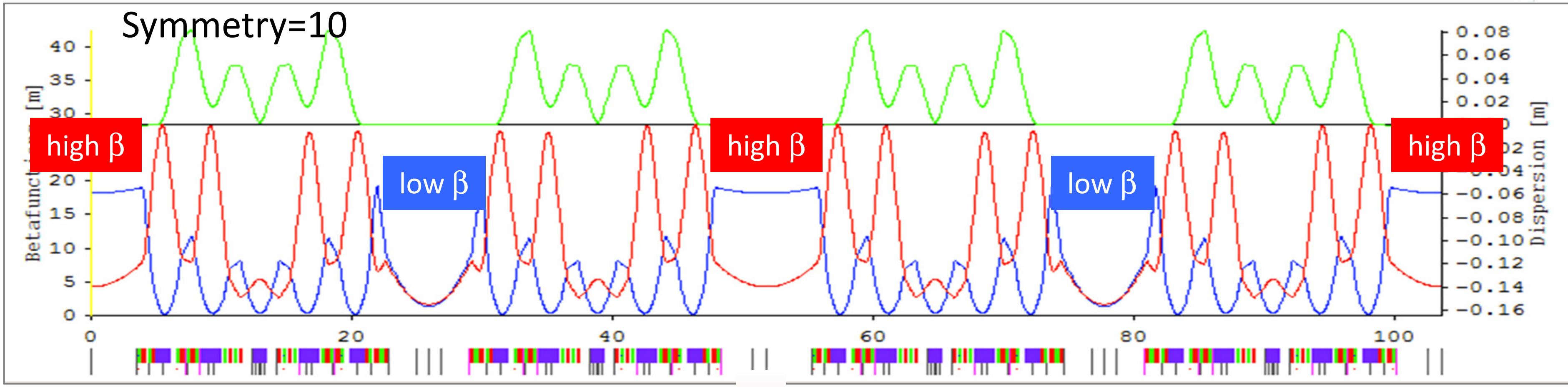

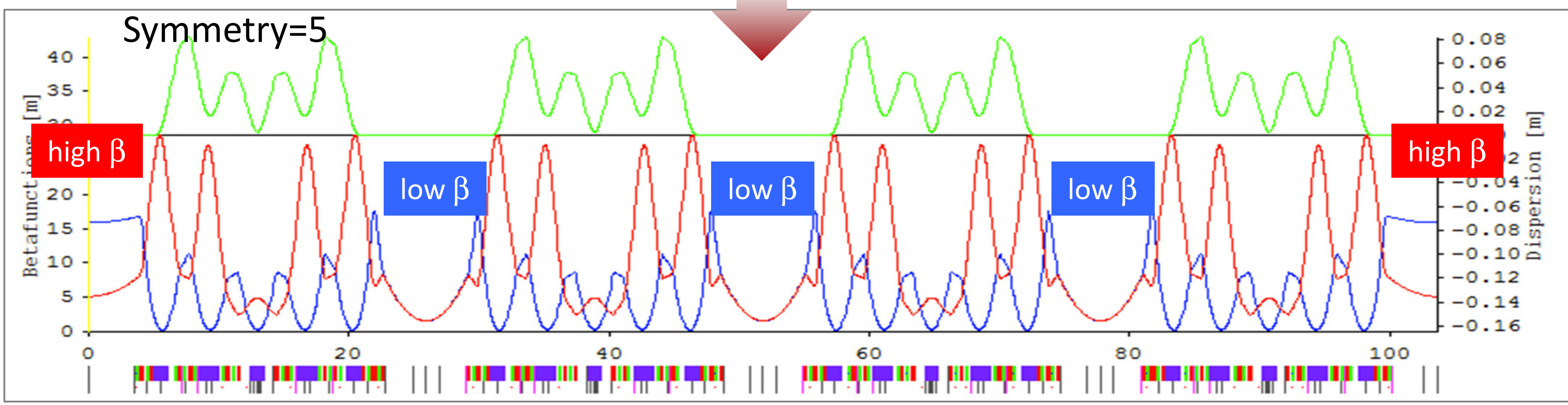

Symmetry 5: 5 high β_x + 15 low β_x

Low β optics: phase-space matching

Courtesy: Harry Westfahl Jr

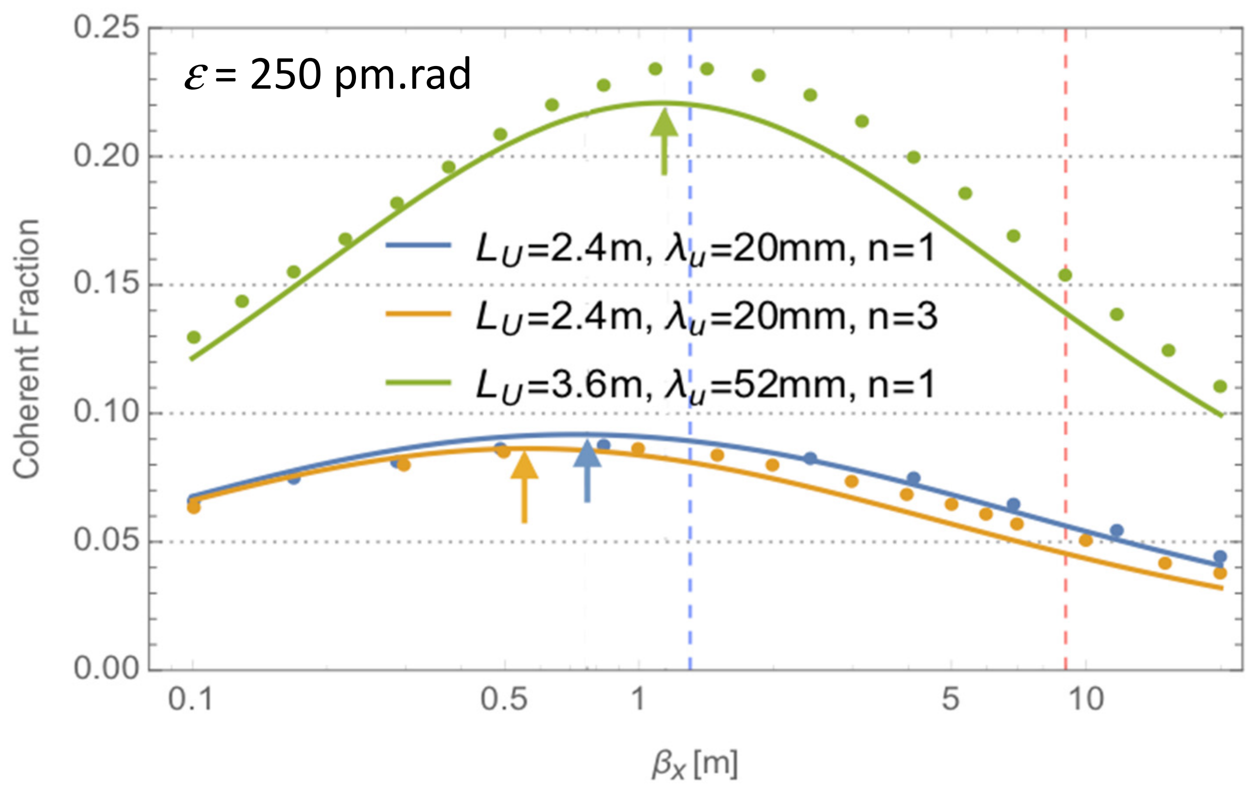

• • • • Numerical integration of Wigner Distribution Function

—— Gaussian approximation of reference [H. Westfahl Jr *et al*, *JSR*, 24, 2017]

Low β optics: phase-space matching

Courtesy: Harry Westfahl Jr

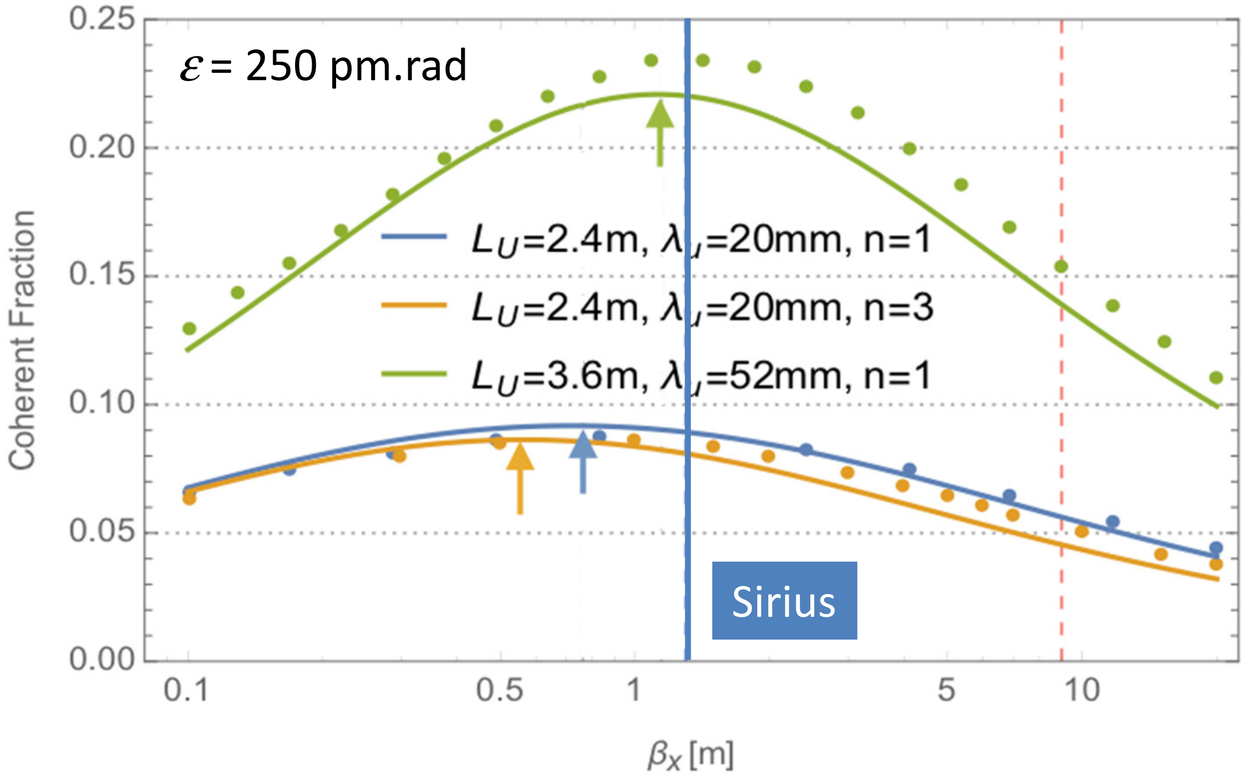

• • • • Numerical integration of Wigner Distribution Function

—— Gaussian approximation of reference [H. Westfahl Jr *et al*, *JSR*, 24, 2017]

Low β optics: phase-space matching

Courtesy: Harry Westfahl Jr

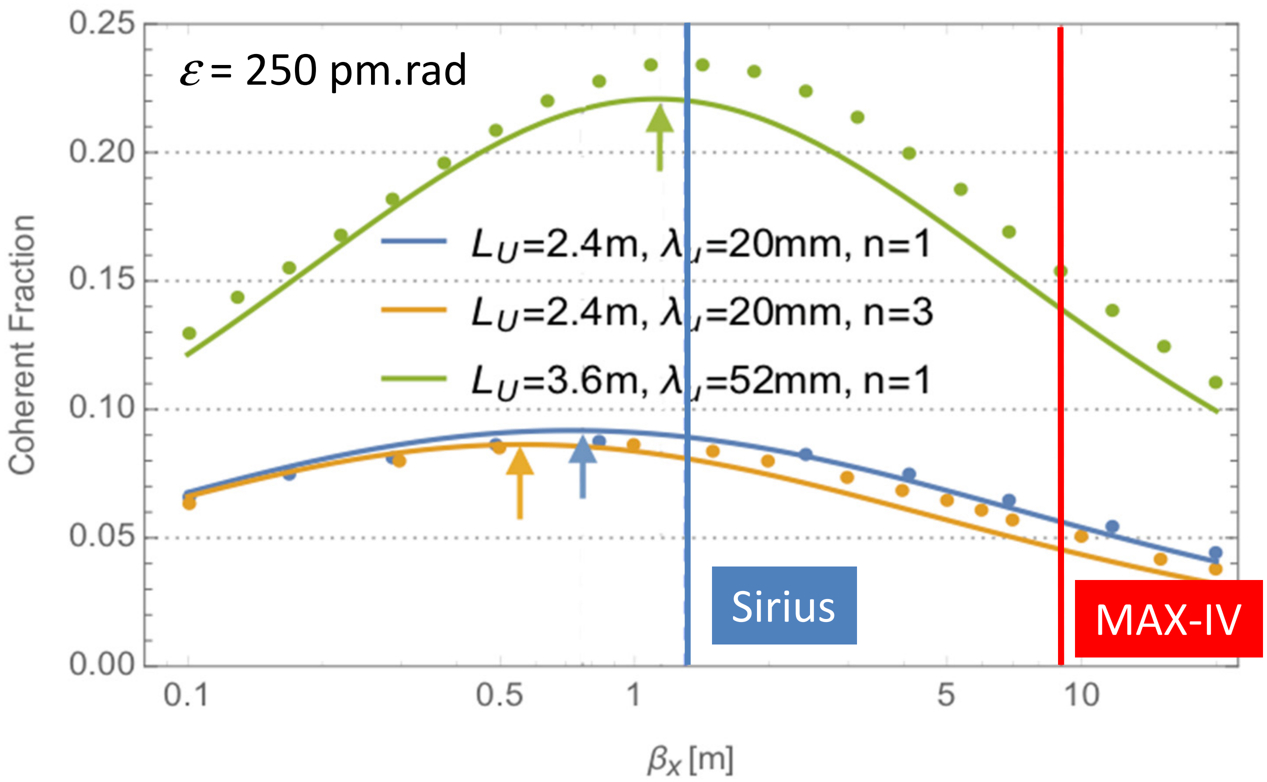

• • • • Numerical integration of Wigner Distribution Function

——— Gaussian approximation of reference [H. Westfahl Jr *et al*, *JSR*, 24, 2017]

Low β optics: Beam Stay-Clear

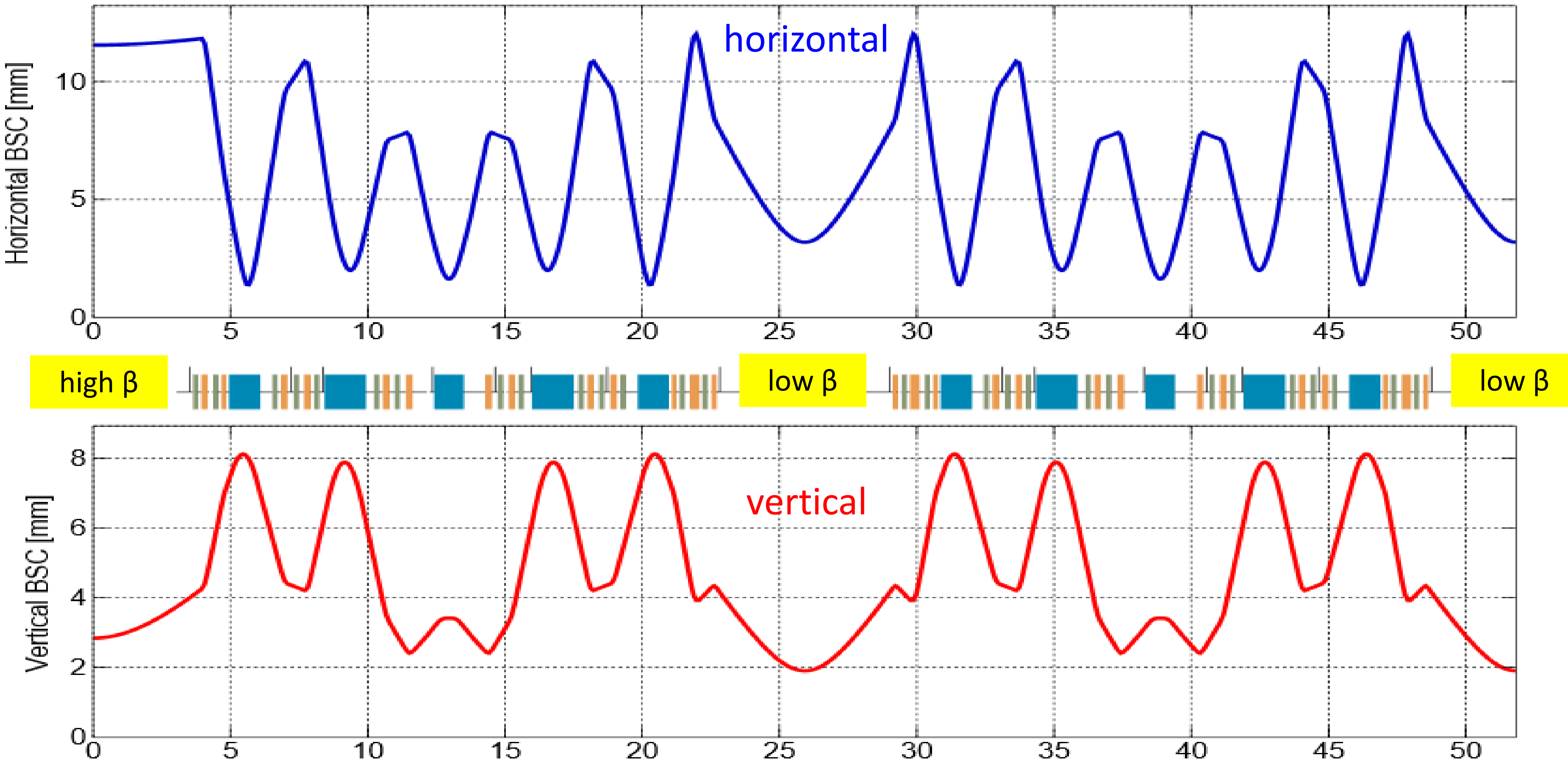

Low β optics: Beam Stay-Clear

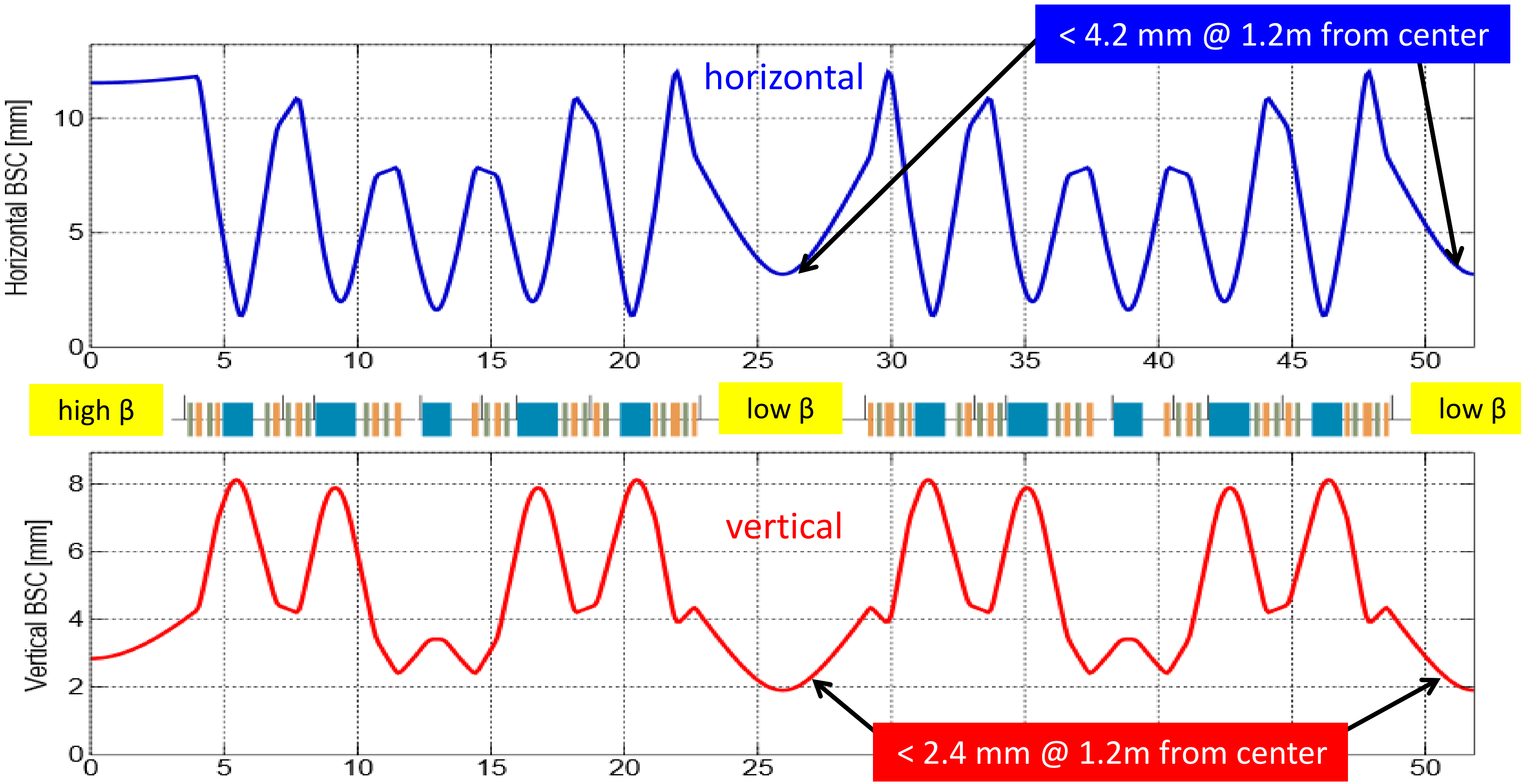

Low β optics: Beam Stay-Clear

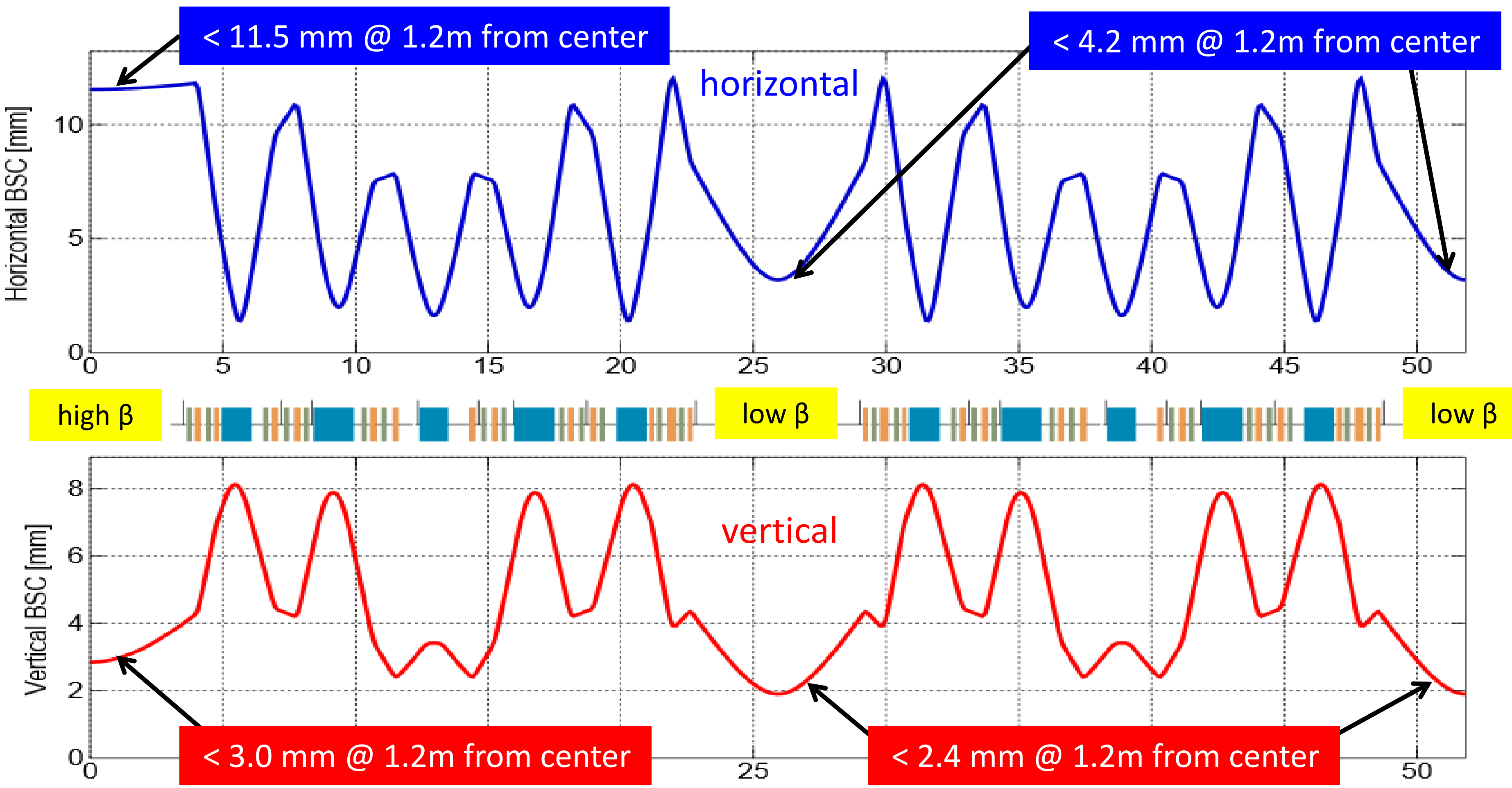

Low β optics: Beam Stay-Clear

Sirius IDs will be based on Delta and APU undulators.

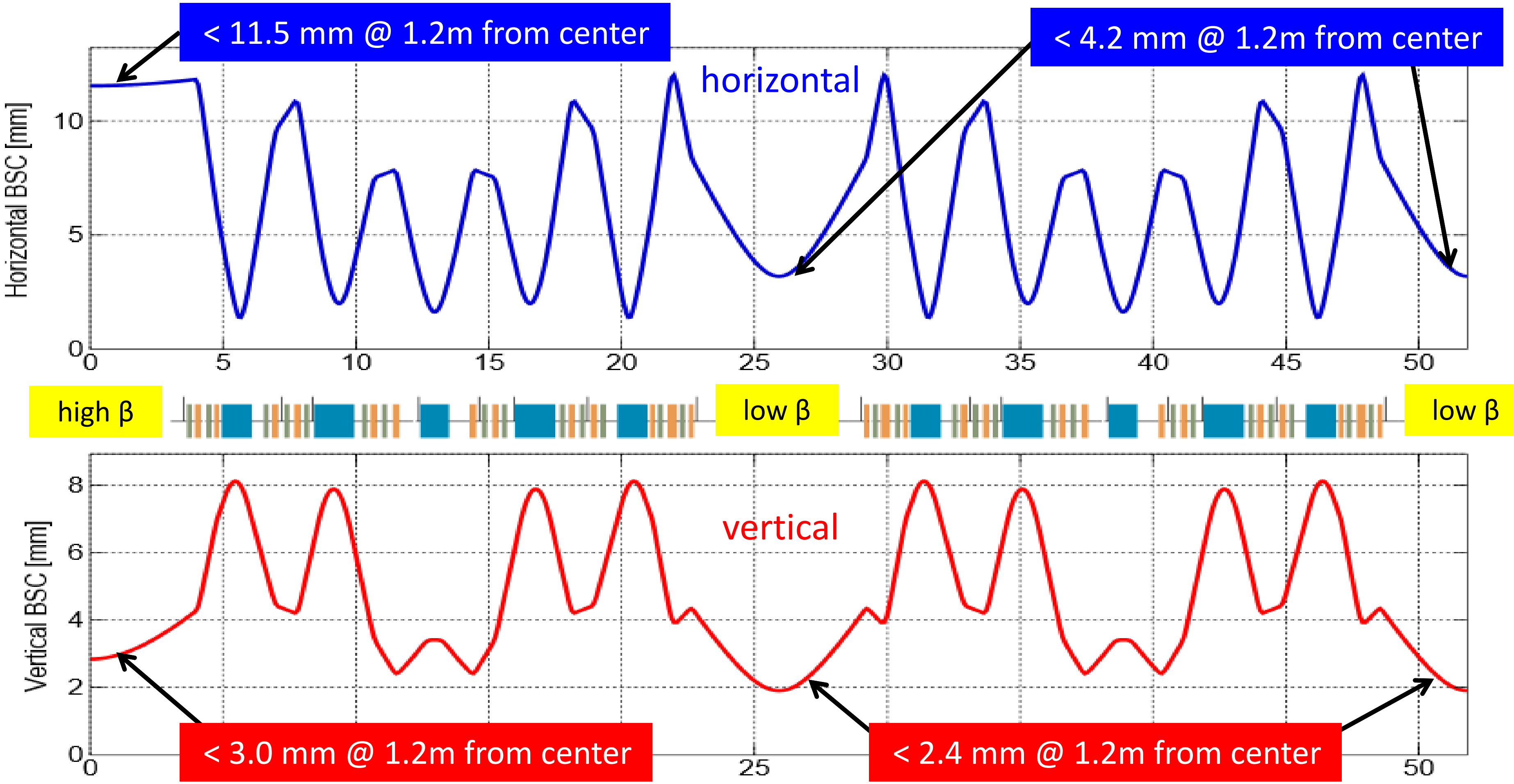

Low β optics: Insertion Devices

- Delta Undulators
  - Possible for Sirius due to small Hor. BSC
  - Smoother K changes
  - Horizontal, Vertical and Circular x-ray polarizations on the same energy range
  - Do not introduce strong harmful multipoles

	B_0 [T]	λ [mm]	L [m]	K_{max}	Diag. gap [mm]
Delta21	1.12	21	2.4	2.2	7.0
Delta52	1.19	52	3.6	5.85	13.85

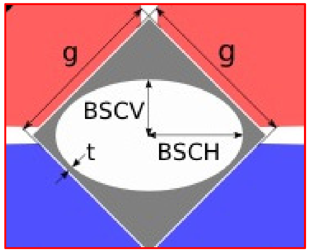

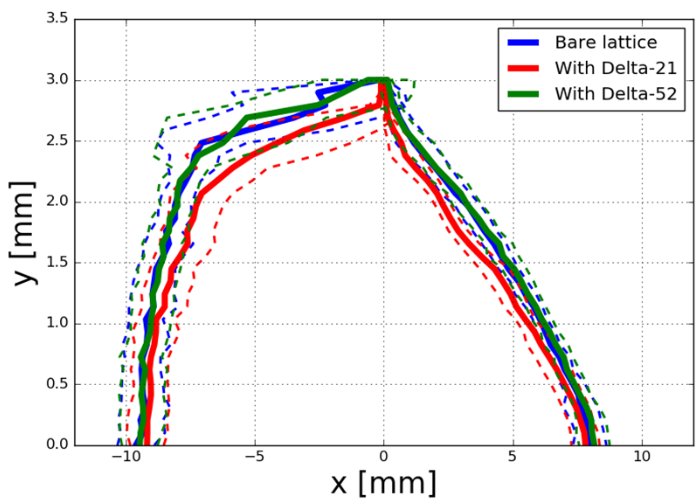

Effect of 14 Delta21 and 14 Delta52 on DA
7 in each polarization (H/V) distributed in low beta sections

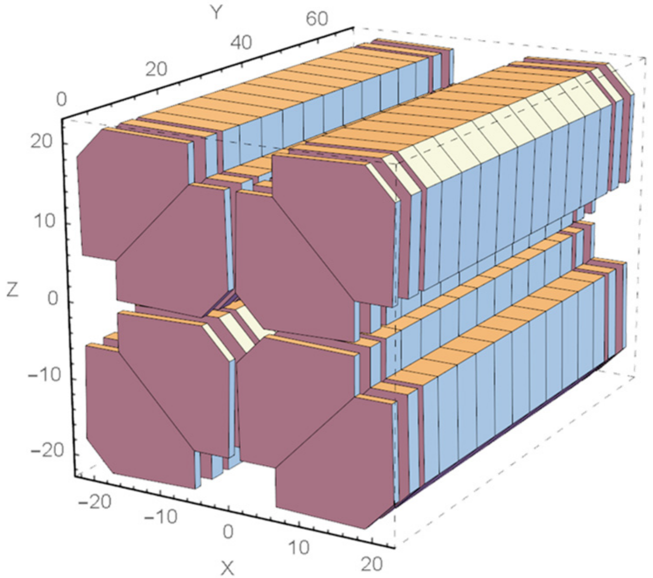

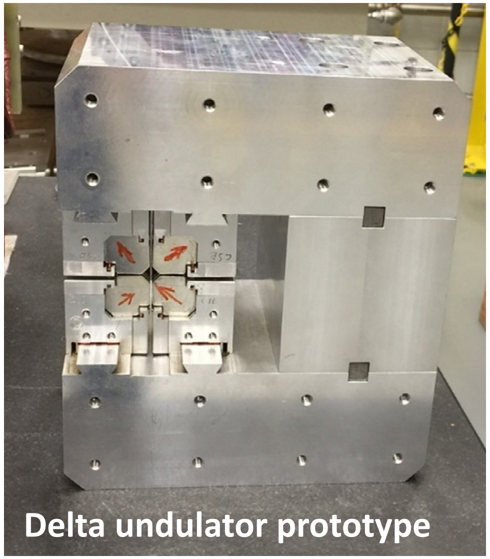

Effect of IDs on emittance and energy spread

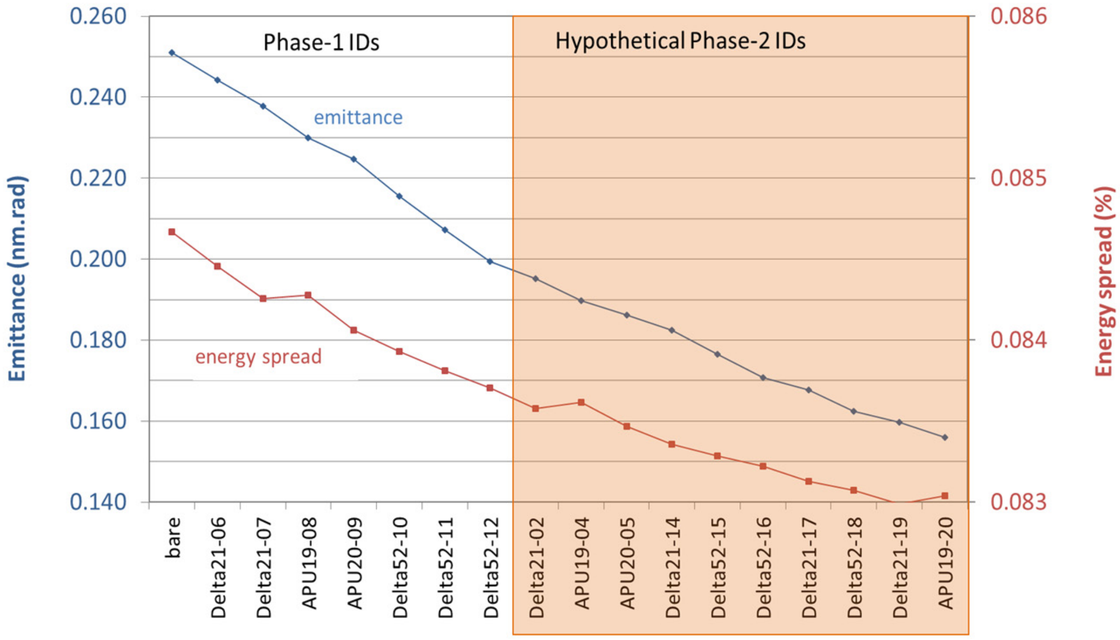

Sirius Phase-1 Beamlines

Beamline	ID Type	SS	β_x
CARNAÚBA	Delta21	06	low
EMA	APU19	08	low
CATERETÊ	Delta21	07	low
IPÊ	Delta52	11	low
SABIÁ	Delta52	10	low
MANACÁ	APU20	09	high
PGM++	Delta52	12	low

Sirius IDs

ID Type	B_0 [T]	λ [mm]	L [m]	K_{max}	gap [mm]
Delta21	1.12	21	2.4	2.2	6.92
Delta52	1.19	52	3.6	5.85	13.85
APU19	1.28	19	2.4	2.3	5.0
APU20	1.07	20	2.4	2.0	6.2

Sirius: initial phase beamlines (2019-2020)

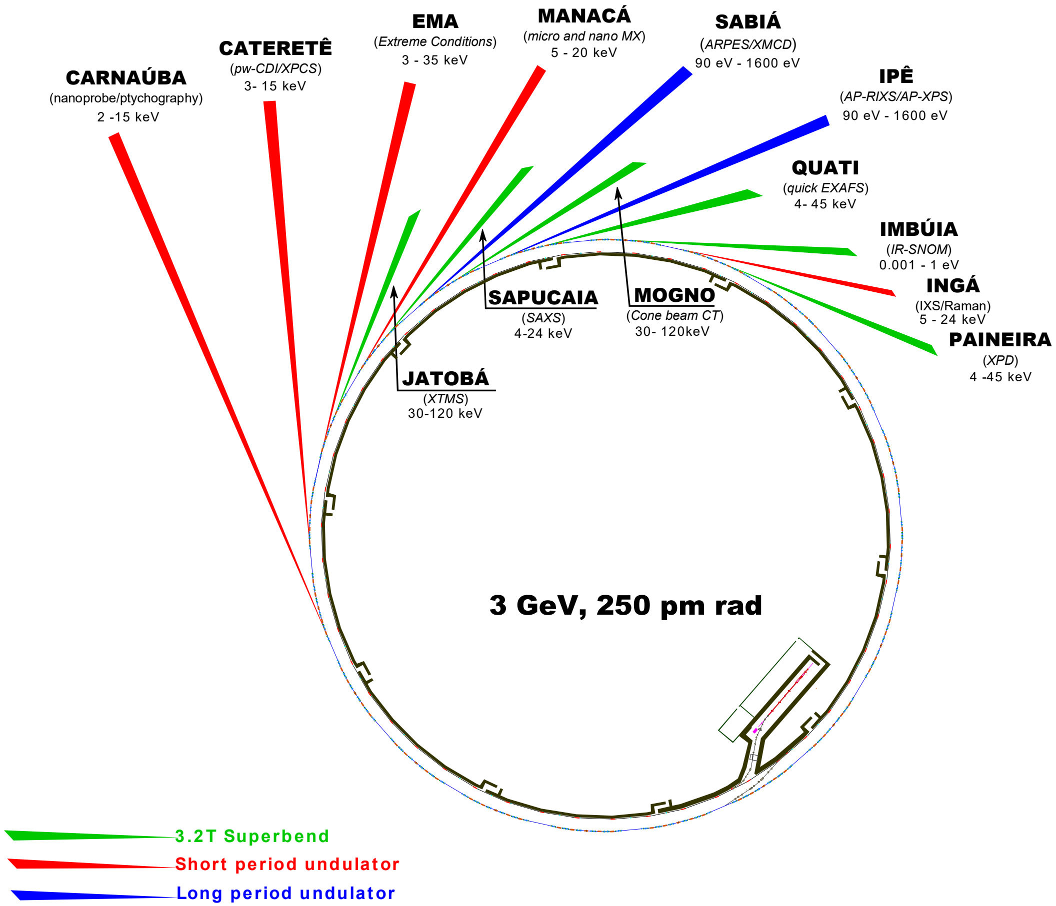

– **Experimental Programs**

- Tender nano-probe for spectro-ptychography
- Large FOV (30 μm) Coherent Diffraction Imaging
- Bragg CDI/XRD/XAFS under extreme conditions
- Serial micro and nano MX
- Tender x-ray RIXS
- AP-RIXS/XPS
- ARPES/PEEM
- Cone beam High Energy Tomography
- Quick-EXAFS
- 3D X-Ray Diffraction Microscopy
- High-Throughput SAXS
- Time Resolved Powder Diffraction
- nano-FTIR

Brilliance Comparison

- Even with future upgrades, Sirius will be competitive in the energy range of tender X-rays.

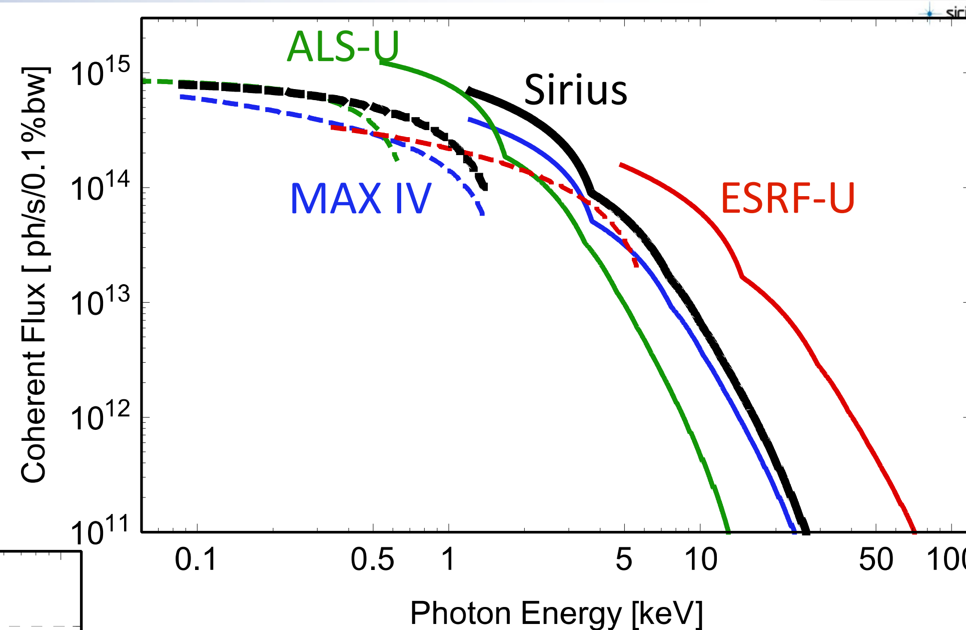

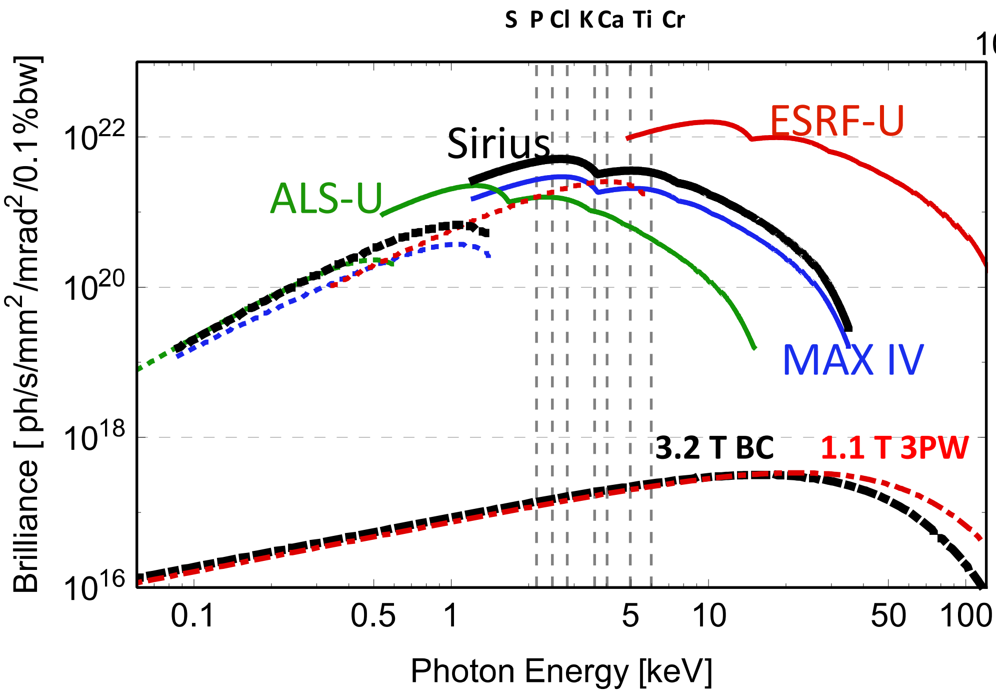

Courtesy: Harry Westfahl

Brilliance Comparison

- Even with future upgrades, Sirius will be competitive in the energy range of tender X-rays.

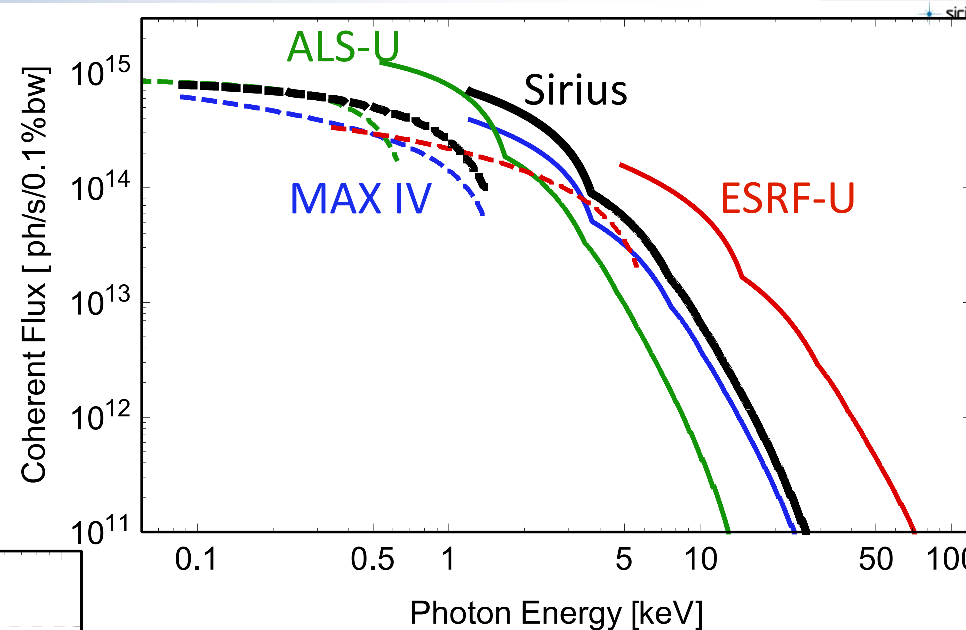

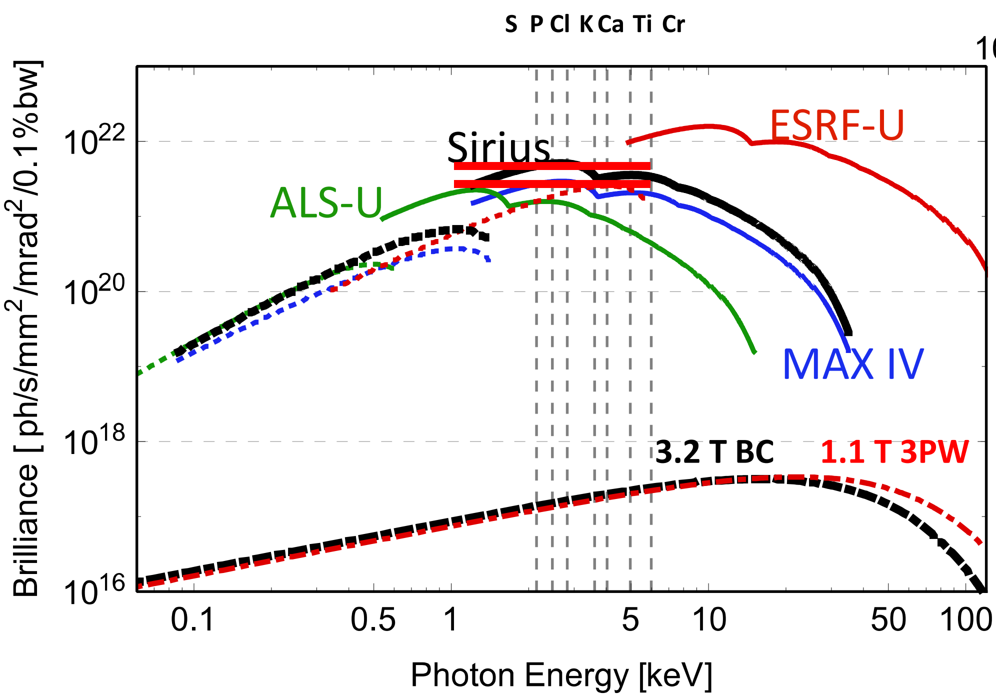

factor ~2 comes from betatron function matching

Courtesy: Harry Westfahl

Scanning X-ray microscope

$$Photon\ Flux \sim Brilliance(NA \times \delta)^2$$

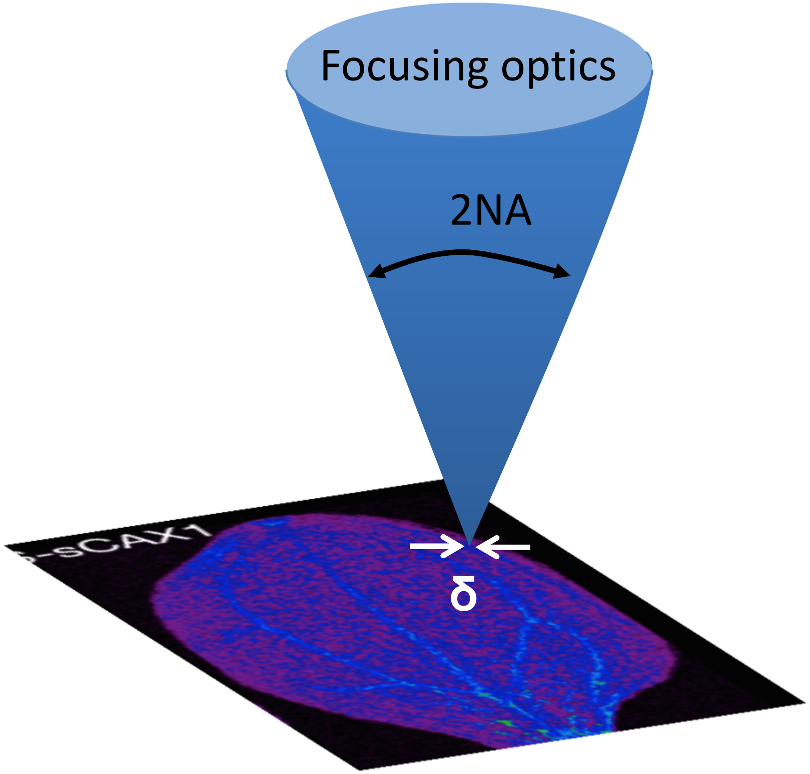

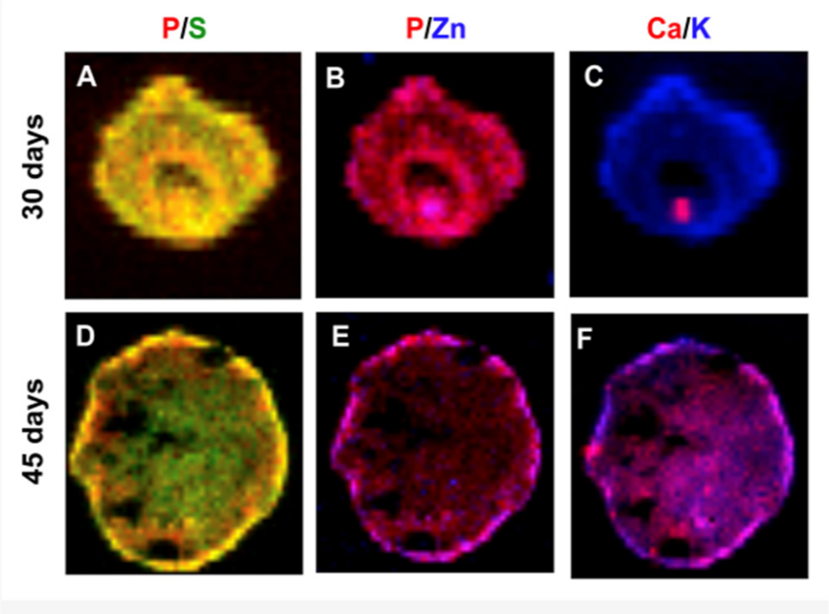

@ LNLS today: micronutrients during brain Formation 1 mm cerebral organoids Rafaela C. Sartore *et al.* (2017)

20 µm (@ LNLS today) → ***20 nm*** (@ Sirius in 2019)

Combining coherent lensless X-ray imaging and fluorescence

Junjing Deng et al (2017) done at APS

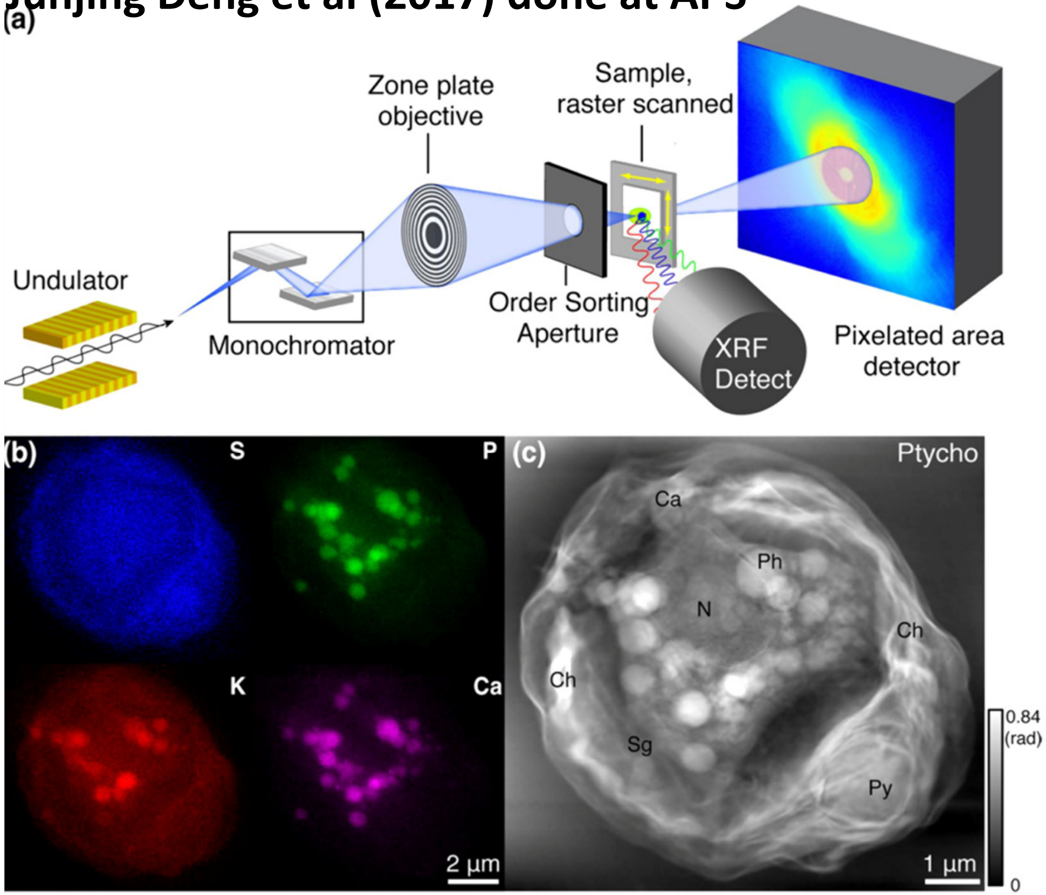

green algae Chlamydomonas reinhardtii
model cell for studying photosynthesis

Combining coherent lensless X-ray imaging and fluorescence

Junjing Deng et al (2017) done at APS

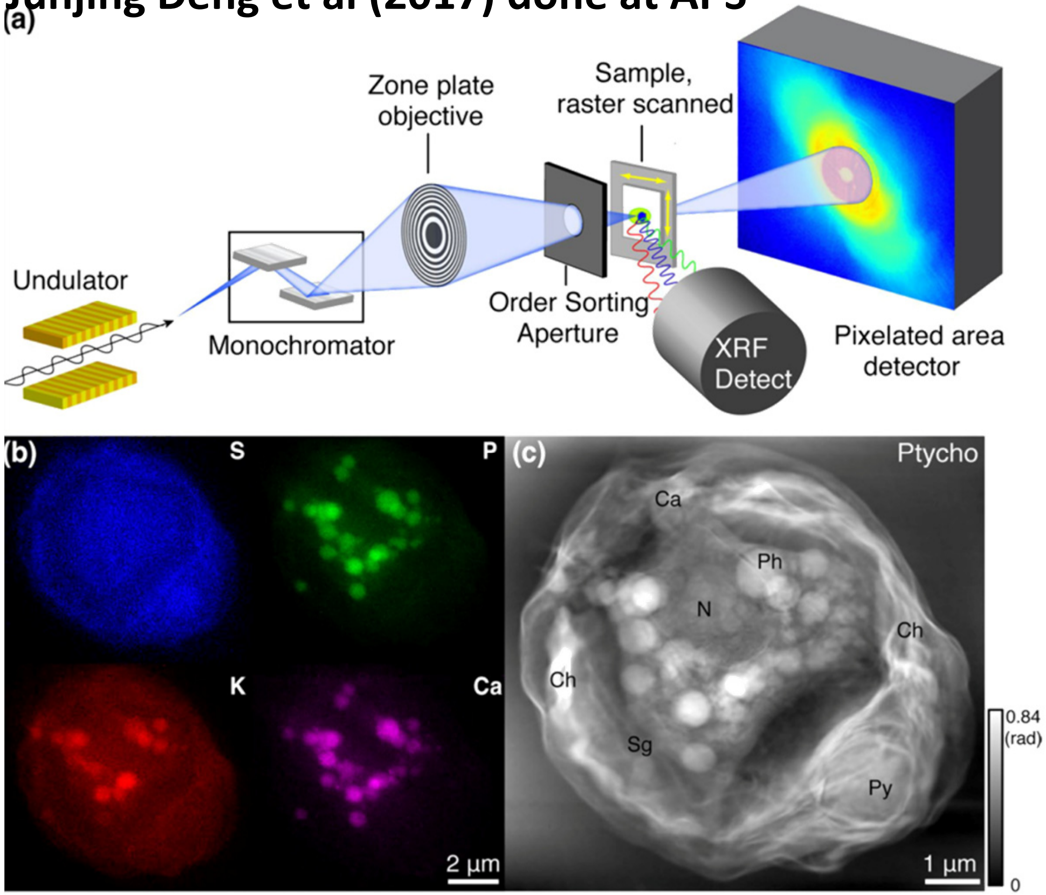

100 nm pix

green algae Chlamydomonas reinhardtii
model cell for studying photosynthesis

Combining coherent lensless X-ray imaging and fluorescence

Junjing Deng et al (2017) done at APS

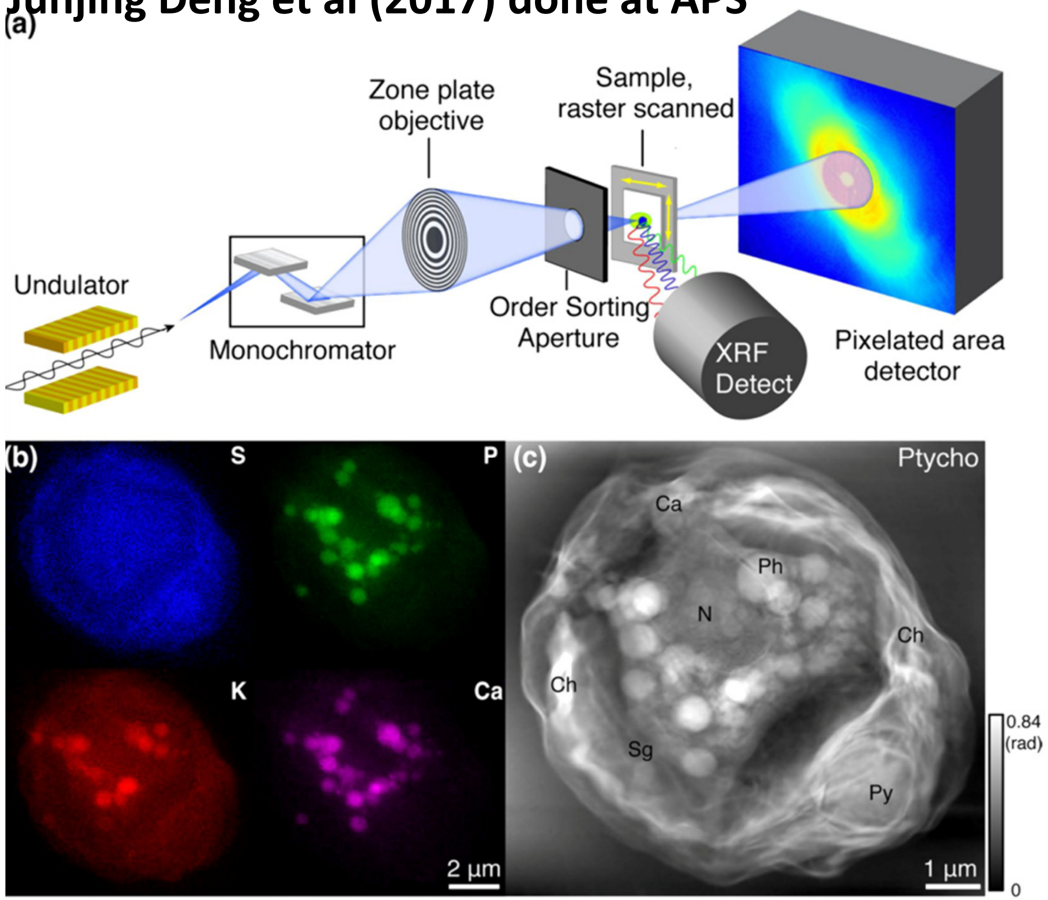

100 nm pix

18 nm pix

green algae Chlamydomonas reinhardtii
model cell for studying photosynthesis

Combining coherent lensless X-ray imaging and fluorescence

Junjing Deng et al (2017) done at APS

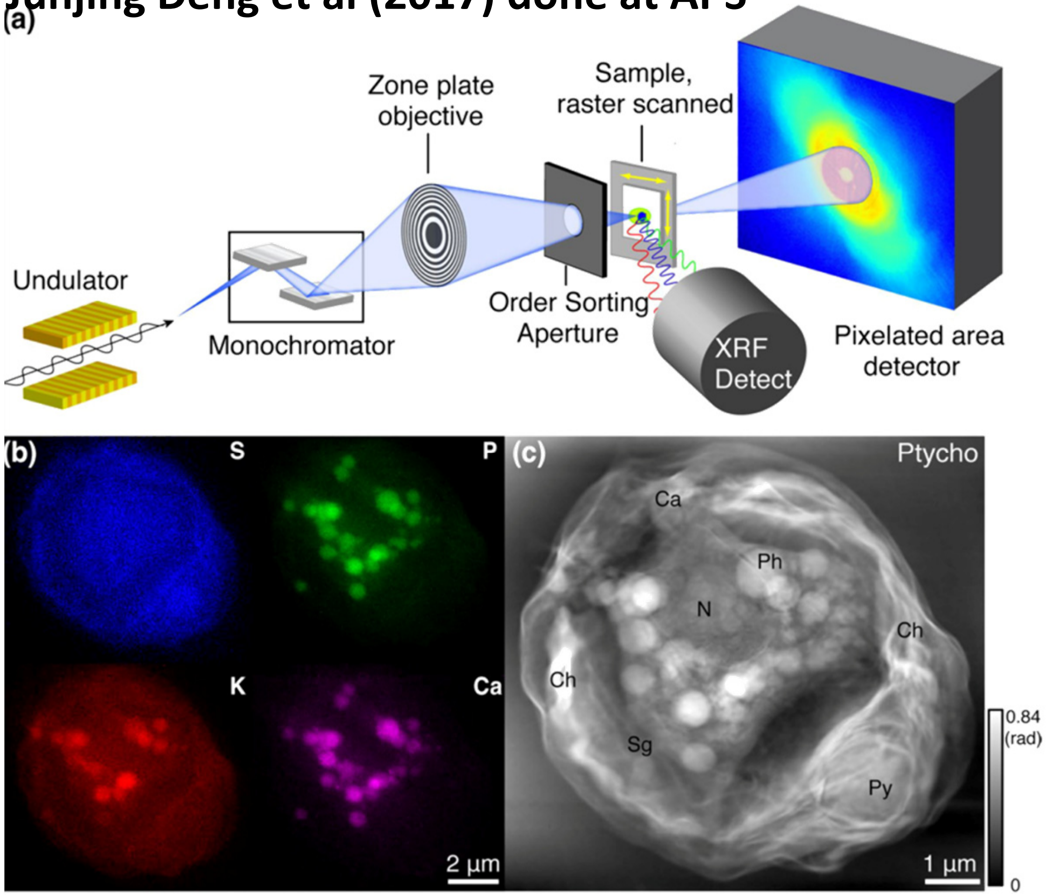

100 nm pix

18 nm pix

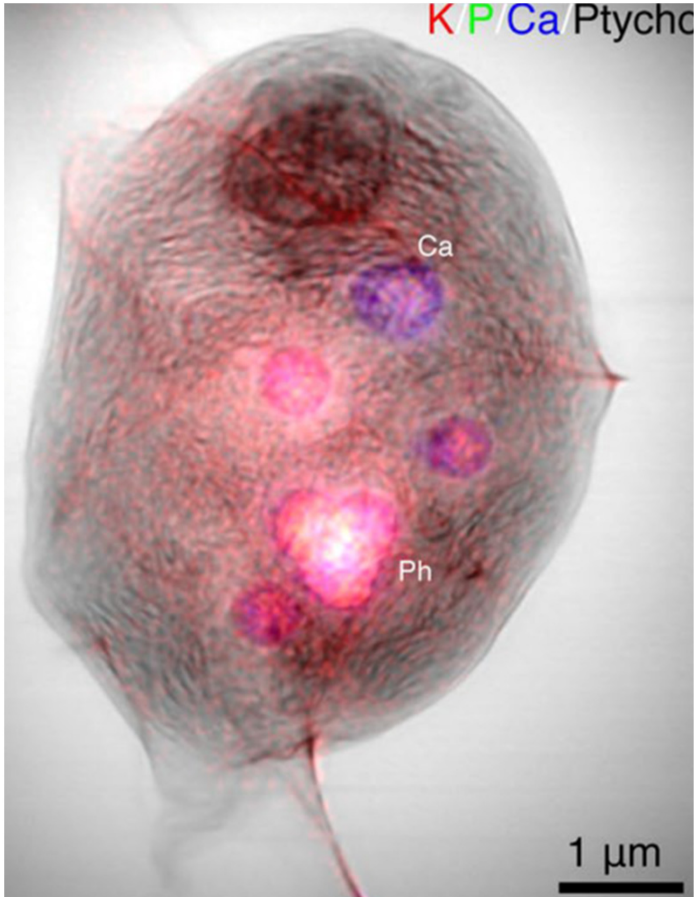

green algae Chlamydomonas reinhardtii
model cell for studying photosynthesis

Overlay of the two measurements

Combining coherent lensless X-ray imaging and fluorescence

Junjing Deng et al (2017) done at APS

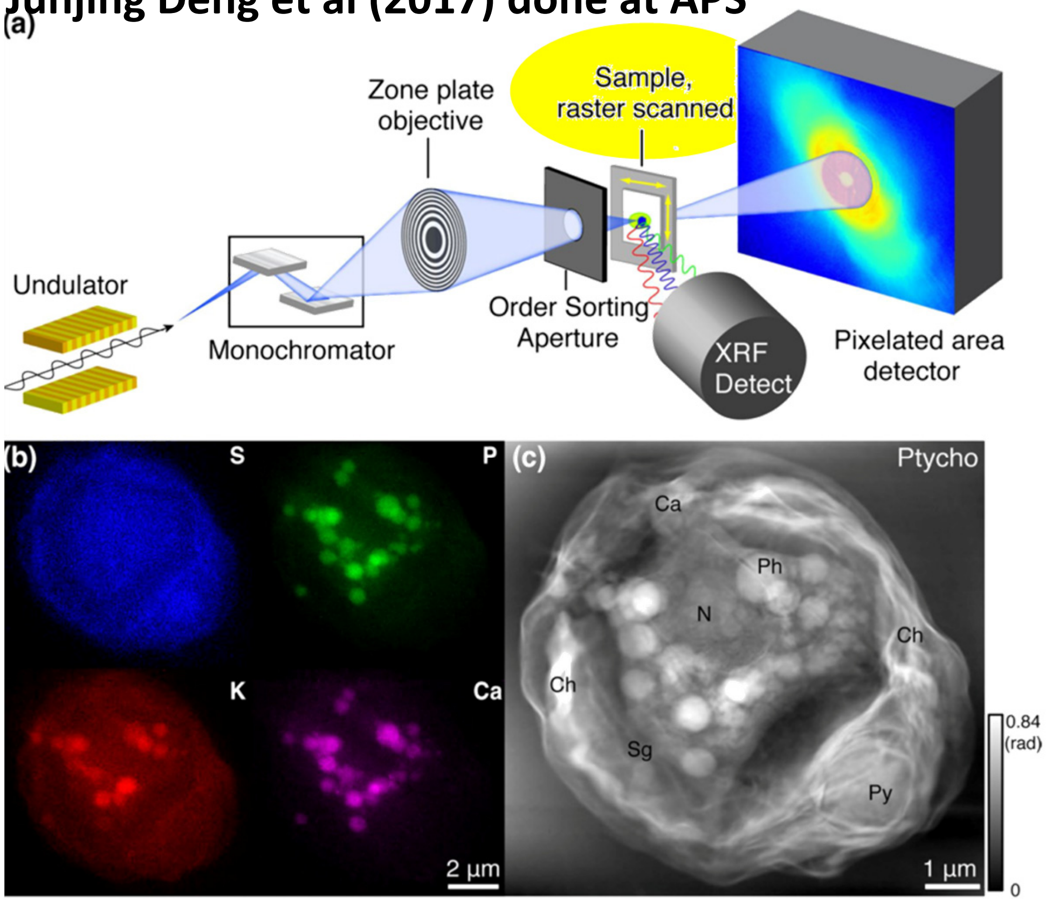

100 nm pix 18 nm pix

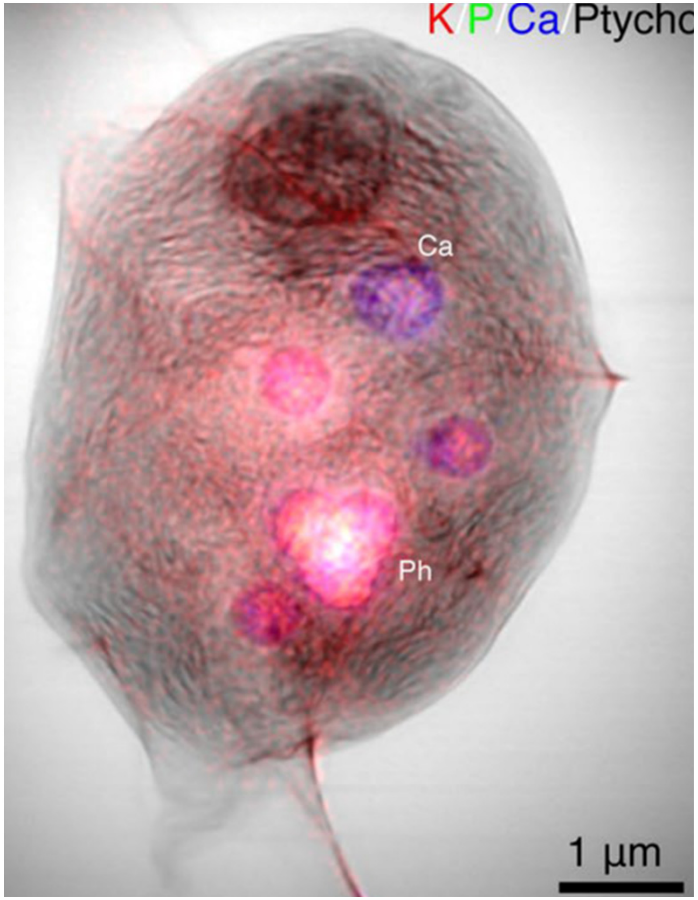

green algae Chlamydomonas reinhardtii
model cell for studying photosynthesis

Overlay of the two measurements

CARNAÚBA

(Coherent X-Ray Nanofocus Beamline)

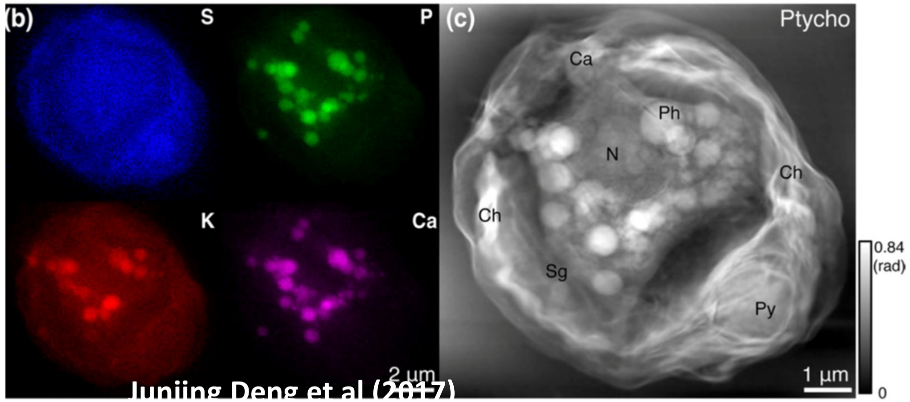

Fluorescence: ~100 nm pix   Lenseless imaging: ~18 nm pix

@ APS today:

Acquisition time (2D):

~0.1 s/pixel & ~75 min/image

~10^4 photons/nm^2 at 5.2 keV

CARNAÚBA
(Coherent X-Ray Nanofocus Beamline)

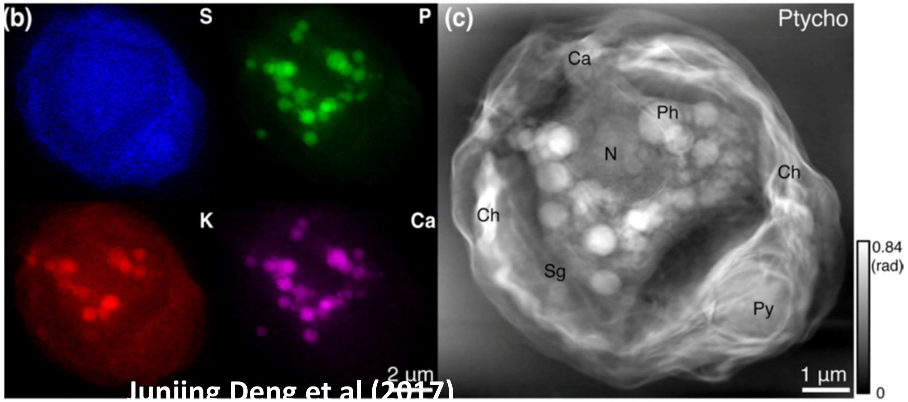

Fluorescence: ~100 nm pix   Lenseless imaging: ~18 nm pix

@ APS today:

Acquisition time (2D):

~0.1 s/pixel & ~75 min/image

~10^4 photons/nm^2 at 5.2 keV

Sirius

50 nm pix

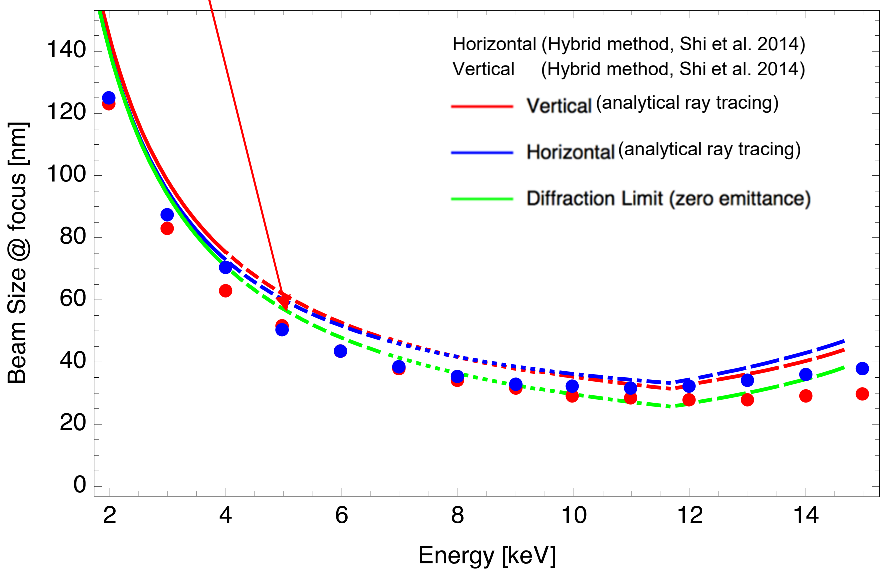

CARNAÚBA

(Coherent X-Ray Nanofocus Beamline)

Sirius

50 nm pix

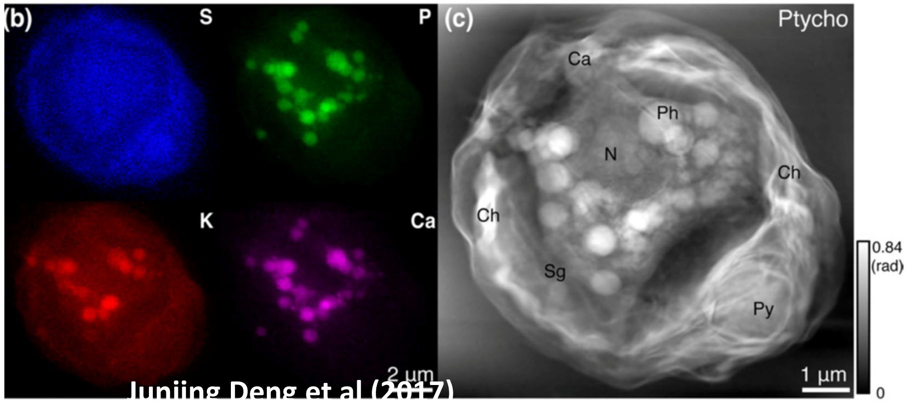

Fluorescence: ~100 nm pix Lenseless imaging: ~18 nm pix

@ APS today:

Acquisition time (2D):

~0.1 s/pixel & ~75 min/image

~10^4 photons/nm^2 at 5.2 keV

Sirius

~10^8 photons/nm^2 at 5.2 keV

~10 µs/pixel & ~1s/image

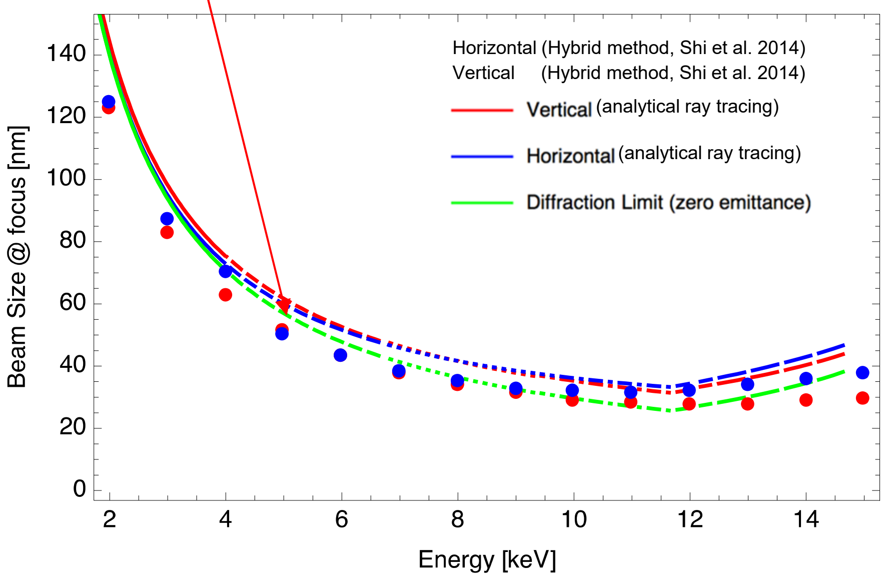

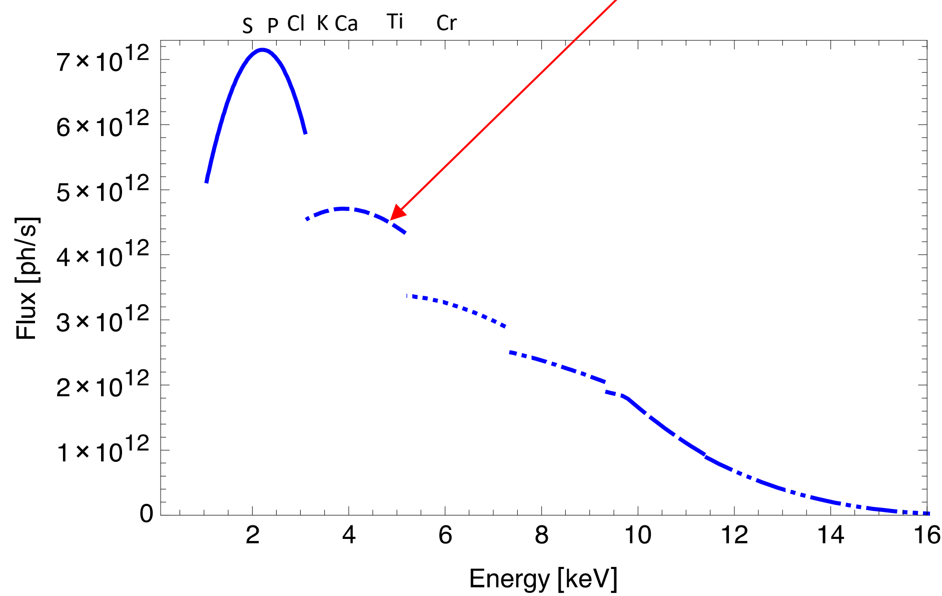

Machine & Beamline teams integration: Source scanning for ptychography

M. D. de Jonge et al. J. Sync. Rad. (2014)

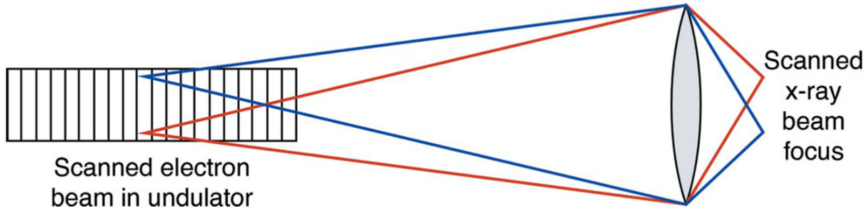

- Scanning the source position with corrector strengths of ±400μrad can result in scanning ranges of ±400μm in each direction.

Machine & Beamline teams integration: Source scanning for ptychography

M. D. de Jonge et al. J. Sync. Rad. (2014)

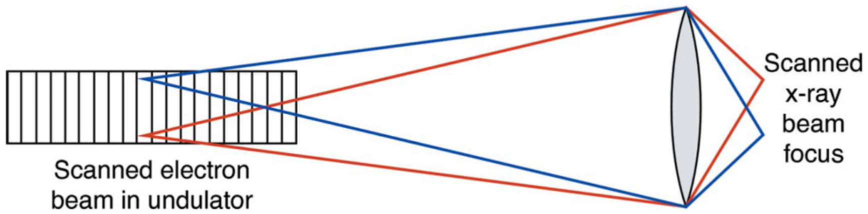

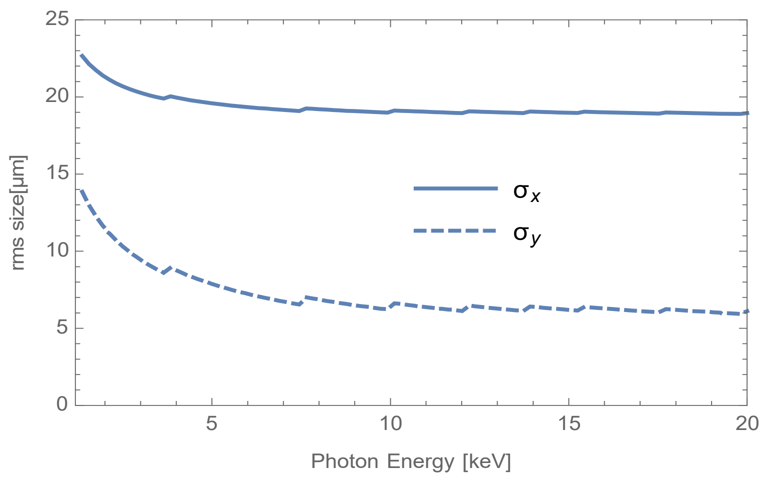

- Scanning the source position with corrector strengths of ±400µrad can result in scanning ranges of ±400µm in each direction.
- Step sizes of σ_x and σ_y result in ~ 40 x 100 overlapping scanning points for ptychography.

Machine & Beamline teams integration: Source scanning for ptychography

M. D. de Jonge et al. J. Sync. Rad. (2014)

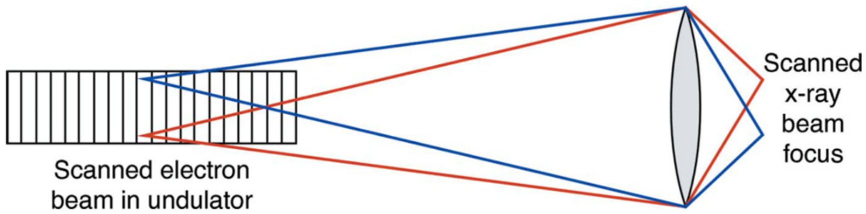

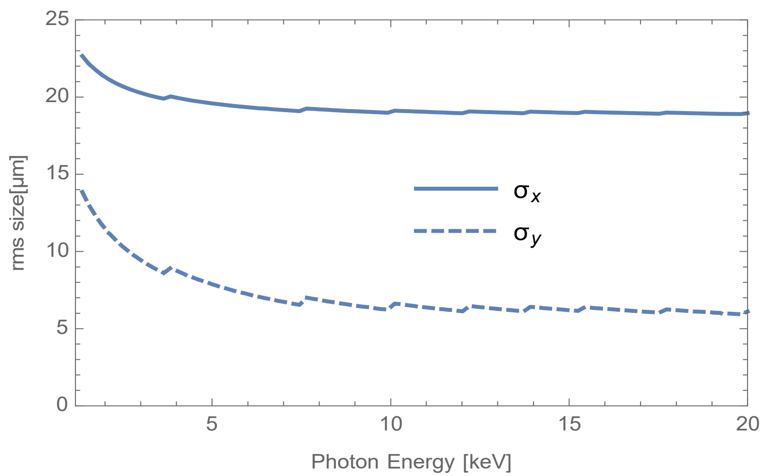

- Scanning the source position with corrector strengths of ±400µrad can result in scanning ranges of ±400µm in each direction.

- Step sizes of σ_x and σ_y result in ~ 40 x 100 overlapping scanning points for ptychography.

- Local beam bumps can be created with 4 correctors in the low beta straight section.

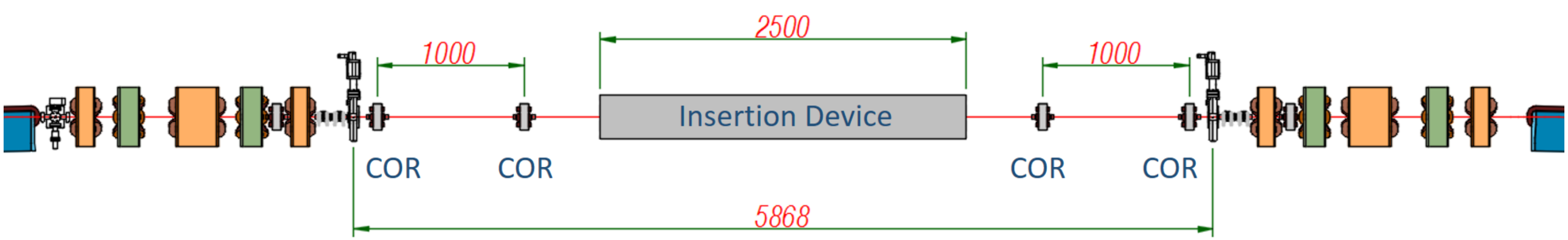

Conclusions

- The Synchrotron Radiation Light Source community is going through a very exciting time, with many new developments under way both in the machine and scientific application sides. Many new machines and machine upgrades are expected for next years.

Conclusions

- The Synchrotron Radiation Light Source community is going through a very exciting time, with many new developments under way both in the machine and scientific application sides. Many new machines and machine upgrades are expected for next years.

If you are a student or a young person starting in this field: you'll have lots of fun! ☺

Conclusions

- The Synchrotron Radiation Light Source community is going through a very exciting time, with many new developments under way both in the machine and scientific application sides. Many new machines and machine upgrades are expected for next years.

  If you are a student or a young person starting in this field: you'll have lots of fun! ☺

- It is important to integrate machine and beamline teams in the optimization of experiments.

Conclusions

- The Synchrotron Radiation Light Source community is going through a very exciting time, with many new developments under way both in the machine and scientific application sides. Many new machines and machine upgrades are expected for next years.

  If you are a student or a young person starting in this field: you'll have lots of fun! ☺

- It is important to integrate machine and beamline teams in the optimization of experiments.
- This is an open community and international cooperation is one of the most important sources for learning and advancing in this area.

Thank you!

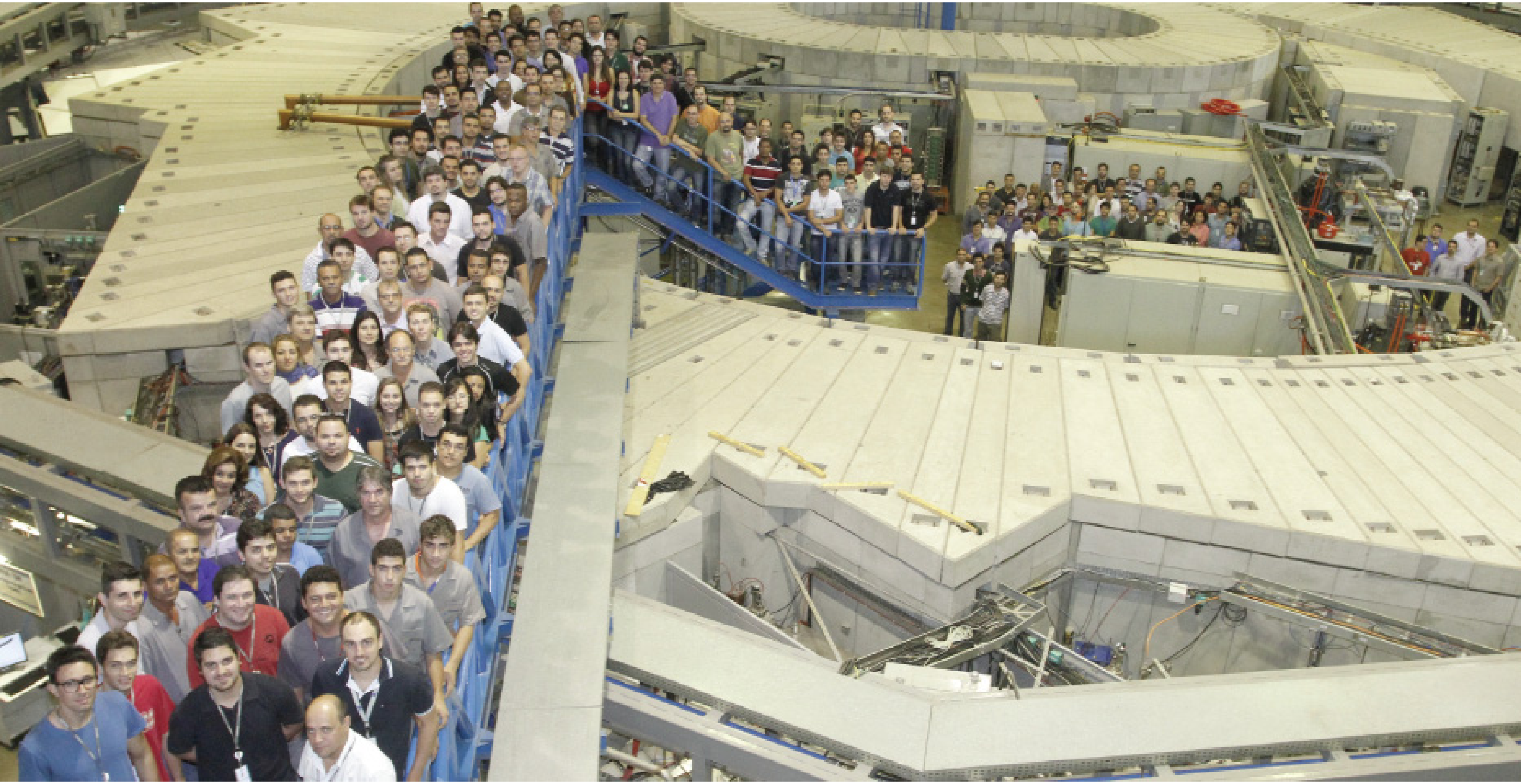

Sirius Team – a small but highly motivated and integrated team!